Laura Tiemeijer

Spatial Control of Angiogenesis by Engineered Patterns of Notch Ligands

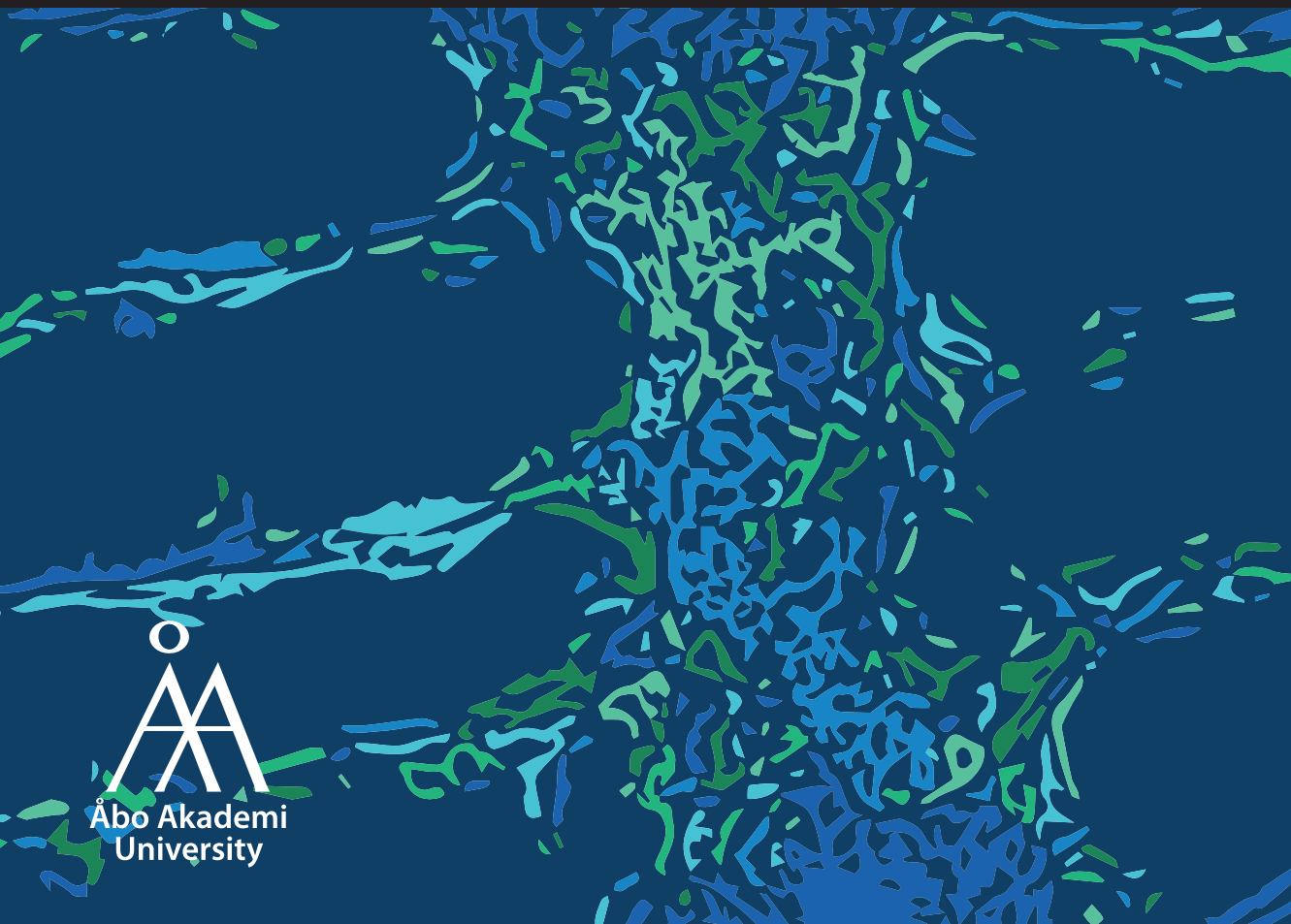

Åbo Akademi University

Laura Tiemeijer

Born 1991

Previous studies and degrees:

Master Regenerative Medicine and Technology, Eindhoven University of Technology, 2016

Bachelor Biomedical Engineering, Eindhoven University of Technology, 2013

Spatial Control of Angiogenesis by Engineered Patterns of Notch ligands

Laura Tiemeijer

Cell Biology, Faculty of Science and Engineering
Åbo Akademi University, Turku, Finland
Biomedical Engineering, Soft Tissue Engineering and Mechanobiology
Eindhoven university of Technology, Eindhoven, The Netherlands

From the Faculty of Science and Engineering, Cell Biology, Turku Doctoral Network in Molecular Biosciences, Åbo Akademi University and the department of Biomedical Engineering, Soft Tissue Engineering and Mechanobiology, Eindhoven University of Technology

Supervisor
Prof. dr. C.M. Sahlgren
Faculty of Science and Engineering, Cell Biology, Molecular Biosciences, Åbo Akademi University and the department of Biomedical Engineering, Soft Tissue Engineering and Mechanobiology, Eindhoven university of Technology

Co-supervisor
Prof. dr. C.V.C. Bouten
Department of Biomedical Engineering, Soft Tissue Engineering and Mechanobiology, Eindhoven University of Technology

Reviewed by
Prof. dr. L. Moroni, Maastricht University
Prof. dr. A. Teixeira, Karolinska Institutet

Opponent
Dr. Stephan Huveneers, University of Amsterdam & AMC (Academic Medical Center)

Custos
Prof. dr. C.M. Sahlgren
Faculty of Science and Engineering, Cell Biology, Molecular Biosciences, Åbo Akademi University and the department of Biomedical Engineering, Soft Tissue Engineering and Mechanobiology, Eindhoven university of Technology

ISBN 978-952-12-4218-2 (Printed)
ISBN 978-952-12-4219-9 (Digital)
Painosalama, Turku, Finland 2022

"*What we know is a drop, what we don't know is an ocean*"**–** Isaac Newton

Summary

Spatial control of angiogenesis by engineered patterns of Notch
In tissue engineering and regenerative medicine, proper vascularization of engineered tissues is imperative, as diffusion of nutrients, oxygen and waste is limited in constructs larger than a few cells thick. Therefore, tissue vascularization has been extensively researched. However, most approaches rely on preset structural support for the cells provided by scaffolds and micro fluidic chips to instruct vascular organization, which limit the integration into engineered and native tissues. Self-assembly of vascular constructs by combinations of support material, cells and growth factors shows promise but is not capable of dictating structure and organization of the engineered vasculatures. Therefore, spatial control over vascularization is required for tissue engineered constructs to remain alive and functioning.

The growth of vasculature from existing vessels towards the oxygen gradient, is a process called angiogenesis. During angiogenesis, migrating tip cells emerge from the vascular endothelium and sprout towards the oxygen gradient. Proliferating stalk cells follow their path and form a vascular tube. The selection of tip and stalk cell phenotypes is regulated via several cell signaling pathways, among which the Notch signaling pathway has a predominant role.

The Notch signaling pathway is a highly conserved cell-cell signaling pathway involved in numerous cell fate decisions and the patterning of tissues. The Notch receptor Notch1 and ligands Dll4 and Jag1 are involved in angiogenesis. Here, Dll4/Notch1 signaling is responsible for tip and stalk cell selection and Jag1 modulates Dll4/Notch1 signaling, though the role of Jag1 in angiogenesis needs to be further elucidated. Notch signaling is involved in several (genetic) cardiovascular diseases as well as cancer. For therapeutic targeting of Notch, mostly soluble molecules have been used to inhibit signaling. However, systemic administration of these molecules gives rise to adverse effects and toxicity. Local activation of Notch signaling, especially to target angiogenesis has not been widely addressed.

In this thesis, we have developed an *in vitro* method where we used spatial patterns of parallel lines of Notch signaling ligands to locally modulate endothelial tip/stalk cell selection and thereby gained spatial control over endothelial sprouting. The technical details of the protocol, optimization, important considerations and alternative approaches are also provided. Using the developed technology we have found that line patterns of Dll4 induced controlled unidirectional and restricted sprouting on the lines, resulting in localization of endothelial sprouts between the lines (negative patterning).

Next, we used our method to investigate the role of Jag1 in endothelial patterning. In contrast to Dll4, we have found that Jag1 patterns did not exert control over endothelial sprouting location and direction. Gene expression profiles did not provide significant difference upon stimulation with Dll4 and Jag1 to explain the difference in control observed. Computational modeling of Notch signaling endothelial cells on patterns of ligand, revealed that underlying differences in signaling dynamics between Jag1 and Dll4 are likely the cause for the lack of control over endothelial sprouting exerted by Jag1.

To study the potential of ligand patterning further, alternative techniques for complex patterning of ligands were considered and investigated, though further optimization is needed for their application.

In summary, we have shown that the use of local presentation of the Notch ligand Dll4 results in spatial control over endothelial sprouting. Additionally, the potential of engineered patterns of ligands to control endothelial sprouting during angiogenesis is valuable for the design of biomaterials and engineering of organized vasculature for tissue engineering as well as for regenerative medicine. Furthermore, the method developed in this thesis allows for the screening of functional engineered ligands and could aid in revealing disease phenotypes by screening for mutations in ligands.

Sammanfattning

Spatial kontroll av angiogenes genom konstruerade mönster av Notch-ligander

I vävnadsteknik och regenerativ medicin är vaskularisering av konstruerade vävnader nödvändigt, eftersom spridningen av näringsämnen, syre och avfall är begränsad i konstruktioner som är större än några celler i tjocklek. Därför har vävnadsvaskularisering i omfattande grad utforskats. De flesta infallsvinklarna är dock beroende av förbestämda stödstrukturer och mikofluidiska chip för att instruera vaskulär organisation, vilket begränsar integrationen i levande vävnader. Självkonstruktion av vaskulaturen genom kombinationer av celler och tillväxtfaktorer är lovande, men kan inte diktera strukturen och organisationen. Därför är spatial kontroll av vaskularisering nödvändig för att vävnadstekniska konstruktioner skall vara funktionella.

Tillväxten av vaskulatur utgående från existerande kärl mot syregradienten är en process benämnd angiogenes. Under angiogenes framträder migrerande spetsceller från det vaskulära endotelet och rör sig mot syregradienten. Snabbväxande stjälkceller följer deras bana och bildar en vaskulär tub. Urvalet av spets- och stjälkceller styrs genom ett flertal cellsignaleringsvägar, av vilka cellsignaleringsvägen Notch har en framträdande roll.

Notchsignaleringsvägen är en i hög grad konserverad cell-cell signaleringsväg inblandad i ett flertal cellödesbeslut och vävnadsmönstring. Notchreceptorn Notch1 och liganderna Dll4 och Jag1 är viktiga för angiogenes. Här är Dll4/Notch1-signalering ansvarig för spets- och stjälkcellsurval och Jag1 modulerar Dll4/Notch1-signalering. Dock bör rollen Jag1 spelar i angiogenes vidare utforskas. Notchsignalering är inblandad i flera (genetiska) hjärt- och kärlsjukdomar samt cancer. För terapeutiska interventioner inriktade på Notch har till största delen lösliga molekyler använts för att hämma signalering. Systemisk administrering av dessa molekyler ger dock upphov till skadliga effekter och toxicitet. Lokal aktivering av Notchsignalering, framförallt inriktad på angiogenes har inte i omfattande grad studerats.

I denna avhandling har vi utvecklat en in vitro-metod där vi använde spatiala mönster av parallella linjer av Notchligander för att lokalt modulera urvalet av endotela spets- och stjälkceller och därmed få kontroll över endoteltillväxten. Vi har funnit att linjemönster av Dll4 inducerade kontrollerad enkelriktad och begränsad tllväxt vilket resulterade i endoteltillväxt mellan linjerna (negativ mönstring).

Vi använde även vår metod för att utforska vilken roll Jag1 hade i endotelmönstring. Till skillnad från Dll4 påverkade Jag1 inte endoteltillväxtens plats och riktning. Genutrycksprofiler visade ingen

signifikant skillnad efter stimulering med Dll4 och Jag1 som skulle förklara de observerade skillnaderna. Datamodellering av Notchsignalerande endotelceller på ligandmönster visade att underliggande skillnader i signaleringsdynamik mellan Jag1 och Dll4 sannolikt är orsaken till bristen på kontroll över endoteltillväxt hos Jag1.

För att studera potentialen hos ligandmönstring vidare utforskades alternativa tekniker för komplex mönstring av ligander, dock krävs vidare optimering innan de kan tas i bruk

I sammanfattning har vi visat att användningen av lokal presentation av Notchliganden Dll4 resulterar i spatial kontroll över endoteltillväxt. Mönster av ligander för att kontrollera endoteltillväxt vid angiogenes är värdefullt för skapandet av biomaterial och konstruktion av organiserad vaskulatur för vävnadskonstruktion samt regenerativ medicin. Slutligen möjliggör metoden utvecklad i denna avhandling screening av funktionella konstruerade ligander och kan bistå i avslöjandet av sjukdomsfenotyper genom screening av muterade ligander.

Table of contents

List of publications included in this thesis

Laura A. Tiemeijer, Jean-Phillipe Frimat, Oscar M. J. A. Stassen, Carlijn V. C. Bouten and Cecilia M. Sahlgren - Spatial patterning of the Notch ligand Dll4 controls endothelial sprouting in vitro. *Scientific Reports*. 8, 6392 (2018).

Laura A. Tiemeijer*, Tommaso Ristori*, Oscar M. J. A. Stassen, Jaakko J. Ahlberg, Jonne J. J. de Bijl, Christopher S. Chen, Katie Bentley, Carlijn V. C. Bouten and Cecilia M. Sahlgren - Engineered patterns of Notch ligands Jag1 and Dll4 elicit differential spatial control of endothelial sprouting. *iScience.* 25, 104306 (2022)

---

* These authors contributed equally to this work

Publication not included in this thesis

Laura. A. Tiemeijer*, Sami Sanlidag*, Carlijn V. C. Bouten and Cecilia M. Sahlgren – Engineering tissue morphogenesis: Taking it up a Notch. *Trends in Biotechnology* (2022)

* These authors contributed equally to this work

Author contributions

I. The author contributed to designing the experiments, performing the experiments, analyzing the data and writing and reviewing the manuscript. The author, J-PF and CMS wrote the main manuscript text. The author together with J-PF, CVB and CMS designed experiments. The author and OMJAS performed experiments. J-PF provided microfabrication masters. The author and CMS analyzed data, all authors reviewed the manuscript.

II. The author contributed to the conceptualization of the method and design, performing the experiments, analyzing the data and writing and reviewing the manuscript. The author, together with TR and CMS was responsible for conceptualization, methodology, validation and project administration. The author, together with TR, JJJB, JJA and OMJAS performed the experiments. The author, together with TR and OMJAS performed the formal analyses. The author, together with TR provided the visualization and wrote the original manuscript. TR and JJJB provided the software. CSC, CVCB, CMS provided the resources for this study. CSC, KB, CVCB, CMS supervised the study. The author, TR, OMJAS, CSC, KB, CVCB, CMS reviewed and edited the manuscript.

Abbreviations

μCP	Micro contact printing
2D	Two Dimensional
3D	Three Dimensional
ADAM	A Disintegrin And Metalloproteinase
BSA	Bovine Serum Albumin
CADASIL	Cerebral Autosomal Dominant Arteriopathy with Subcortical infarcts and leukoencephalopathy
CSL	CBF1, Suppressor of hairless, Lag-1
CVD	Cardiovascular disease
DAPI	4′,6-diamidino-2-phenylindole
DAPT	N-[N-(3,5-Difluorophenacetyl)-L-alanyl]-S-phenylglycine t-butyl ester
Dline	Parameter for the model: Number of Dll4 molecules in the line pattern
Dll	Delta-like ligand
DSL	Delta/Serrate/Lag
EC	Endothelial Cell
ECM	Extra cellular matrix
Ecs	Efficiency of controlled sprouting (Study I)
EFBN2	Ephrin-B2 gene
Efcs	Efficiency of controlled sprouting (Study II)
EGF	Epithelial Growth Factor
EMT	Endothelial-to-mesenchymal transition
FGF	Fibroblast Growth Factor
FGF	Fibroblast Growth Factor
GSI	γ-secretase inhibitor
HEPES	4-(2-hydroxyethyl)-1-piperazineethanesulfonic acid
hESC	Human embryonic Stem cell
HSC	Hematopoietic Stem Cell
HUVEC	Human Umbilical Vein Endothelial Cell
IgG	Immunoglobulin G
Jag	Jagged
Jline	Parameter for the model: Number of Jag1 molecules in the line pattern
LLC1	Lung carcinoma Tumor Cells
MAML	Mastermind-like
MI	Myocardial Infarction
MSC	Mesenchymal Stem Cell
NECD	Notch Extracellular Domain
NICD	Notch Intracellular Domain
PBS	Phosphate buffered Saline

PDGF	Platelet derived growth factor
PDGFRβ	Platelet-Derived Growth Factor Receptor Beta
PDMS	Polydimethylsiloxane
PEG-PLL	Polyethylene glycol – poly-l-lysine
PLGA	Poly (lactic-*co*-glycolic acid)
PLL	Poly-L-lysine
PLPP	4- benzoyl benzyl-trimethylammonium chloride
PTEN	Phosphatase and tensin homolog gene
RGD	Arginylglycylaspartic acid
ROI	Region of Interest
SCC	Squamous cell carcinomas
siRNA	Small interfering RNA
TE	Tissue Engineering
TGF-β	Transforming Growth Factor Beta
TMD	Trans membrane domain
UV	Ultraviolet
Vascular adhesion molecule 1	VCAM1
VEGF	Vascular Endothelial Growth Factor
VEGFR	Vascular Endothelial Growth Factor Receptor
VSMC	Vascular Smooth Muscle Cell
VWF	Von Willebrand Factor
WT	Wild type
α-SMA	α-Smooth Muscle Actin
γ-secretase	Gamma-secretase

Introduction

Cardiovascular Disease (CVD) is the leading cause of death globally[1,2] and responsible for 32% of the total number of deaths in 2019[1]. While the World Health Organization strongly supports prevention by spreading awareness of the benefits of healthy lifestyle changes, there is a need to treat genetic and acquired CVDs. Tissue engineering (TE) provides the opportunity to replace organs, vessels and (cardiac) tissues with engineered tissue constructs, that can grow and adapt to the body, in contrast to donor (allografts and xenografts) or synthetic replacements which require lifelong immunosuppressive therapy[3,4]. While larger vasculature constructs such as vessels and valves have been successfully developed, the engineering of vessels with smaller diameters and microvasculature, remains challenging[3,5]. In TE and regenerative medicine applications a functional vasculature is imperative for successful engraftment of the engineered tissue into the native tissues[5,6] as larger engineered tissue constructs cannot rely on diffusion of oxygen nutrients and waste[7].

The engineering of vasculature is under intensive research[5,6,8]. However, the common approaches rely on preset structural support for the cells provided by scaffolds, micro fluidic chips, 3D printing etc. to guide vascular structure, which limits the integration into engineered and native tissues. Self-assembly of vascular constructs, by combinations of support material, cells and growth factors shows promise but is not capable to dictate the structure and organization of the engineered vasculature. Therefore, spatial control over vascularization is needed and required[6,9,10]. Consequently, this thesis concentrates on engineering a patterned functional microvasculature e.g. to ultimately support larger engineered constructs.

The native response to hypoxic conditions and the required transport of nutrients and waste is the process of angiogenesis[11]. Here, new vessels sprout from existing blood vessels towards the hypoxic tissue to create new vasculature and restore the normal blood supply, normalizing the local oxygen levels. At the start of this process an endothelial tip cell is first to emerge from the endothelial lining of an existing vessel, followed by proliferating endothelial stalk cells. This process is tightly regulated by cell-cell signaling pathways such as the Notch signaling pathway[12,13].

The Notch signaling pathway is a highly conserved, dose dependent, cell-cell signaling pathway involved in numerous cell fate decisions and the patterning of tissues[14]. Angiogenesis is regulated by the Notch ligands Dll4 and Jag1 and the Notch1 receptor[12,15]. Upon hypoxia, Dll4/Notch1 signaling is responsible for the selection of tip and stalk cells in angiogenesis[12,13,16]. Dll4/Notch1 signaling induces a stalk cell phenotype in the receiving cell,

while the sending cell adopts a tip cell phenotype[12,17]. Jag1 has been shown to have an opposite function to Dll4 and induces tip cell formation and sprouting, by modulating the Dll4/Notch1 signaling pathway[16,18]. Together, Dll4 and Jag1 regulate the induction of a tip and stalk cell pattern during the onset of angiogenic sprouting. The Notch pathway is also involved in a larger number of (genetic) CVDs and cancers[19,20].

From a therapeutic point of view, targeting of the Notch signaling pathway has been of interest in many studies that focus on cancer angiogenesis[20]. Here, soluble molecules, such as soluble ligands, decoys and inhibitors of the Notch signaling pathway have been used to target cancer angiogenesis. However, systemic administration of these molecules gives rise to adverse effects and balancing toxicity and efficiency is key[20,21]. Activation of the Notch signaling pathway to engineer vasculature has not been widely addressed.

The immobilization of Notch ligands on materials is important for activation[22], though there are a few considerations for the design of Notch ligand functionalized biomaterials. However, the immobilization of Notch ligands is a valuable tool for local and controlled induction of cell fate for many purposes[14], among which the expansion and differentiation of progenitor cells for transplantation[23] or dental TE[24].

To gain spatial control over angiogenesis for engineering vasculature, we believe that local activation of the Notch signaling pathway can be used to dictate cell fate and drive tissue organization. Therefore, in this thesis, we explore the ability of the Notch ligands to locally induce cell fate to spatially control angiogenesis. We develop an *in vitro* method where we use spatial patterns of Notch ligands to locally induce endothelial tip or stalk cells, thereby gaining spatial control over endothelial sprouting. We explore the spatial control exerted by patterns of both Dll4 and Jag1 and compare the efficiencies of this control over endothelial sprouting. Additionally, we try to unravel the mechanisms behind the ligand-mediated control over endothelial sprouting by combination of *in vitro* and *in silico* models.

The knowledge we obtained with this research could be applied for the development of a novel approach to vascular engineering, where endothelial sprouts are induced to self-organize via of patterns of Notch ligands, thereby spatially dictating vascular structure without the limitations of supporting structural constructs. We believe that gaining spatial control over endothelial sprouting is beneficial for engineering of vasculature for therapeutic and TE applications. Additionally, we believe that obtained knowledge might aid in the design of biomaterials for engineered vasculature and regenerative medicine, as well as the development of future therapeutic strategies for cancer angiogenesis and cardiovascular pathologies.

Review of the literature

1 The Vasculature

The vasculature acts as an efficient delivery system for blood in order to transport oxygen, nutrients and waste throughout the human body. The heart pumps the blood through the system of blood vessels that make up the vasculature. Generally, blood vessels can be divided into five categories: arteries, arterioles, capillaries, venules and veins. From the heart the blood is pumped into the arteries, which are the largest in size and lumen diameter, and act as a highway to distribute the blood efficiently. From the arteries, the blood enters arterioles, which are smaller in size and acts as gate keepers for the perfusion of tissues, responding to neural, hormonal or local chemical stimuli.
Next, the blood enters the capillaries to exchange its cargo with the interstitial fluid of the recipient organs, tissues and cells. Afterwards, the blood enters the venules and veins to be transported back to the heart and lungs[25].

The structure of the blood vessels correlates with their function and thus differs between the five categories. However, in general, blood vessels are made up of three layers; the tunica intima, the tunica media and the tunica externa (Figure 1). The tunica intima consists of a layer of endothelial cells (EC) providing the barrier between the blood in the lumen and the vessel. The tunica media consists mostly of layers of vascular smooth muscle cells (VSMC) and elastin. The muscle layers enable vasoconstriction and vasodilation and can influence the blood flow and pressure by changing the vessel diameter. The tunica externa is the outer layer of the blood vessel and consists mostly of collagen fibers that reinforce the vessel and provide anchoring to the surrounding tissue. Arteries and arterioles contain the largest tunica media to regulate blood flow and pressure, while in veins the tunica media is smaller. Capillaries do not have a tunica media as their primary function is to exchange nutrients, oxygen and waste and therefore only contain of a single layer of ECs and a basement membrane with the odd pericyte, to ensure perfusion[25] (Figure 1).

1.1 Microvasculature

The exchange of oxygen, nutrients and waste with tissues and organs occurs in the capillary beds. Depending on the tissue or organ the vascular bed resides in, the structure of the endothelial layer in the capillary differs to allows for different functions, such as control over vascular permeability, coagulation and anticoagulation, inflammation and angiogenesis[26].

Generally, the endothelium of capillaries can be classified into three classes: continuous non-fenestrated, continuous fenestrated, and discontinuous fenestrated (Figure 1). Continuous non-fenestrated endothelium can be found in the brain, skin, muscle, heart and lung, where the endothelium functions as a barrier. Here, tight- and adherence junctions ensure the barrier function[27]. The transport of molecules over the barrier is achieved via the active process of transcytosis[26]. Continuous fenestrated endothelium allows for rapid exchange of molecules via fenestrae, transcellular pores of approximately 70 nm diameter[28]. This type of endothelium can be found around tissues and organs that require filtration of the blood, such as the kidney and endocrine glands[26]. Discontinuous fenestrated endothelium contains large heterogeneous fenestrae (100 to 200 nm in diameter)[29], and can be found in sinusoidal vascular beds of the liver and bone marrow. These capillaries don't have a basement membrane[26]. Apart from endothelial specification towards an arterial, veinous or lymphatic fate, the heterogeneity of the ECs themselves contributes to the varied responses of different vessel beds to diseases and pathological stimuli[26].

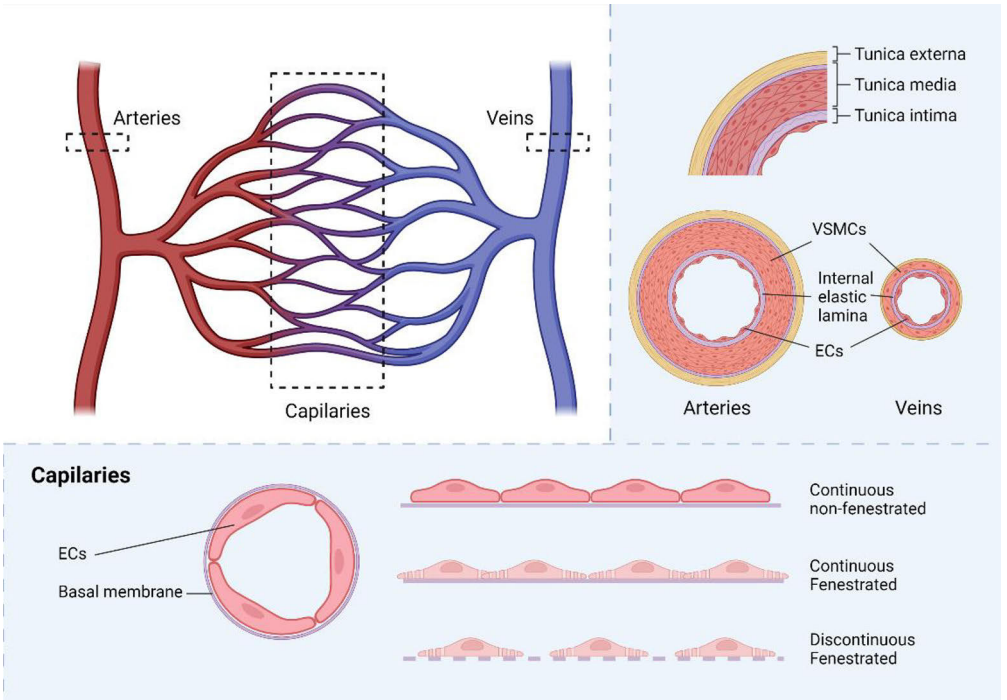

Figure 1. Schematic representation of the components of the vasculature. As blood flows from the heart, it goes through arteries towards the capillaries where transport to the tissue takes place. The blood then flows with more waste and less oxygen back to the heart via the veins. Vessels are composed of the tunica externa, tunica media and tunica intima, with different cell types

residing in each layer. Capillaries are composed of ECs and a basement membrane to allow optimum transport of nutrients, oxygen and waste. The endothelium types of capillaries differ between tissues based on their transport requirements.

1.2 Angiogenesis

In response to injury or when the demand for oxygen and nutrients and the removal of waste in tissue is greater than any short term autoregulatory mechanisms can control, there is a need to extend the vasculature[25]. As nutrient and oxygen deprived tissue becomes hypoxic, newly formed blood vessels are needed to return the local oxygen tension to a normal level[11]. Vascular endothelial growth factor (VEGF) is consequently released by the hypoxic tissue, stimulating vessels to sprout from existing vessels, a process called angiogenesis[12,13,30].

During angiogenic sprouting, one EC is first to emerge from the parent vessel and leads the sprout through the tissue to anastomose with other vessels to create a vascular loop. This first EC adopts a 'tip cell' phenotype, expressing numerous filopodia and lamellipodia, and shows a migratory and non-proliferative behavior. Behind the tip cell, 'stalk cells' follow its path. Stalk cells contain less filopodia than tip cells and have a proliferative nature. Importantly, the stalk cells form the lumen of the new blood vessel. They polarize and initiate exocytosis to adjust their shape and orientation to rearrange their junctions and open up a lumen[30]. During maturation of the vessel, the recruitment of mural cells such as VSMCs and pericytes, formation of a basement membrane and initiation of flow contribute to stabilization and remodeling towards a functional vessel[30,31]. Oxygenation of the tissue results in establishing a quiescent state of the ECs and the vessel (Figure 2). Angiogenesis is involved in several pathologies, including cancers and inflammatory, infectious, autoimmune and ischemic disorders[11].

Numerous signaling pathways are involved in the complex interplay for the regulation of angiogenesis[12,13,30]. A selection of these signaling pathways and their involvement in angiogenesis are addressed in the following sections.

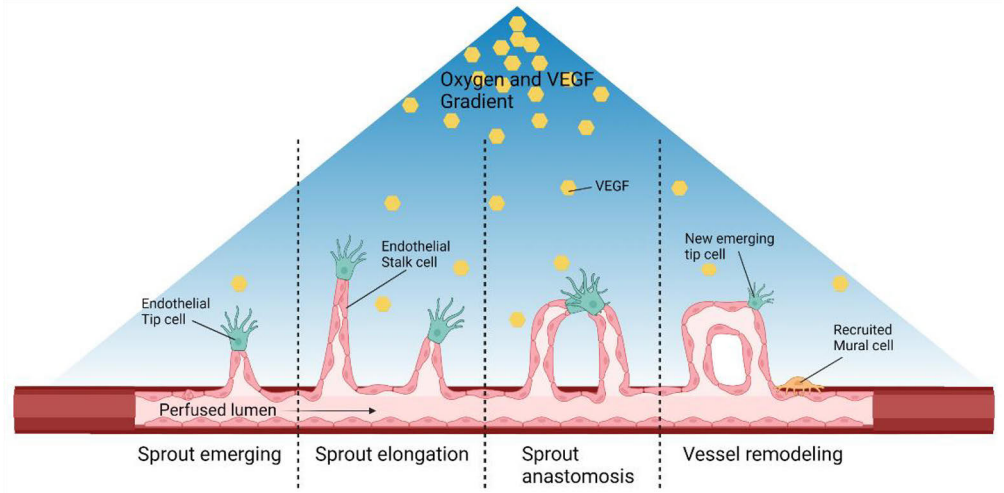

Figure 2 Schematic overview of the process of angiogenesis. Upon hypoxia, under de influence of VEGF ECs are activated and a tip cell emerges first from the vessel and migrates towards the VEGF and oxygen gradient. Proliferating stalk cells trail its path. When two tip cells meet and merge a vascular loop is formed, which by perfusion of the lumen remodels and attracts mural cells to mature the vasculature[32].

2 Engineering vasculature

The human body has limited capacity to regenerate[3]. If the tissue is damaged or diseased, tissue replacement is necessary. Long standing treatment options are the use of autografts (such as bypasses), allografts (tissues from donors), xenografts (bovine or porcine tissues) or artificial protheses (mechanical, synthetic or assist devices). However, these replacements have limited capacity to adapt and grow with the body and may require the patients to take immunosuppressive medication for the duration of their lives. Therefore, research has focused on engineering functional tissue as an alternative option for replacement therapies within the field of tissue engineering (TE)[4]. As the research field has broadened, it has included regenerative medicine, which couples multiple approaches, such as *in vitro* -, *in vivo* - and *in situ* TE and cell therapy[3]. In order for engineered tissues to be functional, vascularization of the tissue constructs is essential, as engineered constructs are mostly larger than the diffusion

limit of 200 μm[7]. Therefore, engineering of micro vasculature for the support of engineered tissues has become very important in TE.

The engineering of vasculature, both macro (TE vessels and valves) and micro (engineered vascular bed for engineered tissues) is important, though challenging. From a functional point of view, the engineered vasculature must be able to transport the needed nutrients, oxygen and waste, while withstanding the hemodynamic forces (larger vessels and valves). Additionally, the implantability of the engineered vasculature is equally important[33,34]. Not only in the engineering of vasculature, but in the engineering of multiple tissues, spatial control over cellular fate, organization and patterning has been highlighted as key to engineering functional tissues[5,6,8–10,34].

Over the years, there have been many approaches to engineer micro vasculature[5,6,8,10,33,35]. Generally, these approaches can be divided in top-down or bottom-up approaches. In top-down approaches, the focus lies on the final structure of the engineered vasculature, and the approach is chosen based on reaching the structure of the vascular network[5]. While in bottom-up approaches, the ability of the cells to self-assemble and remodel into the final vascular structure is the guiding principle[5].

2.1 Scaffold driven approaches (Top-down)

Structure-based top-down approaches have been heavily investigated and reviewed in the past couple of years[5,6,8,10,35–42]. These approaches control the organization of the vasculature by dictating the location of cell seeding, either by providing physical structures for the cells to adhere to, or by combining pre-developed endothelial tissue structures to obtain the desired geometry and organization of the engineered vasculature.

One way this is achieved is by seeding hydrogels containing ECs in channel-like structures made out of polydimethylsiloxane (PDMS), giving direct guidance to ECs to form a tube[38]. 3D printing of vascular structures is also a great option to control the organization of the engineered vasculature[5,6,8,36]. Variations include direct printing with bio ink containing live cells or printing a sacrificial material that has the capability to be removed once the whole structure is embedded in a hydrogel, to leave channels for the cells to be seeded into and provide the cells with the necessary structural guidance[39,41]. The limits of 3D printing is in its achievable dimensions, as the size of the channels are a direct result from the printing method, and for example, range between 1 mm and 200 μm[39,41] with larger hydrogel constructs around the channels and are thus not suitable for the generation of smaller vasculature.

A third option is to layer multiple cellular sheets, a “sandwich culture”, to obtain the desired vasculature structure[5,36,40]. Though rapid, this approach is limited to dictating structural organization as the absence of

scaffold material allows for remodeling of the vasculature, and is therefore more susceptible to other angiogenic factors such as hypoxia[40]. Many more approaches such as laser drilling, electrospinning and fiber disposition are used as well[5,6].

It is believed that by obtaining a highly optimized structure and organization of the engineered vasculature, the implantation into the host tissue is made easier[5,6]. However, the structural aids used are not always compatible with implantation[35]. Especially when microfluidic chips are used, the engineered vasculature is particularly developed as a model for disease research[37,43] or as a drug delivery model[37,42].

2.2 Self-organization - based approaches (Bottom-up)

Though bottom-up approaches borrow idea's from top-down approaches, the formation of the vasculature is still dictated by the cells themselves[5,36].

Generally, there are two different ways to achieve this. One is based on vasculogenesis, where ECs and a support structure, such as a hydrogel, are mixed in combination with the possible addition of stromal cells and additional growth factors, such as VEGF and Platelet-derived growth factor (PDGF). After a period of culturing a self-assembled vasculature is formed[5,44–47].

The other is based on angiogenesis, whereby top-down approaches are used to from two channels lined with ECs, which will sprout through the interlaying hydrogel or extra cellular matrix (ECM) forming a vasculature network[5,37,45,48].

The successful outcome of both approaches relies heavily on the choice of material, cells and growth factors used[9,10,36], as for example, the density of the ECM influences the angiogenic growth as the stiffness of the matrix influences neo vessel formation[49] (Figure 3). However, in terms of dimensions, the resulting engineered vasculature is noticeably smaller then in 3D printed approaches. For example Moya *et al.* achieved perfused vasculature of 15-20 µm diameter vessels[46].

There are still several limitations with these approaches, especially those relying on microfluidic chips to perfuse or initiate self-assembly of the networks[37,46], which hinders integration into native or engineered tissue. Additionally, the lack of organization of the vasculature and multiple vessels branches hinders surgical anastomosis during integration into native tissue[5].

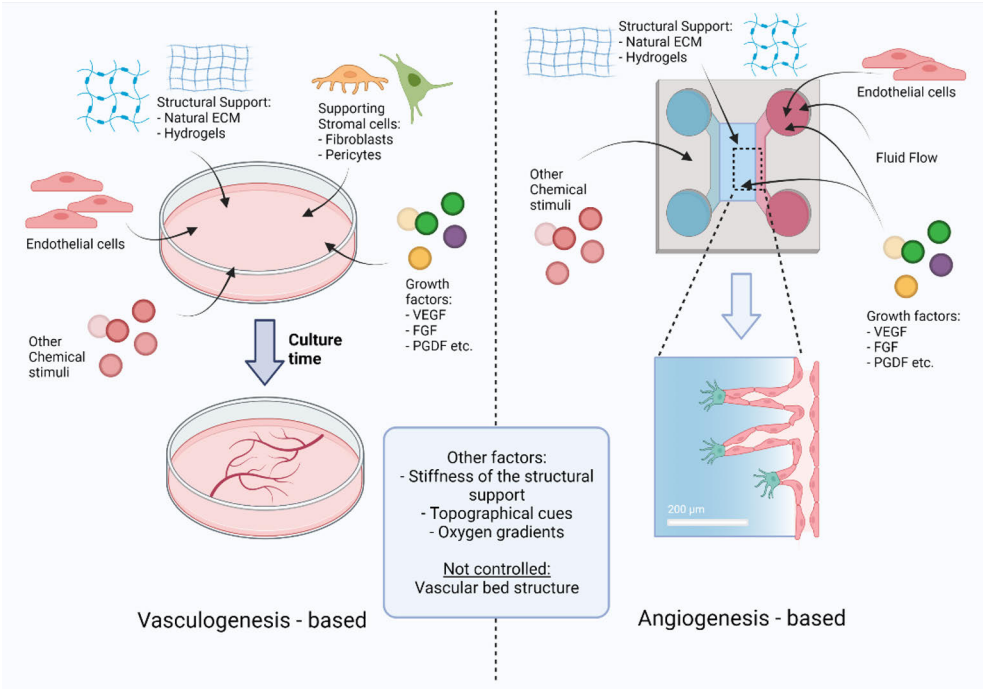

Figure 3 Schematic overview of the two main approaches in bottom-up vascular engineering and the most common factors influencing the outcome. In vasculogenesis-based approaches all factors, cells, structures and stimuli are brought together to self-assemble into an in vitro vasculature. In angiogenesis-based approaches, endothelial cells are first seeded into a tube or in a channel before stimulation with fluid flow, (oxygen) gradients and biochemical stimuli to sprout into the structural support. Both approaches do not exert spatial control over the structure of the engineered vasculature.

2.3 The missing link: inducing spatial organization in self-organized vasculature

While top-down approaches provide a highly organized vasculature, their dimensions are generally 5-20x as large than the tissue diffusion limit of 200 µm[7] which hinders their applicability for smaller tissues. Additionally, their reliance on structural scaffolds of synthetic material hinders their integration into the native tissue. Bottom-up approaches lack organization and require longer culture times.

Spatiotemporal control over the formation of vasculature has been highlighted as a key factor in engineering vasculature and angiogenesis[5,6,8–10]. To achieve spatial control, material induced patterning, for example with cell adhesive molecules and growth factors, structural patterning, such as sacrificial 3D printing materials, or direct cell patterning with cell-laden ink

have all been mentioned and investigated[8]. However, to achieve the level of organization of the top-down approaches, with the scale and integration potential of the bottom-up approaches, we will have to focus on patterning at a cellular and molecular level to manipulate the organization of self-assembled vasculatures. Therefore, more knowledge is needed about the drivers of angiogenic vascularization and vascular patterning.

Several signaling pathways driving angiogenesis have been used in the engineering of vasculature[5,9,10,36]. For example, VEGF has been extensively investigated for the induction of sprouting[50–53] and for therapeutic growth of vasculature for hind limb ischemia[54,55]. Though the VEGF loaded biomaterials enhance vascularization, it does not induce spatial and structural control.

The Notch signaling pathway, a key regulator of sprouting angiogenesis, has also been utilized to enhance micro vascularization and promote angiogenesis, via either by making use of a Notch signaling inhibitors or soluble ligands[51,54,55], which can act as decoys for the Notch receptors and inhibit Notch activation[15,56]. However, the possibility to target and activate Notch signaling to control the organization and structure of the vasculature has not been addressed.

3 The Notch signaling pathway

The Notch signaling pathway is a crucial regulator of cell fate decisions including proliferation, differentiation, and apoptosis, and orchestrates numerous important biological processes during tissue development and homeostasis as well as in disease[57,58].

The signaling pathway operates through cell-cell contact. A “sending” cell presents a Notch ligand which interacts with the “receiving” cells Notch receptor. In mammals, the Notch signaling pathway is comprised of four heterodimeric transmembrane receptors (Notch 1, 2, 3, and 4) and five ligands (Jagged (Jag) 1,2 and Delta-like ligands (Dll) 1, 3, and 4), where the relevance of the receptor-ligand pairings in a particular biological process is determined by the cell-context[59]. The ligands and the receptors contain large extracellular domains, which consist of epidermal growth factor (EGF) like repeats, which interact with each other in the extracellular space in between the cells. In general Jag ligands differ from Dll ligands by having a cysteine rich domain[15,60] as well as in the number of the EGF-like repeats and EGF-like repeats that bind calcium are only present in Jag ligands and not in Dll ligands[15,60–62]. The ligands bind to the EGF-like repeats 11-13 of the receptor, where EGF-like repeat 12 is the most crucial and all three repeats bind calcium[15,61,62]. The binding between ligand and receptor is further influenced by the presence of Fringe enzymes and O-Glycosylation of the ligand- binding region[62]. Additionally, the bond between ligand and

receptor is prolonged by the tensile forces, indicating a "catch bond" behavior[60].

Notch signaling is initiated upon receptor-ligand interactions, followed by two consecutive proteolytic cleavages (S2 and S3) on the Notch receptor, catalyzed by ADAM metalloproteinases and γ-secretase, respectively[63]. S3 cleavage releases the intracellular domain (NICD) of the Notch receptor, which translocates into the nucleus and interacts with the CSL transcription factor to drive the expression of Notch target genes[59] (Figure 4).

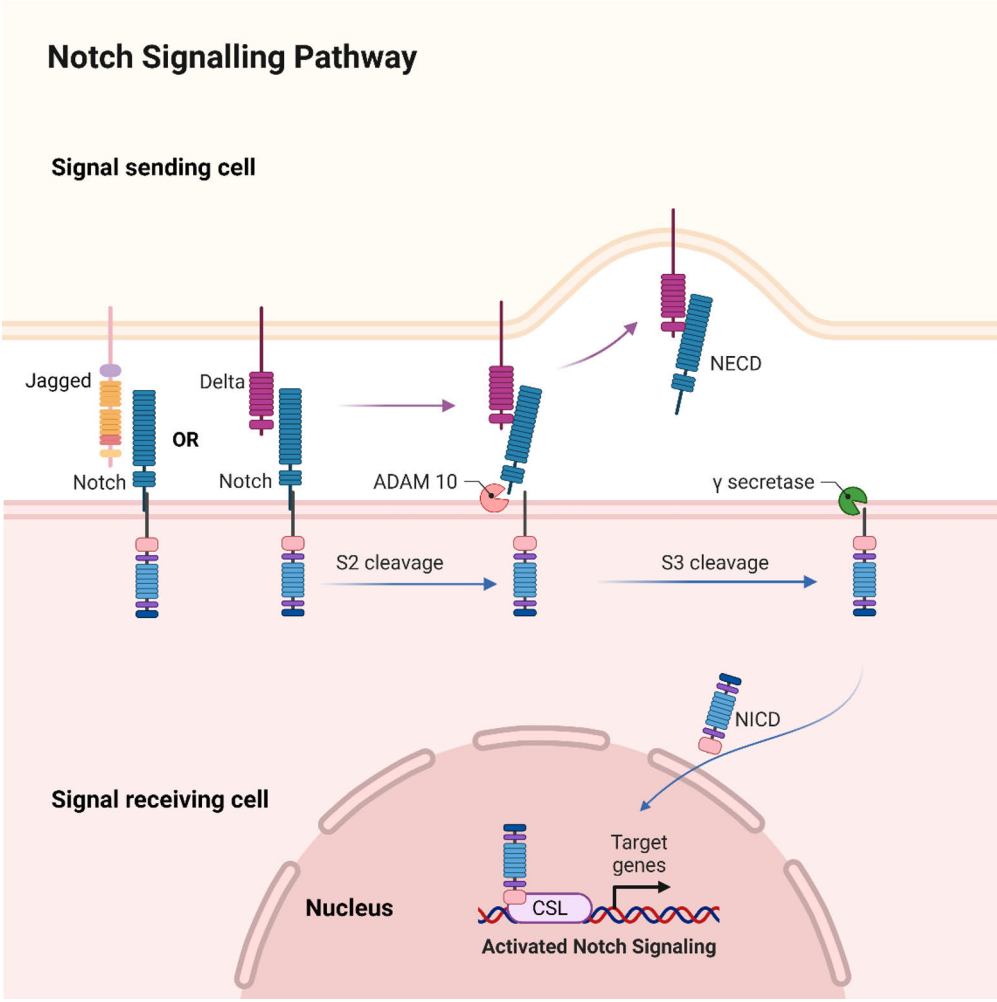

Figure 4 Simplified schematic overview of the Notch signaling pathway. Here, a Notch ligands, either a Jagged family member or Delta family member, interacts with the extra cellular domain of the Notch receptor (NECD). Upon binding, the receptor is consequently cleaved by ADAM10 and γ- secretase, and

the inter cellular domain (NICD) is transported to the nucleus of the signaling receiving cell, where it aids in the transcription of target genes. NECD bound to the ligand, is endocytosed by the signal sending cell. Adjusted from "Notch signaling pathway", by BioRender.com (2021). Retrieved from https://app.biorender.com/biorender-templates)

General target genes of the Notch pathway include Hey1 and 2, Hes1, CyclinD1 and Notch1 itself[64]. The resulting Notch signal either propagates to the next cell by promoting signal-receiver cells to express more ligands, in a process called lateral induction (Figure 5B) or prevents the propagation of the signal by repressing the expression of Notch ligands, in a process called lateral inhibition (Figure 5A). Lateral inhibition amplifies the existing sender-receiver relationship between the juxtaposed cells, resulting in different cell fates[14]. Additionally, during development, lineage decisions can be initiated, by asymmetrical inheritance of Notch regulators in daughter cells[15]. Since Notch signaling is key in cell fate decisions[14,15,65], it is not surprising that the signaling pathway is involved in stem cell maintenance and tissue morphogenesis and tissue patterning[66,67].

Non-canonical Notch signaling, independent of ligands and/or CSL, has been shown in human embryonic stem cells (hESC) to negatively regulate Wnt signaling, via active β-catenin interactions[68,69]. Another non-canonical Notch signaling process, involving the trans membrane domain (TMD), has been suggested to be involved in regulating the vascular barrier function[70].

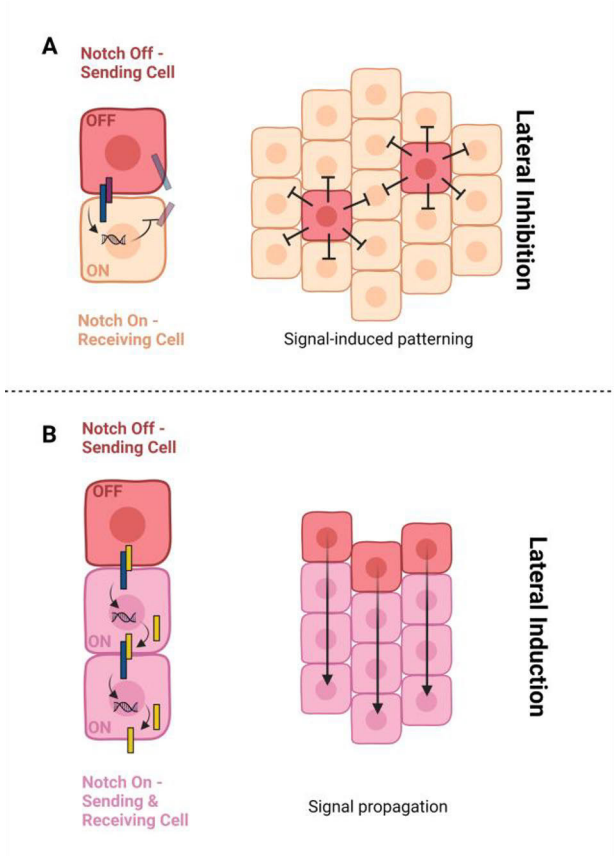

Figure 5. Schematic representation of signaling processes of lateral inhibition and lateral induction. A) In lateral inhibition the signaling cells induces notch signaling in the receiving cell, upon which the receiving cell downregulates its Notch ligands. The cell fate difference between the two cells becomes more pronounced. This process contributes to patterning of tissues. B) In lateral induction the signal receiving cells upregulates the expression of ligands, and can thus function as a sending and receiving cell, propagating the signal through layers of cells. This process contributes to tissue homeostasis[14].

3.1 Notch signaling in the vasculature

Notch signaling is a key regulator of cellular fate, via lateral inhibition, lateral induction or asymmetric cell division[14] and is therefore important in development, homeostasis and disease of the vasculature[14,71–74].

To maintain vascular homeostasis, the ligand receptor combination of Dll4/Notch1 in the endothelium and Jag/Notch2 and Notch3 in the vessel

wall are important[71]. In larger vessels, the ECs that are exposed to the blood flow, will experience flow induced shear stress, which leads to the upregulation of Jag1 and downregulation of Dll4[75,76] and reorganization of the Jag1 ligands and Notch1 receptors in the endothelial cells[75,77]. ECs presenting Jag1 ligands can subsequently communicate with VSMCs, which is required for vascular development and vessel maturation [78]. This communication is established via Jag1/Notch3 signaling[79] and contributes to the development of the multilayered VSMC wall via lateral induction[74]. The regulation of the thickness of the VSMC wall via Notch signaling is linked to hemodynamic forces [80] and to vimentin[81], which indicates several mechanosensitive roles for Notch signaling in the vasculature[77,82].

Additionally, the Notch signaling pathway can reprogram endothelial specification towards arterial over venous fates, as overexpression of Notch signaling increases arterial EC markers in venous compartments and inhibition of Notch signaling increases venous EC markers in arterial compartments[83].

3.2 Notch signaling in angiogenesis

Several signaling pathways are involved in regulating angiogenesis, including VEGF signaling and Notch signaling[12,13,84]. In ECs, several Notch receptors and ligands are expressed, including Dll1, Dll4, Jag1, Jag2, Notch1 and Notch4, alongside the key signaling components; Rbpj, Hey1, Hey2, MAML1, Numb and Nrarp[12]. Together, these components regulate several aspects of angiogenesis such as tip versus stalk differentiation, arterial versus venous specification[85], proliferation, motility, filopodia protrusion, matrix production and cell adhesion, and vessel stability and maturation[86,87]. The upstream modulators of Notch signaling in angiogenesis are hypoxic conditions and VEGF signaling[88].

Via Dll4 knock-out models and γ-secretase inhibition, it was shown that non-functional Dll4/Notch signaling in ECs enhances the number of tip cells in the vasculature, whereas inhibition of Jag1/Notch signaling resulted in a decreased number of tip cells[17]. Therefore, Dll4/Notch1 signaling between ECs was proposed to be responsible for the restriction of tip cell formation in response to VEGF, promoting an adequate ratio of tip versus stalk differentiation in ECs. Additionally, Dll4 expression in ECs is induced by VEGF signaling, resulting in a negative feedback loop with VEGF[89]. Inhibition of Dll4/Notch signaling increases vascular proliferation, while inducing defective vessel maturation, lumen formation, recruitment of mural cells and perfusion, indicating Dll4 as possible target for tumor angiogenesis[90]. Recently, it was shown that Dll4/Notch1 signaling is responsible for the generation of new coronary vessels to vascularize the expanding myocardium in late fetal development[91].

3.2.1 Notch signaling regulates tip/stalk cell differentiation

To answer the question of what the exact mechanism is for Dll4/Notch1 signaling to regulate EC differentiation into a tip or stalk cell phenotype, mechanistic models have been proposed by several research groups[12,13,84,92,93].

Generally, Dll4, Jag1 and Notch1 cooperate with VEGF signaling to dictate the ratio of tip versus stalk cells[12,13,30,93] (Figure 6). Upon binding of VEGF-A to the VEGF receptor (VEGFR) ECs upregulate the expression of Dll4[12]. The EC that expresses more Dll4 transmembrane protein than their neighbor, induces Notch signaling in the neighboring cell. The signal receiving cell adopts a stalk cell phenotype, while the sending EC adopts a tip cell phenotype. The signal receiving (stalk) cell subsequently down regulates VEGFR2 and upregulates VEGFR1. As VEGFR1 acts as a decoy for VEGF-A, signaling receiving (stalk) cells will detect less VEGF-A, and are thereby less likely to adopt a migratory cell behavior, leading to the proliferative stalk cell phenotype[17,89,94,95].

This feedback loop of Dll4/Notch1 signaling with the VEGF signaling pathway, is thought to be the prime reason for the tip/stalk cell pattern in the early stages of angiogenesis[96,97]. The pattern is dynamic, as tip and stalk cells actively compete for the positions[98]. During sprouting, several stalk cells will follow the leading tip cell towards the VEGF gradient[12].

Upon merging of a tip cell with another EC, the tip cell's transmembrane Dll4, in the junction with the stalk cell, is released, resulting in a decrease in the stalks cells Notch signaling activity, which allows for the stalk cells to adopt a tip cell phenotype[13].

3.2.2 A different role for Jag1 in angiogenesis

As stated above, ECs also express Jag1, and Jag1 appears to have a pro-angiogenic role[95,99]. Jag1 is mostly expressed in stalk cells and has a lower potential to bind to Notch1 than Dll4[95]. Jag1 has been shown to have an opposite function to Dll4 and induces tip cell formation and sprouting, by modulating the Dll4/Notch1 signaling pathway[95] (Figure 6). As Notch1 has a lower affinity for Jag1 compared to Dll4[60], Jag1 is thought to be responsible for a lower Notch1 activation in tip cells, influencing their susceptiveness to VEGF-A[95,99]. Alternatively, Jag1 has been suggested to activate Notch in order to suppress sVEGF-1/Flt-1 levels, which antagonizes VEGF-A/VEGFR2 signaling[61].

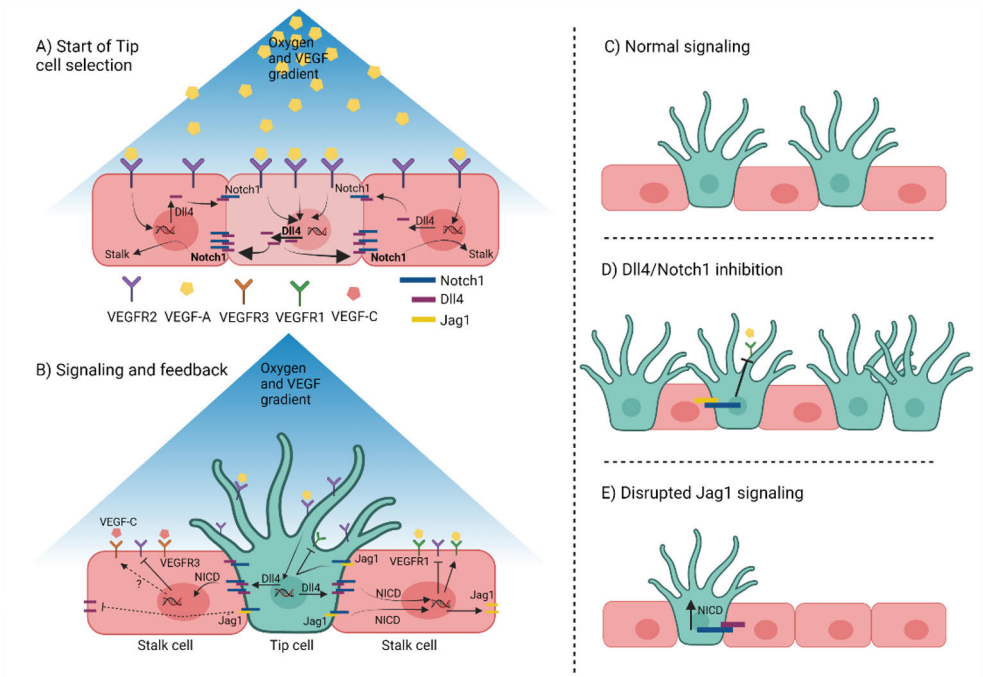

Figure 6 Schematic representation of the signaling pathways in sprouting angiogenesis. A) The selection of a tip cell is induced by the VEGF-VEGFR signaling that upregulates the expression of Dll4. The cells that presents more Dll4 than their neighbor can induce Notch signaling in that neighbor, inducing a stalk cell phenotype. B) Upon Dll4-Notch1 signaling the stalk cells will upregulate the expression of VEGFR1 acting as a decoy for VEGF-A, preventing VEGFR2-VEGF signaling and the consequent upregulation of Dll4. The role of VEGFR3 in the feedback loop is still not clear. Jag1 signaling acts as antagonist for Dll4/Notch1 signaling. C) Upon normal signaling, a salt and pepper pattern of tip and stalk cells can be observed. D) When Dll4/Notch1 signaling is inhibited, Jag1 signaling is most prominent, inducing an increase of the number of tip cells. E) Upon the disruption of Jag1 signaling, Dll4 on stalk cells is also able to induce Notch signaling in tip cells, resulting in a reduction of the number of tip cells.

3.3 Notch signaling in disease

3.3.1 Notch signaling in vascular disease

In some vascular (congenital) diseases Notch signaling is directly related to the pathology[19,20,87,100]. Mutations in the Notch3 gene leads to degeneration of VSMCs characteristic for Cerebral Autosomal-Dominant Arteriopathy with Subcortical Infarcts and Leukoencephalopathy syndrome (CADASIL). This degeneration of VSMCs is a result of the

reduction of platelet-derived growth factor (PDGF) signaling by a decrease of downstream PDGF receptor PDGFR-β[100]. The degeneration of VMSCs in CADASIL results in unstable blood vessels, causing strokes in the brain[20]. In contrast, over-expression of Notch3 causes pulmonary arterial hypertension[20].

Additionally, Notch signaling is involved in the Alagille syndrome pathology as Jag1 and Notch2 mutations lead to loss of function of specialized vascular development in tissues and organs including the kidney, liver, heart and eyes[19,20,87,101]. In humans Jag1 mutations have been found in 60-70% of the Alagille cases[87].

Though not directly related to pathology, Notch signaling is involved in the development of arteriosclerosis, as endothelial Dll4 (and debatably Dll1) interacts with macrophages' Notch1 and Notch3 receptors, promoting the pro-inflammatory M1 phenotype opposed to the immunosuppressive M2 phenotype[102].

3.3.2 Notch signaling in cardiovascular and valvular disease

A genetic mutation in the Notch1 gene, leading to loss of function of the Notch1 receptor is responsible for the development of aortic valve disease[19]. Here, the aortic valves consist of two leaflets, instead of three. Though, the disease is mostly benign, it can lead to aortic valve stenosis or hypoplastic left heart syndrome.

As Notch signaling is an important regulator of the maintenance of vasculature homeostasis, it's therapeutic application in ischemic and cardiovascular disease has been of interest[20,54,103]. For example, activation of Dll4 via mesenchymal stem cells (MSC) modified with miRNA was beneficial in the generation of functional neo-vessels after myocardial infarction (MI) in mouse models[104]. Inhibition of Dll4 after ischemia counteracts the natural upregulation of Dll4 ligands, resulting in disordered capillary sprouting, non-functional vascular interconnections, enhanced leukocyte infiltration, which all aggravate the condition[105].

In cardiac tissue regeneration and repair, Notch signaling is regarded a major player and could be used for modulation of regeneration after MI[106,107].

3.3.3 Notch signaling in cancer angiogenesis

Notch signaling is involved in multiple types of cancer, for example, brain, breast, skin, head and neck, lung colorectal, pancreatic tumors and leukemia[108]. Additionally, Notch signaling is involved in several phases of cancer, such as endothelial-to-mesenchymal transition (EMT), immunomodulation, angiogenesis, tumor growth and cancer stem cell function[108].

Tumor angiogenesis is a response to the interactions between tumor cells and ECs, growth factors and extracellular matrix components[109]. Zeng and colleagues found that in squamous cell carcinoma (SCC) Jag1 was up-

regulated, and thereby promoted and guided angiogenesis, supporting the growth of head and neck SCC tumors[110]. Growth factors like transforming growth factor-β (TGF-β) and EGF, induce Jag1 expression via MAPK activation in the tumor and therefore trigger the Notch dependent crosstalk between ECs and tumor cells.

Dll4 also participates in tumor angiogenesis and is up-regulated by VEGF secreted by tumor cells, leading to activation of Notch4, which induces abnormal vessel remodeling by up- regulating ephrinB2[111]. Another interaction exists between Dll4/Notch/TGF-β signaling, involving SMAD2/3, which results in the proliferation of lung carcinoma tumor cells (LLC1), where Dll4 presented by the tumor infiltrating myeloid cells initiates the signaling cascade[112].

Although both Jag1 and Dll4 promote tumor angiogenesis, their roles differ[113]. Dll4 overexpression decreases the number of vessels, but enhances vessel size, while Jag1 knockdown decreases the number of sprouts. Jag1 was found to enhance angiogenesis, but not via antagonizing Dll4. Jag1 induces Dll4 expression, but not as much as Dll4 does.

Based on knowledge about Dll4/Notch signaling, several anti-angiogenic pharmacological treatments have been developed, including anti-Dll4 antibodies, soluble Dll4-Fc, DNA vaccination, γ-secretase inhibitors (GSIs) and anti-Notch receptor antibodies[20,114]. The inhibition of Dll4 results in excessive but non-functional sprouting, reducing tumor growth[12]. In ongoing clinical trials, the focus lies on GSIs and ligand or receptor specific inhibition[20]. GSIs are not specific and are accompanied by severe gastrointestinal toxicity, which limits their therapeutic efficacy[20,114]. Improvement of specificity is therefore key in constraining these side effects, so ligand specific blockade of Notch signaling has been assessed[61], resulting in Notch decoys with minimal gastrointestinal toxicities. The blocking of Jag1 with decoys had an anti-tumor effect as well[61], endorsing the role of Jag1 in tumor angiogenesis.

Endothelial Notch signaling also promotes metastasis, as it was found that sustained levels of NICD in the vasculature results in pro-inflammatory and senescent ECs, while high levels of NICD in EC lead to increased expression of vascular adhesion molecule 1 (VCAM1) on the cell surface, which promotes tumor cell homing[115].

3.4 Computational models for Notch signaling in the vasculature

The mechanisms of Notch signaling for specific tissue homeostasis and organization are hard to isolate biologically, as the signaling pathway is involved in processes widespread throughout the (human) body. Additionally, the biological effects are ligand- and receptor-specific and complex cross talks with other signaling pathways exist.

In sillico computational models aid in unraveling the mechanisms and dynamics of Notch signaling by focusing on- and isolating single phenomena, while neglecting systemic changes. Therefore, they can be a valuable tool to study molecular mechanisms of Notch signaling as well as genetic disorders caused by mutations in members of the Notch signaling pathway in CVD[116].

The model proposed by Boareto *et al.* (2015)[117] which is based on the cis- and trans-signaling of Jag and Delta with the Notch receptor determines cell fate into a sender, receiver and a sender/receiver hybrid cellular phenotype based on the protein levels of ligand and receptor in the cells. This model was used as a basis for another model that explored the lateral induction in VSMCs in the blood vessel walls[80,118]. Here, the modeled thickness of the vascular wall depended on the genetic input of levels of Notch signaling components influenced by *in vitro* applied mechanical strain, highlighting the importance of hemodynamic forces on Notch signaling and vascular homeostasis[80,81].

Later, this model was developed further to include cellular connectivity in a 2D setting, revealing that the influence of cellular connectivity was inferior the Notch signaling dynamics of lateral induction[118]. Cellular connectivity is shown to be of influence in another computational model, which reveals the contact-area dependence for cell fate patterning in lateral inhibition[119].

These examples highlight the new insights gained with the application of computational models for unraveling Notch signaling dynamics.

3.4.1 Computational models describing Notch signaling in angiogenesis

The process of angiogenesis is a complex process, which restricts computational modeling of angiogenesis from including all mechanisms regulating angiogenesis. Therefore, different computational models describing angiogenesis have been focusing on different aspects of angiogenesis, based on the research questions behind the developed model[120]. For example, some models which focus on the progression of the vascular tree as influenced by VEGF gradients, chemical guidance and hypoxia have neglected Notch signaling[121,122]. Others, focused on the initial tip-stalk cell selection have not focused on gradients or cellular processes such as the formation of filopodia[123,124]. However, computational combination of both Notch signaling and movement based on chemo-, hapto-, duro- or mechanical taxis is achievable[96,125].

An agent-based model which includes the VEGF feedback loop with Dll4/Notch1 signaling with VEGF gradients and filopodia[96], is the basis for multiple studies which elucidate several aspects of angiogenesis. Examples are the role of VE-Cadherin and tight junctions in the dynamics of tip/stalk cells selection[97], the formation of hybrid tip/stalk cell phenotypes and the

dynamics of tip/stalk cell selection[126], the role of temporal dynamics of vascular patterning in angiogenesis[127] and the requirement of filopodia for timely development of the tip and stalk cell pattern[124].

The role of Jag1 in the VEGF – Dll4/Notch1 signaling feedback loop has been mostly ignored and seldom incorporated in angiogenic computational models[123,125] despite several observations on the importance of Jagged in angiogenesis. Computational models that did include Jag1 observed that an increased expression of Jag1 leads to pathological vasculature[125], and overexpression of Jag1 is responsible for a hybrid tip/stalk cell phenotype[123]. The latter finding is in agreement with experimental results where Jag1 was demonstrated to act as antagonist for Dll4/Notch1 signaling[95,128].

In sum, computational models shed light on several different aspects of angiogenesis, and can therefore aid in unraveling complex Notch signaling dynamics during endothelial sprouting.

4 Modulating Notch signaling with biomaterial approaches

As the Notch signaling pathway has such wide spread functions throughout the body, as well as being involved in several pathologies[129], targeting of the Notch signaling pathway is of interest for therapeutic, regenerative and tissue engineering applications as well as tissue morphogenesis[130] (details on approaches for tissue patterning and morphogenesis can be found in Tiemeijer & Sanlidag *et al.* (2022), not included in this thesis). However, conventional targeting by the use of pathway interfering molecules to inhibit signaling is inadequate for precise control over tissue pattering. Activation by use of traditional co-culture systems provide poor specificity and give rise to unrelated cellular responses[131] in addition to their limited relevance for applications outside the research lab.

Active molecules such as recombinant Notch ligands, ligand-mimicking peptides, receptor agonist/antagonist or inhibitory antibodies, and small molecules modulating receptor processing, such as ADAM and γ-secretase inhibitors, are used mainly in soluble form to manipulate Notch signaling[20,132–136]. Though effective in the lab, the use of these molecules in soluble form for other applications is limited. This is due to two reasons:

1) Activation of the Notch receptors requires ligands to be surface bound. Soluble ligand function as decoys and compete with membrane-bound ligands, which causes Notch signaling inhibition instead of activation[20,136].

2) Spatial and temporal precision of Notch signaling modulation is needed to dictate cell fate without unwanted side effects in surrounding tissues, as Notch-mediated regulation of cell fate is stage- and context- dependent, with cellular outcomes dependent on the amplitude and waveform of the NICD signal[137–142].

Therefore, in order to spatially activate Notch signaling and better understand the biology of Notch signaling in the control of cell fate for regenerative and therapeutic approaches functional platforms that can mimic the membrane-dependent receptor-ligand interactions and selectively modulate Notch activity are needed[130].

4.1 Design considerations of Notch functionalization of biomaterials

Biomaterials functionalized with Notch signaling regulators have been developed in the last couple of decades, targeting numerous tissues and multi-cell processes, such as the immune system[23,143–153], dental tissue[24,154–157], epithelial tissue[150,158–160], cardiac tissue[131,161,162], cancer[114,137,138,163] and stem cells[161,164] (Table 1).

Based on the application, Notch-functionalized materials allow either activation or inhibition of Notch signaling. Materials that inhibit Notch signaling can serve as tools for site-specific delivery of soluble molecules that interfere with Notch signaling. Materials that activate Notch signaling utilize immobilized ligands and or receptors to substitute native cell-cell interactions with controlled targeting of cell fate. Due to the complex tandem of spatiotemporally controlled physical and biochemical phenomena in the native Notch activation process, functionalization of materials with Notch ligands is less straightforward than with structural biomolecules, such as ECM proteins.

*Table 1 Overview of studies of Notch ligand functionalized biomaterials and their respective target tissues. ¥ = no specification of ligand indentity was mentioned. * = Peptide was included in the study. Table adjusted from* [130].

Ligand	Cell/Tissue Type	References	Notes
Dll1	Muscle	22,165	
	Immune/Blood	23,143,146,148,149,166,167	
	Dental	168	
	Cardiac/Stem cells	161	
	-	169	
Dll4	Hepatic	170	
	Reporter cells,	171	
	Immune/Blood	151,152	
	Cancer/HeLa	172	
	Endothelial	173	
Delta¥	Reporter cells	174	
Jagged1	Immune/Blood	144,153,175	
	Epithelial,	150,158–160*	* peptide
	Dental	24,154–157	
	Muscle,	165	
	Cardiac	131, 162*	* peptide
	Reporter cells, Stem cells	164, 135,176,177*	* peptide
	Bone	178	
	Hepatic	140	
Inhibition	Cancer	137,179	DAPT
	Hepatic/Pancreas	180	Dibenzazepine
	Immune/Blood	181	SiRNA
	Cancer	163	Notch1 antibody

The method used for ligand immobilization should minimally change ligand bioactivity, while successfully tethering the ligands to the material surface. Therefore, in the design of the Notch functionalized biomaterial the following considerations should be made:

1) Correct ligand presentation and orientation, to ensure ligand recognition at the receptors side[144,153,158,161],

2) The lateral mobility and clustering of the ligands, which affects the ability to activate the Notch receptor[20,171],

3) Ligand affinity and the cellular pulling forces required for S2 cleavage,

4) Other factors, including lipid binding on the receptor-ligand complex, post-translational modifications, and Ca^{+2} binding on the Notch extracellular domain (NECD), which fine-tune the activation criteria for distinct ligand-receptor pairs[182,183],

Additionally, immobilization of ligands to the material surface in a spatially well-defined manner can be an important engineering tool for spatiotemporal control over the Notch signaling[130].

4.1.2 Immobilization techniques

Generally, the three most used approaches of functionalizing Notch ligands to materials in the past are direct immobilization by physical adsorption, direct immobilization by crosslinking or covalent binding to the material, and indirect immobilization via a docking molecule, which exploits the strong affinity of the dock molecule to the (recombinant) Notch ligand, for example IgG/Fc pairs (Figure 7).

Based on the different approaches, different important design criteria are met. For example, indirect immobilization via protein A/Fc lead to increased functional orientation of Jag1 on glass to stimulate hematopoietic stem cell (HSC) proliferation[153]. The Notch inducing efficiency of peptides mimicking the highly conserved DSL domain instead of full length (recombinant) ligands, also depend on the choice of immobilization approach in specific material applications. For example, while covalent binding of Jag1 peptides at culture surfaces appears successful for inducing myogenic differentiation[162], the processing of Jag1 peptides into supramolecular scaffolds proves less successful in inducing Notch signaling than coating with the full length protein[135].

However, the variation of approaches and outcomes leaves room for tailored spatiotemporal control over cell fate. For example, micropatterning of ligands for controlled differentiation of stem cells towards liver progenitors[170], or controlled proliferation of HSCs[148]. In addition, spatiotemporal control over stem cell differentiation can be achieved by photochemically regulated Notch ligand presentation in hydrogels[140,184]. The divers and specific tailoring of the incorporation of Notch ligands into materials allows for locally dictating cell fate, by either inducing or inhibiting signaling and is therefore a useful tool for tissue engineering[130].

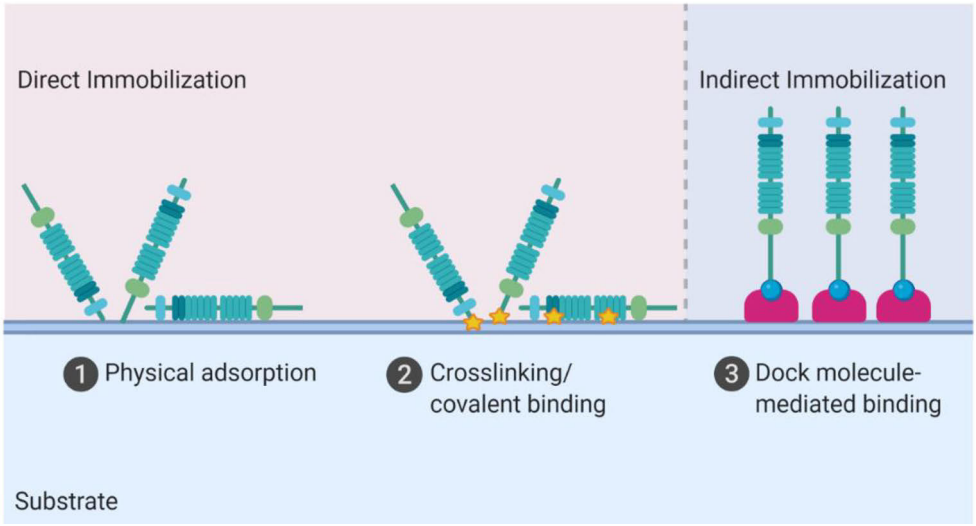

Figure 7 Current immobilization approaches for Notch ligands: Two most common approaches for the immobilization techniques of Notch ligands are direct immobilization and indirect immobilization. Direct immobilization can either be by 1) Physical adsorption of the ligand on the substrate or 2) Crosslinking or covalent binding of the ligand to the substrate. Both approaches have limited control over ligand orientation. 3) In indirect immobilization a secondary dock molecule, such as protein G/A or Streptavidin, is attached to the substrate, while the strong affinity between the dock molecule and the (recombinant/modified) ligand ensures more control over orientation of the ligand. Image courtesy of Sami Sanlidag, with permission.

4.2 Modulating Notch signaling in Angiogenesis

As Notch signaling is an important cell fate determinant in angiogenesis, the therapeutic application of Notch signaling for targeting cancer angiogenesis has been extensively explored[20]. Generally, targeting Notch activity via soluble molecules, such as antibodies targeting the Notch1 receptor[185], Dll4[186,187] or Jag1, with more specific decoys[61] or peptides[56,188], have been investigated previously with a common goal to disrupt functional angiogenesis and cause tumor starvation and hypoxia, leading to necrosis of the tumor. However, the systemic administration of the soluble molecules can be unsafe, therefore, balancing toxicity and efficacy is highly important[21].

The use of Notch signaling ligands in biomaterials to stimulate angiogenesis, has not been extensively studied. Such an approach potentially opens doors for vascularization and regeneration of ischemic tissues, and can be used to stimulate and control vascularization of engineered tissues. Indirect modulation of Notch signaling with

biomaterials has been utilized to induce tissue healing via Notch mediated angiogenesis[189]. Here, poly (lactic-co-glycolic acid) (PLGA) particles loaded with tazarotene promoted deep tissue wound repair via activation of the VEGF/VEGFR and Notch1/Dll4 signaling pathways in angiogenesis. Additionally, a combination of VEGF and the γ-secretase inhibitor DAPT in an injectable hydrogel induced endothelial cell proliferation, migration and sprouting in 2D and 3D cultures, as well as improved blood vessel density and tissue perfusion in hind limb ischemia in diabetic mice[54]. In myocardial repair, injection of a hydrogel containing a peptide mimic of Jag1 improved cardiac function and increased the endothelial vessel density in infarcted rat hearts[190].

While spatiotemporal control has been highlighted as a key factor in biomaterial modulation and stimulation of angiogenesis[52], and has been applied using spatial placement of growth factors for vascularization of bone[191], spatiotemporal control over Notch ligands to control angiogenesis has not yet been investigated.

This is surprising, as Notch signaling is highly local-, context depended-, and its cell fate dictating- potential provides the excellent opportunity to spatially dictate cell fate. Spatial control of Notch activity has the capability to control initiation of angiogenesis and the organization of the vasculature.

Outline and key aims of the thesis

A functional micro vasculature is essential for transport of oxygen, nutrients and the removal of waste in tissues larger than 200 μm[7,11]. Therefore, engineering vasculature is imperative for successful regenerative medicine[6,8–10,192,193]. The current protocols for vascular engineering lack either methods for spatial and structural control over new engineered vasculature or have limitations in the integration of the vasculature with native or engineered tissues[35].

Through angiogenesis, new micro vasculature is created via endothelial sprouting from existing vessels[11,30]. This process is regulated by cell signaling pathways, such as Notch[12,13,30,84,194]. Notch is also involved in several (cardio) vascular pathologies and cancer angiogenesis[19,106,114,129,195–197]. During angiogenesis, the migratory tip cells containing filopodia lead endothelial cells towards the oxygen gradient, while the proliferating stalk cells follow. In this highly dynamic process[126,198–201], Notch signaling is a critical regulator of tip or stalk cell specification[17,89]. The Notch pathway thus provides a potential therapeutic handle to spatially regulate endothelial cell fate and sprouting[14], and thereby controls the organization and structure of the (micro) vasculature.

In this thesis we explore the possibilities of using patterns of Notch signaling ligands to provide spatial control over endothelial sprouting and elucidate the underlying mechanisms of ligand-mediated control of sprouting angiogenesis.

The obtained knowledge might aid in the design of biomaterials for engineered vasculature and regenerative medicine and help the development of future therapeutic strategies for cancer angiogenesis and cardiovascular pathologies.

The key aims of this thesis are:

- To investigate the possibility to spatially control endothelial sprouting by distinct patterns of the Notch ligands Jag1 and Dll4.

- To gain mechanistic insight in the ligand-mediated control of endothelial sprouting.

Experimental Procedures

More information and additional protocols regarding materials and methods can be found in the original articles (study I and II). An overview of all methods used can be found in Table 2.

Additional material and methods:

Human endothelial cell culture

Human Umbilical Vein Endothelial Cells (HUVECs) (Lonza, pooled) were cultured in Endothelial Cell Base Media 2 (Promocell) with addition of the supplement pack endothelial cell GM2 (Promocell) with final concentrations of 0.02 ml/ml Fetal Calf Serum (FCS), 5 ng/ml human recombinant Epidermal Growth Factor (hEGF), 10 ng/ml human recombinant basic Fibroblast Growth Factor (hbFGF), 20 ng/ml human recombinant Insulin-like Growth Factor (R3-IGF-1), 0.5 ng/ml human recombinant Vascular Endothelial Growth Factor 165 (VEGF), 1 µg/ml ascorbic acid, 22.5 µg/ml heparin, and 0.2 µg/ml hydrocortisone and was supplemented with additional 1% penicillin/streptomycin. Cell culture flasks were coated with 0.1% gelatin (Porcine, Sigma) before culture in 37 °C, 5% CO_2. Cells with passage numbers of 3-6 were used for the experiments.

Thick gel method for endothelial sprouting

Pre-cooled 48 wells plate and 200 µl pipets tips were kept on ice, and coated with 150 µl/well of Corning® Matrigel (growth factor reduced). After a 10 min incubation period at room temperature, the Matrigel was left to set at 37 °C 5% CO_2 for 30 min. HUVECs in media were seeded on top of the gels at density of 60.000 cells/well. They were cultured for 48 hours before fixating with formalin, permeabilized with 0,5% triton X-100 and stained with fluorescent probes for the cytoskeleton (Phalloidin) and nuclei (DAPI). They were stored topped with PBS at 5 °C until use of the microscope.

Endothelial alignment under flow

HUVECs of 800.000/ml in warm media at 5% CO_2 were seeded into Ibidi µ-Slide I Luer and cultured at 37 °C, 5% CO_2 until confluency. Next, they were attached to the Ibidi flow pump and a flow of 1 Pa was performed for 18 hours. The alignment of the cells along one direction was observed with the help of the CytoSMART Lux2 at 37 °C, 5% CO_2, and the direction was analyzed with Directionality Plugin of Image J.

Preparation of micro contact printing ink containing Notch ligands

50 µl (10 µg/ml) of active human Dll4 protein fragment ab108557 (Abcam) or 4.3 µl (200 µg/ml) of recombinant human Jagged1/fc chimera (R&D systems) or 0.2 µl (2.2mg/ml) ChromePure human IgG Fc fragment(Jackson Immuno Research) was incubated with 100 µl (0.1% w/v) protein G fluorescent particles (Spherotech, purple, 0.4–0.6 µm) overnight at 5 °C or 1 hour at RT resulting in µCP ink with a maximum of 0.5 µg of Dll4 ligand immobilized to the beads per sample or its molar% equivalents of Jagged1 and fc fragments.

Micro contact printed lines of ligands for non-confined cell culture conditions

Before inking the µCP stamps with 150 µl Dll4 mixture or 105 µl Jag1 / Fc mixture, the stamps were made hydrophilic by treatment with atmospheric plasma for 9 s (Corona Discharge Generator, Tantec HF). µCP stamps and ink were incubated for 30 min at room temperature and dried using N_2 gas prior to printing in sterile 6 well plates. The µCP stamps were left to adhere to the glass for 30 min at room temperature before removal in one swift stroke. The wells were coated with 1 ml of 1% gelatin solution and incubated for 10 min 37 °C, 5% CO_2, before careful removal of the gelatin. HUVECs were seeded at 75.000 or 300.000 cells per well and left to adhere for 2 hours before addition of 15% Matrigel in 3 ml of media. After 24-hour culture at 37 °C, 5% CO_2 the cells were fixated for 30 min with formalin, permeabilized with 0.5% triton X-100 and stained with the fluorescent probes for cytoskeleton (phalloidin) and nuclei (DAPI). Washing buffer used was PBS, and this was also used as storage buffer (at 5 °C) before imaging.

Confined cell seeding using inserts

Inserts were placed on top of µCP lines of ligands in 12 well plates with sterile tweezers. Ideal orientation of the cross section of the inserts was an angle of 90° with the lines. 100 µl of 0.1% gelatin in PBS was added to each well of the insert and was incubated for 10 min at 37 °C before excess fluid was removed. 100 µl of 262.000 cells/ml was seeded in each well of the two diagonally facing wells of the insert. The HUVECs were cultured for 1-3 hours at 37 °C, 5% CO_2 until adhered. Inserts were removed with sterile tweezers, and additional 20 v% Matrigel was added in 800µl media, and the cells were left to sprout for 24 hours at 37 °C, 5% CO_2, until fixation and fluorescent staining.

Confined cell seeding using micro fluidic channels

Microfluidic channels were placed on the printed glass slides orientated perpendicular to the ligand functionalized lines and gently pressed to contact the substrate and seal the microchannels. Sterile P200 pipette tips (without filter) were placed in the inlets of the channels as fluidic reservoirs that allowed feeding of the system by gravity. The channels were coated with 1% gelatin in PBS, pipetted in one of the tips, for 5 min at 37 °C, 5% CO_2, followed by careful flushing out of the gelatin solution with prewarmed media (18 h at 37 °C, 5% CO_2). Removal of air bubbles was done by careful up and down pipetting, to wriggle the bubbles loose, and careful suction to remove completely. HUVECs in prewarmed media ($5*10^6$ cells/ml) were seeded directly via the pipette tips and were left to adhere for approx. 2.5 hour at 37 °C, 5% CO_2 monitoring against cell aggregates and ensuring sufficient flow through the channels. After adherence the channels were cautiously taken off the glass slides, and Matrigel®matrix (15% in total amount of media, growth factor reduced, Corning; lotnr. 00034014) was placed on top of the HUVECs, after setting shortly followed by remaining media. The HUVECs were left to sprout unconfined for 24 h in 37 °C, 5% CO_2, until fixation and fluorescent staining.

qPCR

The Notch signaling inducing potential of the µCP ink was verified with qPCR. 12-well plates were homogenously coated with 50 µl ink-mixture (bead-Fc, bead-Dll4, bead-Jag1) per well, topped with 0.1% gelatin in PBS, and seeded with 10^5 HUVECs/well. After cell adherence, 15-20 v% of Matrigel®matrix (corning, growth factor reduced, lot nr. 00034014) was added on top to mimic the previous experimental conditions. After 24h the cells were washed with PBS and harvested in RLT Buffer (RNeasy Kit, Qiagen) before overnight freezing in -80 °C. Further RNA extraction was done with the RNeasy Kit (Qiagen) according to manufacturer's instructions. RNA was stored at -30 ° C before cDNA synthesis. 100ng RNA per sample was used to synthesize cDNA. cDNA (0.5ng per well) was amplified using primers (Table 3.) for the Notch gene family including Dll4, Jag1, Notch1, Notch4, Hey1 and Hey2; The VEGF receptor family including FLT1 (VEGFR1, KDR (VEGFR2) and FLT4 (VEGFR3) and the target genes EphrinB2 and PTEN; and reference gene B2M (PrimerDesign) using the iQ Thermal cycler (BioRad). iQ SYBR Green (BioRad) was used as fluorescent dye. N=6 per condition. Non-parametric ANOVA (Kruskal-Wallis) with Dunns multiple comparison was used as a statistical test.

Anti-fouling treatment for cell adherence test's

24-wells plates with sterilized coverslips were coated with 230ul of 0.5; 0.05; 0.02 w/v% PEG-PLL (Sigma) in PBS, or 0.1% gelatin or nothing. After 30 min incubation at room temperature, excess fluid was removed, and the sample were left to dry for 5 min at room temperature. 20.000 HUVECs in 1 ml EBM2+ media (Lonza) were seeded per sample (n=3). Cells were left to adhere and incubate overnight at 37 °C, 5% CO_2 for 23h before 15 min fixation with 3.7% formaldehyde in PBS to obtain samples for fluorescent staining. Permeabilization of the samples was done with 0.5% triton X-100 in PBS for 15 min. PBS was used as washing buffer. To show the cytoskeleton Phalloidin (Atto488) was used and DAPI as a marker for the nuclei. Three representative images per sample were made using the Zeiss Axiovert 200M. Analysis was done by counting the number of (spread) cells and cell aggregates per representative image. A 1-way ANOVA with a Dunett's multiple comparisons test was performed to check the statistical significance of the results.

Photo-patterning using the Alvéole PRIMO

Patterning of the ligand-bead mixture as similar to the μCP ink using the Alvéole PRIMO was based on the protocol of Melero *et al*. 2019[202] which is based on light-induced molecular adsorption (LIAMP) as published by Strale *et al.* 2016[203]. In short, a pattern is designed using the maximum of 1824 pixels length and 1140 pixels width, corresponding to several lines of 100 μm wide with 100μm spacing. The culture surface is sterilized and activated by plasma treatment, before passivation with 500 mg/mL poly-l-lysine (PLL) for 30 min and consequent washing with HEPES buffer (0.1 M (pH 8-8.5)). To complete passivation the surface was incubated with 100 μl of 50 mg/ml mPEG-SVA in HEPES buffer for 1 hour, avoiding drying of the surface, and washed with- and stored in PBS up to 3 days. To pattern, 50 μl of the photo initiator [4- benzoylbenzyl-trimethylammonium chloride (PLPP), Alvéole), was added to the passivated surface, before UV light projection with power of 7,5 mW/mm^2 at a dose of 1000 mJ/mm^2 was directed with the Leonardo software (Alvéole) to remove the passivation agent. Additional washing with PBS was performed before the addition of the ligand-bead mixture. A second UV light projection is then applied to remove the remaining PEG-PLL outside of the patterning side.

For dual patterning, this latter part was skipped and the surface was additionally blocked with BSA, before the second pattern was applied to remove the passivation agent, washed with PBS and addition of the other ligand-bead mixture. After extensive washing with PBS, the patterned surfaces were stored in PBS at 4°C overnight until cell seeding the next day. To visualize the different ligand inks for dual patterning beads with different fluorescent spectra were used, namely Spherotech protein G

fluorescent particles Purple, 0.4–0.6 µm and Spherotech protein G fluorescent particles Yellow, 0.4–0.6 µm.

Tabel 2 Methods. Methods applied in the studies of this thesis. Indication of the studies refers to either the result section of this thesis (R) or the published articles (I and II).

Method	**Study**
Alvéole PRIMO Photo Patterning	R
Cell Culture	R, I, II
Computational modeling	II
Directionallity	R, I, II
Fluorescent stainings	R, I, II
IBIDI culture inserts for scratch assay	R
IBIDI culture system for flow	R
Image Analysis	R, I, II
Micro contact printing	R, I, II
Micro fluidic cell seeding	R, I, II
Microscopy	R, I, II
PDMS stamp and channel fabrication	R, I, II
quantative reverse transcription PCR	R, I, II
Statistical Analysis	R, I, II
Thick gel method for EC sprouting	R

Tabel 3 Primers. Overview of the genes used for qPCR in this thesis. The primer sequences are given for both forward as reverse primer sequence. Indication of the studies refers to either the result section of this thesis (R) or the published articles (I and II).

	Gene	Forward Primer	Reverse Primer	Study
Notch Family	Dll4	CCTCTCCAACTGCCCTTCAAT	GCGATCTTGCTGATGAGTGC	R
	Jag1	AATGGCTACCGGTGTGTCTG	CCCATGGTGATGCAAGGTCT	R and II
	Notch1	CCTGAAGAACGGGGCTAACA	GATGTCCCGGTTGGCAAAGT	R
	Notch4	TGCCAGCCCAAGCAGATATGTA	CCAACCCACGTCACACACAC	R
	Hey1	TGGATCACCTGAAAATGCTG	CGAAATCCCAAACTCCGATA	R
	Hey2	TTTGAAGATGCTTCAGGCAA	GGCACTCTCGGAATCCTATG	R
VEGFR family	VEGFR1 (FLT1)	CAAATAAGCACACCACGCCC	CGCCTTACGGAAGCTCTCTT	R and I
	VEGFR2 (KDR)	CGGTCAACAAAGTCGGGAGA	CAGTGCACCACAAAGACACG	R and I
	VEGFR3 (FLT4)	TGAGAGACGGCACAAGGATG	CTCCACCAGCTCCGAGAATG	R and I
Target	EphrinB2	CTGCTGGGGTGTTTTGATGG	GTACCAGTCCTTGTCCAGGTAG	R and I
	PTEN	CCTCAGCCGTTACCTGTGTG	AGGTTTCCTCTGGTCCTGGTAT	R
Reference	BM2	Primer design		R
	ACTB	Primer design		R and I

Results and Discussion

1 Patterning of recombinant Notch ligands for morphogenic control of angiogenesis

1.1 Practical considerations concerning the optimization of controlled endothelial sprouting in vitro

During our work to develop and design a material-based method to control endothelial sprouting in vitro, several aspects of the handling and techniques needed to be optimized. Here we list some focus points and learning experiences for future reference to take into consideration in the design of future experiments.

1.1.1 Verification of endothelial phenotype

In order to manipulate cell fate of EC towards a tip or stalk cell phenotype, it is important to verify if the ECs used for the experiments still possess an EC phenotype. Here, we used human umbilical vein endothelial cells (HUVECs), which have been widely used to study angiogenesis[204,205]. These cells can either be isolated from umbilical cords by researchers themselves[206] or bought from cell suppliers. We choose for the latter option, as this gave us the option to choose pooled HUVECs from donors of different sex and race, to eliminate intra-donor differences[207].

HUVECs are primary cells and can still lose phenotype upon prolonged culture. For example, in endothelial-to-mesenchymal transition (EMT) ECs loose specific endothelial markers such as VEGFR, VE-cadherin, Von Willebrand factor (VWF) and PECAM in addition to the upregulation of mesenchymal markers such as α-smooth muscle actin (α-SMA), vimentin and N-Cadherin. This process is influenced by several signaling pathways, including Notch signaling and TGF-β signaling, and physiological stressors such as shear stress, hypoxia and oxygenation[208,209]. The first passages of HUVECs normally express all endothelial markers[210] but it is imperative to verify that the sequential passages of HUVECs still possess the functional characteristics of EC.

To check whether the HUVECs possessed to ability to form sprouts when cultured on a gel membrane[210,211], we seeded the HUVECs (P1) on a layer of Matrigel. After 24h of culture we observed that the cells expressed sprouting behavior (Figure 8A and B). As ECs should respond to shear stress by aligning themselves to the flow direction[77,212], we sequentially used microfluidic slides to expose the HUVECs to flows of 1 Pa. We observed a gradual alignment of the HUVECs over time between 0-17h (Figure 8C-F), indicating a flow responding phenotype in the HUVECs. Thus, we concluded that the batch of HUVECs, at the very minimum was suitable for functional

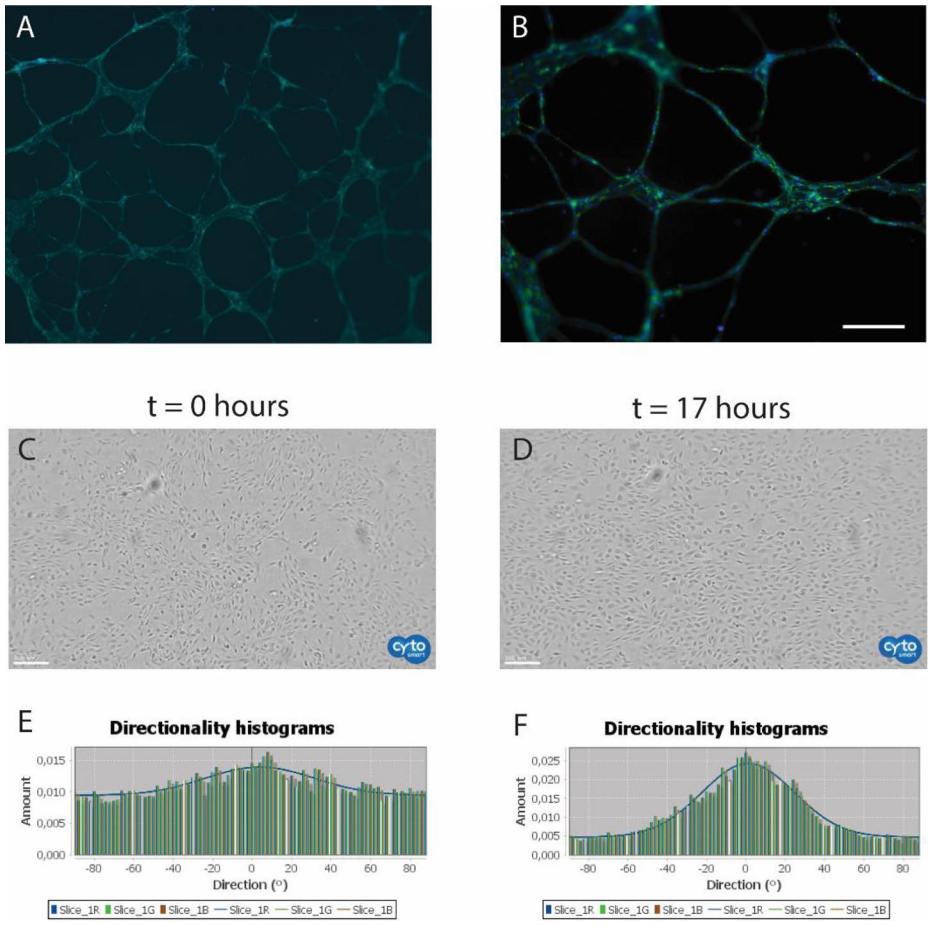

Figure 8 Investigation of HUVEC phenotype. A) HUVECs seeded on top of Matrigel and cultured for 24 hours showed sprouting behavior. Magnification 5x. B) HUVECs seeded op top of Matrigel and cultured for 24 hours showed sprouting behavior. Nuclei in Blue, actin cytoskeleton in green. Magnification 10x. Scalebar represents 100 µm. C) Morphology of HUVECs seeded in Ibidi flow slide on t = 0 hours, show a cobblestone morphology and no preferred alignment. D) HUVECs in Ibidi flow slide on t =17 hours show cobblestone morphology and increased alignment. Images are stills of a CytoSmart based movie. Scalebar represents 200 µm. E) Directionality plugin acquired histogram of average directions based on the still for t = 0 hours. There is no clear preferred direction. F) Histogram of average directions based on the still from t = 17 hours. There is a clear preferred direction of 0 degrees, which corresponds with the direction of the flow through the slides with a magnitude of 1 Pa. n = 1 for Ibidi flow slide analysis.

angiogenesis assays, such as our setup, and was able to reproduce the aligning of the cells upon shear stress as was previously investigated by members of our group[212,213]. Therefore, for the experiments in this thesis, we used HUVECs with passage numbers 3-6 mostly to ensure EC phenotype. The HUVECs were discarded after passage number 7-8.

1.1.2 Practical considerations for micro contact printing patterns of Notch ligands

To achieve spatial patterns of recombinant Notch ligands, we choose to use micro contact printing (μCP). This is a soft-lithography technique based on the use of patterned PDMS stamps, that are made by casting PDMS on top of silicon based masters[214,215]. These masters are the topographical negative of the PDMS stamp and are made with UV light penetrating masks to pattern the photoresist on top of the silicon wafer (Figure 9A and B). The master wafers can be used multiple times to produce larger quantities of PDMS stamps. However, over time, due to frequent use, wafers may lose sharpness and definition of their features.

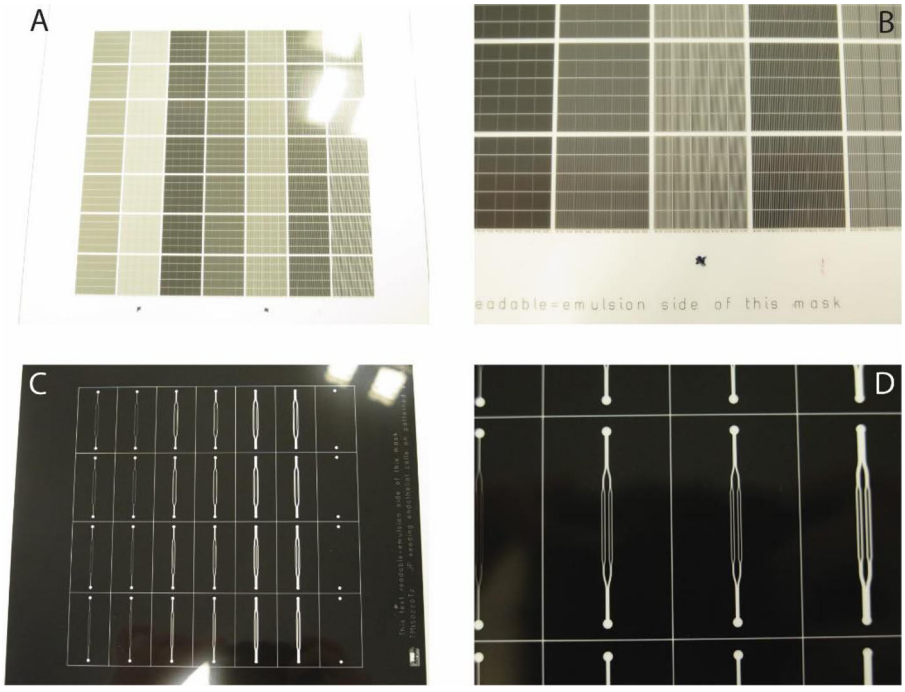

Figure 9 Photographs of the masks used for soft lithography-based creation of PDMS μCP stamps and PDMS micro fluidic channels. A) Overview of the mask for μCP stamps, which offers various sizes of patterns. These ranges as arrays of 100 μm wide lines spaced by 30, 50, and 100 μm or 200 μm wide lines spaced

by 100 and 200 µm, from which we choose 2 as preferred sizes (pen marking). These were line patterns of width 50 µm and spacing of 100 µm and line patterns of width 100 µm and spacing of 100 µm. B) Zoomed in image of the mask with pen markings for line patterns of width 100 µm and spacing of 100 µm. C) Overview of the mask for micro fluidic channels of various sizes. Variation in channel width was 50, 100 and 300 µm for the four subchannels, and variation in spacing between the two sub channels of a main channel and the main channels was 150 and 300 µm and 500- 1000 µm respectively. D) Zoomed in image of the micro fluidic channels which were most frequently used. Those contained channels of 100 and 300 µm width and the largest spacing between sub channels.

As the quality of the line pattern of immobilized Notch ligand is directly related to the quality of the µCP process, it is important to inspect the quality of the stamps and wafers, especially after longer periods of use. Figure 10 shows a comparison of the PDMS stamps produced with the same master wafers after a period of time (approx. 200 times used). Some areas of the master wafers were not able to produce sharp PDMS stamps anymore (Figure 10 bottom row), while other areas still had the definition and sharpness needed for µCP (Figure 10 top and middle row). This illustrates the importance of reviewing the used wafers regularly, and selecting the µCP stamps in the PDMS accordingly, based on local quality of the features.

Alternative to well-published µCP based *in vitro* patterning, where cells were patterned on anti-fouling layers by use of µCP anchoring proteins, such as RGD or ECM proteins[214,216–218], in our design we choose not to use anti-fouling agents. This is due to the need for the ECs to have complete freedom to migrate in any direction they prefer in order to investigate the directionality of endothelial sprouting. Therefore, the contact between the underlayer of glass slides and µCP ink and adhesive capabilities between those two influence the quality of the µCP lines. Consequently, the µCP ink was labelled by a fluorescent agent, to visualize the µCP lines and assess their quality. Additional selection of regions of interest (ROIs) with strict criteria were used to only select areas with lines with sufficient quality.

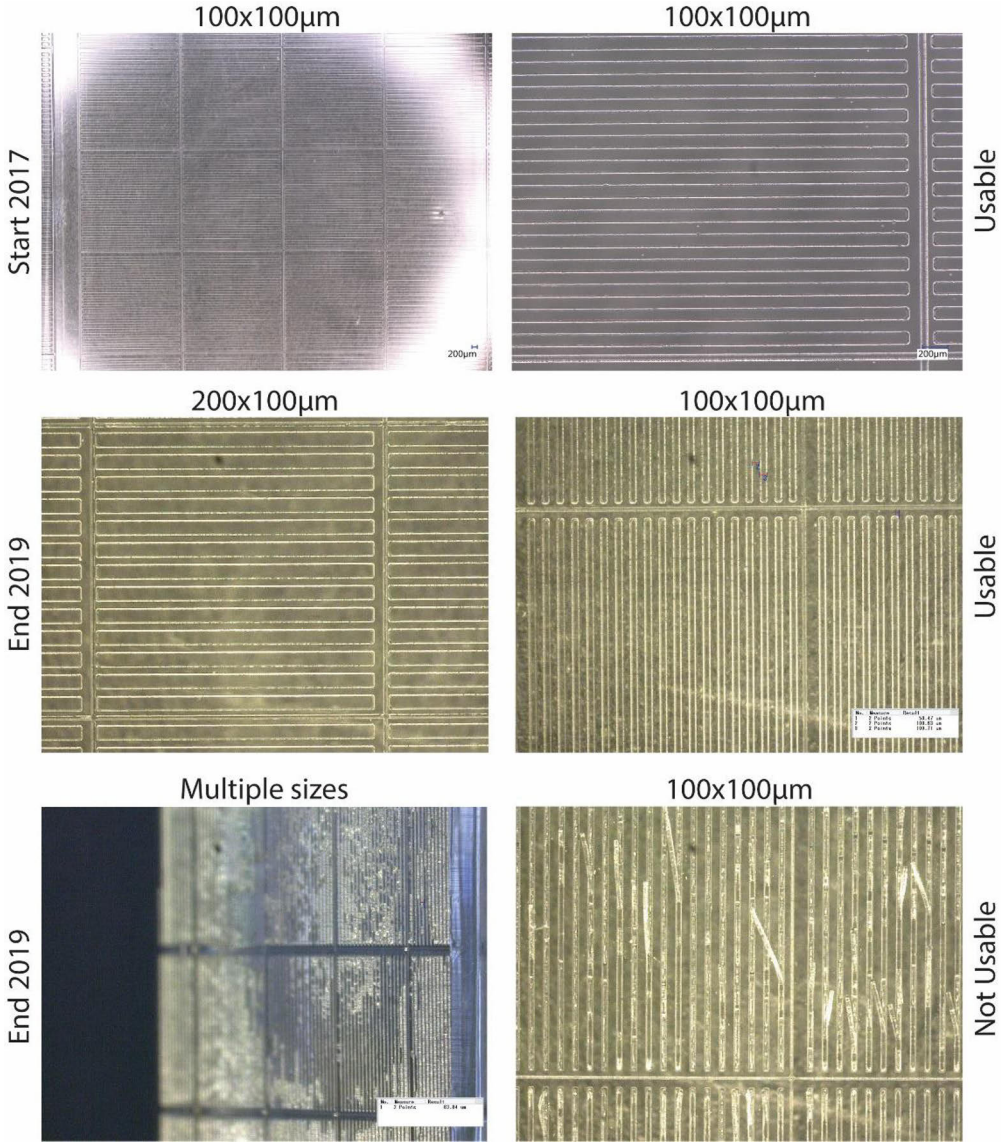

Figure 10 PDMS stamps for µCP. Images of µCP stamps created from the master wavers at the start of the project (top row), and after more than two year of use from the same master wavers (middle and bottom row). The width of the lines and spacing in between the lines are stated above the image. Though the older master wavers still produced adequate PDMS µCP stamps (middle row), some master wavers and spots on those wavers were thus damaged by multiple use, that it could not produce adequate µCP stamps anymore (bottom row). Careful selection of the areas of the adequate regions of the PDMS and cutting of the µCP stamps were required.

1.1.3 Sprouting orientation does not follow μCP patterns of Notch ligands in unconfined cultures of ECs

To verify the requisite of confined EC seeding for inducing spatial control over endothelial sprouting, we seeded EC homogenously in different concentrations on top of μCP lines of Notch ligand in cell culture plates with wells of 9,5 cm^2. After 24h culture and sprouting, the samples were fixed and stained with fluorescent probes for the actin cytoskeleton (phalloidin, green) and nuclei (DAPI, blue) (Figure 11). The ECs seeded at the lower concentration (75.000 per well) did not appear to respond to the μCP lines of Notch ligands (Figure 11 top half). ECs seeded at the higher concentration (300.000 per well) did appear to respond to the printed lines, as they appeared to favor adhering to the area on top of the lines (Figure 11 bottom half).

To quantify differences in sprouting direction we looked at the dispersion parameter using the Image J plugin "directionality" which provides the broadness of the graph fitted to the histogram of average directions, based on the phalloidin staining. No difference was found between samples of the different Notch ligands lines, or even between samples of μCP lines without Notch ligand and sample without μCP lines at all (Figure 11 bottom graph, n=1).

We concluded that homogenously seeded ECs do not respond to spatial patterns of Notch ligands, which indicates that in approaches for engineering vasculature based on vasculogenesis[44–46], exposure to spatial patterns of Notch ligands would not be enough to spatially guide endothelial sprouting. Additionally, we might speculate that the exposure of established vascular beds *in vivo* and/or *in vitro* to spatial patterns of Notch ligands, would similarly not be sufficient to spatially direct the vasculature. We therefore deduct that spatially guiding endothelial sprouting with spatial patterns of Notch ligands, will be possible only at onset of endothelial sprouting, when the selection of endothelial phenotype into tip or stalk cells occurs.

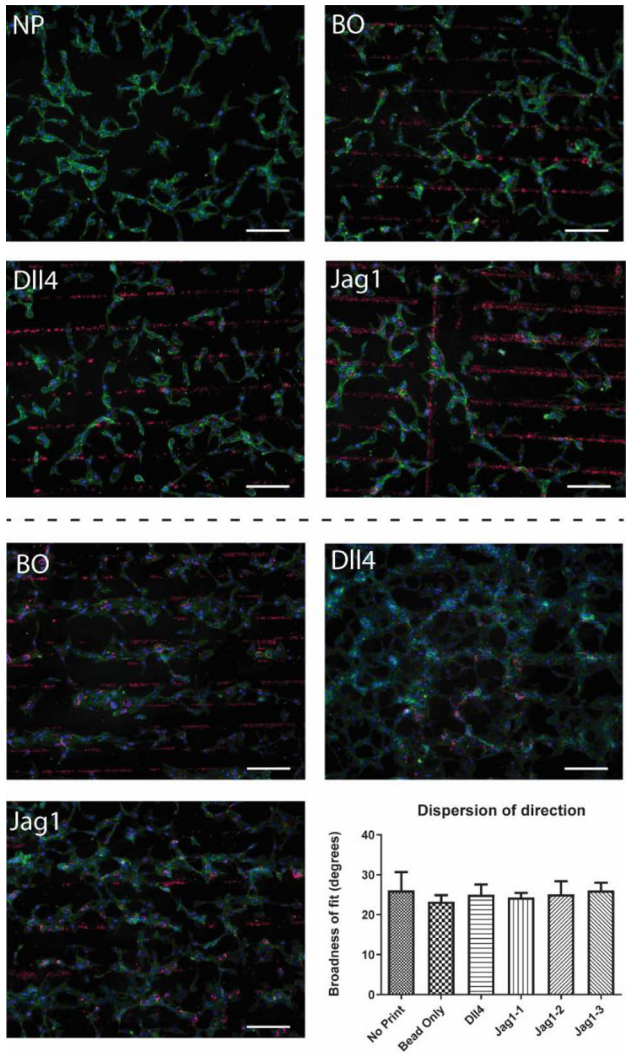

Figure 11 Homogenous seeding of HUVECs on μCP lines does not indicate direction manipulation. Top half of the figure contains fluorescently stained homogenous seeding of HUVECs on top of no lines (NP), Bead-only (BO), Bead-Dll4 lines (Dll4) and bead-Jag1 lines (Jag1). Cellular density was 75.000 cells per well. The HUVEC do not appear to recognize or change their behavior in response to the lines. Bottom half of the figure contains fluorescently stained homogenous seeding of HUVECs with cell density of 300.000 cells per well. The HUVECs appear to respond to the μCP lines. Fluorescent probes are green for the Cytoskeleton and Blue for the Nuclei. Scalebar represents 100μm. The graph represents the dispersion analysis of the samples with a cell density of 300.000 cells per well, using the directionality plugin. Here we observe no difference in dispersion between sample conditions, indication that there is no difference in

efficiency to orient to a preferred direction, between conditions. One experiment, N=4/5 respectively for each sample. Images without clear lines were not included.

1.1.4 The confined seeding method allows for spatial control of endothelial sprouting *in vitro*

We investigated two methods to ensure confined seeding of the ECs. First, we seeded the EC through PDMS microfluidic channels of different sizes (Figure 9C and D). As the ECs are directly seeded on top the μCP lines, containing the signaling ligands, there is no time for establishing a confluent monolayer. A better method that allows for an immediate mimic of the *in vivo* situation is necessary. The use of micro fluidic channels mimics the *in vivo* situation by ensuring high density seeding in a vessel-like fashion. However, seeding of higher concentrations of EC into narrow channels, may lead to occlusions and air bubbles (Figure 12A-C), which severely decreases the through put of the method. Therefore, there was a need to investigate possible alternatives.

Next, we tested Ibidi scratch assay inserts as an alternative, as these consist of 4 open wells with two crossing borders in the middle, which allowed for a gap of 500 μm between two wells and 1000 μm between the four wells in the center of the insert. The rationale was that these gaps would allow for endothelial sprouting and the open well concept would increase the ease of EC seeding, due to decreased possibility of creating air bubbles of clogging of cells due to easy and direct pipetting into the wells. These inserts contained a sticky layer underneath to prevent fluid from leaking at the border of two wells. Additionally, the size of the inserts (17 mm) allowed for the use of cell culture plates, thereby increasing the trough-put. However, the inserts did not increase the efficiency of the method, as hardly any endothelial sprouting could be observed in the gap between the wells. Possible due to the sticky nature of the inserts, the μCP lines between wells were removed upon insert removal (figure 12 D and E). To provide areas in the sample without ECs where "vascularization" was necessary, as well as leave more room for endothelial sprouting, we switched between the seeding of all four wells to just the seeding of two wells. Though, the two well seeded inserts were more comparable to micro fluidic channels than the four wells seeded inserts, switching did not improve the amount of sprouting observed formed the insert-seeded areas.

In both methods we used media containing a constant concentration VEGF, which is an important stimulator of endothelial sprouting[89,199]. It should be noted that the local concentration of VEGF per area of the sample may have differed, based on the geometry of the cell seeding area (long channels vs roundish inserts), and geometry of the cell culture container (long rectangle vs round wells), which may have influenced the sprouting

capability of the ECs. However, we did not observe areas in samples of both seeding methods where we did not have sprouting of healthy cells.

In summary, we acknowledge the advantages and disadvantages of both cell seeding methods and conclude that the micro fluidic channels which mimic the *in vivo* situation most, provide the best circumstances for successful spatial control over endothelial sprouting, even though their efficiency and through-put is limited.

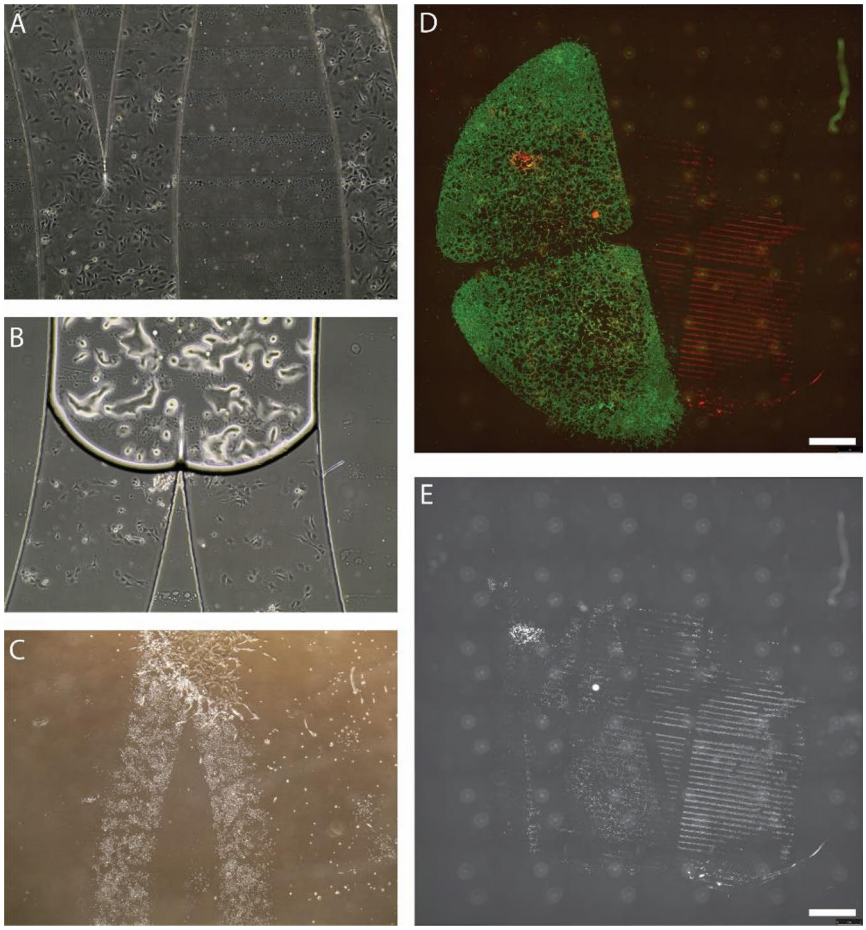

Figure 12 Representative images of seeding of HUVECs using micro fluidic channels or Ibidi scratch assay inserts. A) Bright field imaged pf seeded HUVECs after 2 hours of incubation, right before removal of the channels. The HUVECs look adhered and though not a complete monolayer, the density is sufficient. B) Air bubble appeared after 2 hours of incubation, blocking the cell culture media inlet of the channel and damaging the cells directly below. Removal of the air bubble at this moment in time, will damage the HUVECs around it. C) Representative image of HUVECs after overnight incubation after channel

removal. HUVECs that were damaged by either oxygen and nutrient deprivation during channels seeding caused by either occlusion of cells or air bubbles, perished, while cells directly before occlusion or bubbles survived and sprouted. D) Fluorescent image of HUVECs seeded with the Ibidi inserts sprouted on top of μCP lines of ligand (red). At the left borders of the seeded area, no sprouting can be observed, while in between the two seeded wells, some sprouting is visible, however the μCP lines are not clear there. Green represents the cytoskeleton E) the μCP lines underneath the cells from D, show that at the border of the wells the lines are removed, and underneath the cells the lines are hard to detect. Scale bar represents 2 mm.

2 Patterns of Dll4 spatially control endothelial sprouting

In study I[173], we looked into the potential of Dll4 patterning to control endothelial sprouting. To achieve patterned Dll4 lines, we used micro contact printing (μCP) of fluorescent beads, to which recombinant human Dll4 was immobilized via IgG-Fc affinity binding. To be able to control the seeding of ECs to mimic blood vessels, we used micro fluidic channels to seed HUVECs. We investigated the ability of the Dll4 in the μCP mixture to induce Notch signaling and used immunofluorescence to visualize the effects of the patterns of Dll4 on the sprouting HUVECs.

2.1 Notch signaling is induced by immobilized Dll4

To ensure that the Dll4 in the μCP mixture was able to induce Notch signaling activity, we performed qPCR analyses on all the following experimental conditions; no mixture, bead-only and bead-Dll4, in addition to treating all conditions with the γ-secretase inhibitor DAPT and its vehicle DMSO. Samples consisted of HUVECs seeded without spatial confinement on top of a homogenous coating of the μCP mixture, to ensure enough sample material. Additionally, the choice for a homogenous coating of the μCP mixture instead of patterns eliminates the noise in the signal from HUVECs not exposed to the μCP mixture.

We analyzed fold changes of the three VEGFR genes, and the Notch target gene EFBN2[87] (Study I, Figure 3 and Figure 13). We observed a distinct effect of DAPT treatment on the expression levels of EFBN2 and VEGFR3 (Study I, Figure 3), indicating the gene expression response to Notch signaling, but not in the expression levels of VEGFR2 and VEGFR1 (Figure 13). Furthermore, we observed an increase in gene expression levels of EFBN2 when comparing untreated bead-only and bead-Dll4 conditions, indicating that the immobilization of Dll4 to the beads in the μCP mixture induces Notch signaling activity. We observed the same trends in the gene expression of VEGFR3, though this is was not confirmed statistically. We did not find differences in gene expression levels for VEGFR1 and VEGFR2 (Figure 13).

Current literature indicates that VEGFR1 acts as a decoy to take VEGF-A signaling away from VEGFR2[98,219], while VEGFR2-VEGF-A signaling is responsible for the upregulation of Dll4 in ECs[12,98]. Based on these observations, we would expect an increase in VEGFR1 expression and decrease in VEGFR2 expression when HUVECs are exposed to Bead-Dll4.

However, contradictory findings have been reported where in retinal tip cells VEGFR2 was not essential for Dll4 expression, and Dll4-Notch1 signaling did not down regulate VEGFR2[220]. The function of VEGFR3 during the Dll4/Notch1/VEGF crosstalk in angiogenesis is less clear[98]. Notch

appears to regulate expression of VEGFR3 independently of VEGFR2 signaling[220]. Dll4/Notch1 signaling has been shown to downregulate VEGFR3 expression[221] and in the absence of- or low- Notch signaling, VEGFR3 allows for abnormal angiogenesis[220,221]. In contrast, other reports have found that Notch signaling upregulates VEGFR3 expression, which increases the responsiveness of HUVECs to VEGF-C, and upregulates EFBN2[222]. In turn, EFBN2 modulates angiogenesis by regulation of the internalization of VEGFR3 and VEGFR2[223]. It must be noted that VEGFR3 is mainly expressed in lymphatic endothelium[98,221], and during post-natal angiogenesis[221], as well as recently discovered in late fetal coronary plexus at the ventricular inner myocardium[91], therefore, it not surprising to find VEGFR3 expressed in HUVECs[222].

In sum, we observed context-dependent VEGF/Notch signaling[199], indicating that VEGFR3 regulated angiogenesis might be induced in our system. Additionally, we must note, that here we stimulated the HUVECs with bead-Dll4 homogenously, and not in a spatial pattern, which allows all cells to adjust gene expression to the stimulus, smoothing out the response and restrict us from detecting the cell specific expression normally occurring during angiogenesis. Further, we harvested after 24 hours, which leaves time for the cells to produce more or less mRNA than during their initial response to Dll4 activation. Furthermore, computational modeling has highlighted the importance of Dll4 expression fluctuations in individual cells for normal angiogenic sprouting[224], indicating a role for time dependent expression of Notch components during angiogenesis.

2.2 Microfabrication techniques allow for patterning of Dll4

To pattern lines of Dll4 we used μCP, where "ink" is stamped on a surface in the pattern of the stamp. The stamps were made from PDMS and consisted of lines of 100 μm wide with 100μm spacing or lines of 100 μm wide with 50 μm spacing (Study I, Figure 2A and B). The use of μCP directly on glass slides allowed for the patterning of Dll4 without the use of antifouling agents. The advantage was that this allowed ECs to freely migrate and sprout without physical or chemical restrictions, filtering out those factors from the resulting cellular behavior. Additionally, restricted seeding, by use of reversible microfluidic channels, allowed for a patterned HUVEC monolayer mimicking a larger capillary. Study I, Figure 2C and 2D shows the channel designs and dimensions used in this study, 300 μm and 150 μm wide channels respectively. The use of Matrigel on top, provided the structural ECM for the HUVECs to form sprouts.

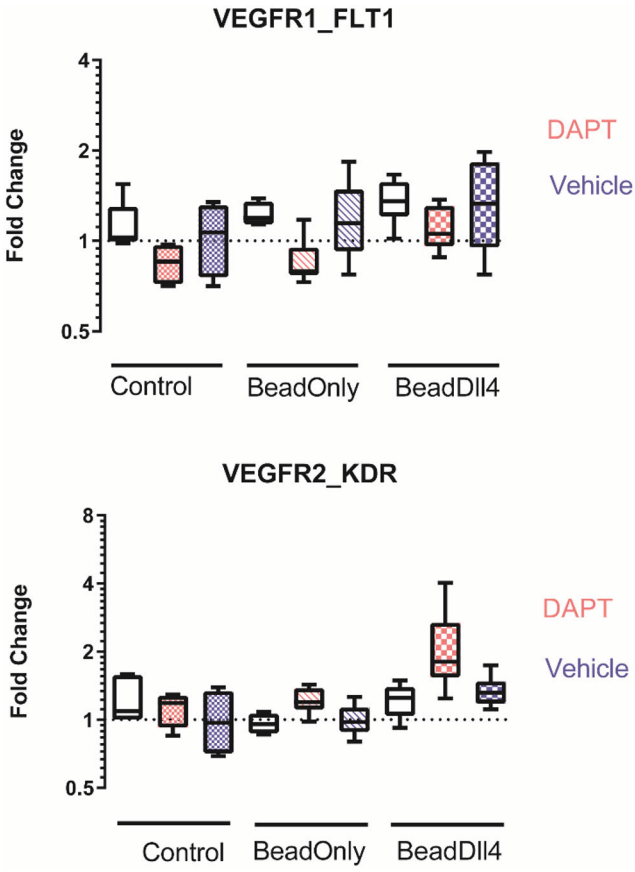

Figure 13 Gene expression levels of FLT1 (VEGFR1, top) and KDR (VEGFR2, bottom) in HUVECs (Control), stimulated with µCP ink without Dll4 (Bead-only) and with Dll4 (Bead-Dll4) after 24 hours. Per condition, untreated (in white), treated with the Notch inhibitor DAPT (in Pink) and treated with vehicle only (DMSO, in blue) where analyzed. Though significant gene expression differences could not be observed for both VEGFRs, trends in increased VEGFR1 expression could be observed between the different conditions for each treatment, while treatment with DAPT suggests a decrease in gene expression level of VEGFR1 per condition. For the gene expression of VEGFR2, it appears that upon inhibition of Notch signaling VEGFR2 is up regulated, which is most prominent in the stimulation with Bead-Dll4.

As the combination of µCP and microfluidic seeding of the HUVECs required many manual handling steps, the need arose to strictly define Regions of Interest (ROI), to ensure quality of the image analysis afterwards. The ROIs were defined as areas where clearly visible lines could be observed either in the area where the HUVECs were seeded or directly adjacent. Additionally, ROIs required sufficiently seeded and adhered

HUVECs in the seeded area, to mimic vessel lining, and those HUVECs sprouted outside of the seeded area. One ROI consisted of the area direct adjacent to the seeded area, that contained one line and one area in between the line, of the same size. With manual handling steps in the method, the samples were prone to mistakes and inconsistencies, which could be filtered out by the strict criteria of the ROI.

We calculated that a maximum amount 0.5 µg of Dll4 immobilized to the beads, per sample, could be achieved. This amount of ligand, has been found sufficient to activate Notch signaling in previous experiments performed by members of our group[225,226]. Regarding the immobilization of the Bead-Dll4, by using an indirect immobilization technique based on IgG-Fc affinity bonds, we assumed that correct orientation of the ligands are presented to the HUVECs, as has been shown previously with indirect immobilization with a docking molecule[227]. Additional fixation of the Bead-Dll4 ink was achieved by gelatin coating of the glass after µCP, making it improbable that the Bead mixture would be transferred after seeding of the HUVECs.

Taken together, we believe that our method of immobilization and patterning of Dll4 can locally restrict Dll4-Notch1 signaling and could be used to spatially stimulate cell-fate decisions.

2.3 Lines of Dll4 stimulate spatial patterning of endothelial sprouts

To assess the effects of spatial Dll4 patterns on sprouting behavior of HUVECs, the samples were fixed after 24h of culture and immunofluorescently stained. In Study I, Figure 4 representative images of the samples of the three experimental conditions used are shown. In NoPrint, the ECs were seeded via the micro fluidic channels, but were not exposed to any µCP lines. In Bead-only the ECs were exposed to µCP lines of the bead-mixture without Dll4 functionalization. In Bead-Dll4, the ECs were exposed to µCP lines with Dll4 functionalization. The samples were stained for the actin cytoskeleton and the nuclei, while the beads pre-possessed their fluorescent ability.

We observed small sprouts in the samples without any lines (Study I, Figure 4, top row), while we observed larger sprouts in the samples with µCP lines of beads only (Study I, Figure 4, middle row), which did not prefer any direction. However, we observed the largest, highly directional sprouts in the samples with µCP lines containing Dll4 (Study I, Figure 4, bottom row). Here, the sprouts appeared to originate from the area in between the lines, indicating that the tip cell leading the sprout started sprouting from that area. Additionally, the sprouts in the samples with µCP lines containing Dll4, could anastomose with the sprouts originating from the opposite channel seeded area (Study I, Supplementary Figure 1).

Related to the dimensions of the μCP stamped Dll4 lines, the endothelial cells were observed to form sprouts from most non-Dll4 line areas. Therefore the distance between sprouts was within the 100-200 μm range, which is physiologically relevant considering the need to overcome the diffusion limit of 200 μm with engineered micro vasculature[7].

Taken together, this data suggests the possibility of spatially controlling a HUVEC-based vessel bed with spatially patterned Dll4 ligands.

2.4 Lines of Dll4 spatially restrict endothelial sprouting

To quantify the amount of control the μCP lines of Dll4 had over the endothelial sprouting, compared to the control condition bead-only, we calculated a parameter we called the efficiency of controlled sprouting (Ecs) for every ROI (Study I, Equation 1). This parameter produces a percentage of the number of cells that reside in between the μCP lines. When the cells reside exclusively in between the lines, the equation produces a percentage of 100%, while Ecs = 0% corresponds to the case where cells reside exclusively on the lines, also called negative patterning and positive patterning respectively.

Four samples were analyzed resulting in a total of 89 ROIs for bead-only and 229 ROIs for bead-Dll4. We observed a clear difference between the control bead-only value of Ecs = 54.5 ± 3.1% (Mean ± SD) and all the Bead-Dll4 values of (A) Ecs = 95 ± 0.9%, (B) Ecs = 81.2 ± 2.4% and (C) Ecs = 74.9 ± 2.6% (Study I, Figure 5). The average Ecs value of the Bead-Dll4 samples was found to be Ecs = 84.7 ± 1.86%, while there were some significant differences between the Bead-Dll4 samples themselves (Study I, Supplementary Figure 3). Therefore, we checked for a possible difference between samples of Dll4-line induced proliferation in the seeded areas, to eliminate its effect on sprouting control (Study I, Supplementary Figure 2). There was no difference in the number of cells in the seeded areas between the samples.

Taken together, our data shows that Dll4 lines locally inhibit endothelial sprouts on the Dll4 μCP lines, driving them to sprout in between the μCP lines, thereby negatively patterning endothelial sprouting.

2.5 Lines of Dll4 induce unidirectional sprouting

As we observed that the sprouts in the samples with μCP lines of Dll4 very clearly preferred one direction, the next step was to quantify this using the Directionality plugin of ImageJ. The plugin returns a histogram of directions per image on which a graph is fitted. From the graph the average direction and dispersion are given as parameters, together with a parameter representing the goodness of the fit on the histogram.

While no clear difference was found between the average direction of the unprinted and the Bead-Dll4 μCP line samples (Study I, Supplementary

Figure 4), there was a difference between one of the Bead-Dll4 samples and the Bead only. However, not all three Bead-Dll4 samples were different. Therefore, we looked at the original histograms, dispersion and fit correctness of the samples (Study I, Figure 6). The dispersion was significantly reduced compared with the unprinted condition and the fit correctness was significantly increased upon μCP lines with Dll4 (Study I, Figure 6A and B). The histograms of all the conditions confirm the hypothesis that upon μCP lines with Dll4, the ECs are more prone to sprout unidirectionally and in parallel to the μCP lines (Study I, Figure 6C-D). While the histograms corresponding to the control unprinted and bead-only conditions show a more random choice in average direction. This suggests that the Dll4 in the lines induces the direction and orientation of the endothelial sprouts.

2.6 Implications of controlling sprouting *in vitro* with spatial patterns of Dll4.

In study I, we were first to show that immobilization of Dll4 in a spatial fashion could be applied to control vascular tissue patterning. In study I, we see a direct relation between the addition of Dll4 to the μCP line pattern, and the outcomes of unidirectional sprouting and increased control over sprout location.

Based on findings from literature, where dose sensitivity of Notch signaling can determine cell fate[14,228], and the size of the contact area between cells influences the Notch signaling strength[119,229], we believe that controlled dose and location, here represented by the μCP lines, induce endothelial cell fate. We suggest that local Dll4 signaling, by means of the μCP lines induces a stalk cell phenotype, leaving the ECs not exposed to the Dll4 lines to adopt a tip cell phenotype. This, in combination with the already established patterning abilities of Dll4-mediated lateral inhibition[14], shows the potential of μCP lines of Dll4 to spatially control endothelial sprouting. This approach could serve as the basis for the development of tools to engineer vasculature for TE applications.

3. The potential of Jag1 in spatial control of endothelial sprouting

Dll4 is not the only Notch signaling ligand involved in angiogenesis, and we were wondering what the exact role of Jag1 in sprouting angiogenesis could be, and importantly, if it is possible to use Jag1 to spatially control angiogenesis. Jag1/Notch1 signaling has been shown to promote tip cell selection and sprouting by antagonizing Dll4/Notch1 signaling[18,99]. Others believe that Jag1 regulates tumor angiogenesis via different mechanisms than Dll4, and not behaving as an antagonist but as a modulator[113]. However, the mechanisms and differences between the signaling modes of Dll4 and Jag1 are still under intense investigation[18,60,61,230–232]. Therefore, the engineering potential as well as angiogenic mechanisms of Jag1 need to be further elucidated. To this end we compared Jag1 with Dll4 in our experimental setups to study controlled endothelial sprouting.

3.1 Comparison of gene expression upon Jag1 and Dll4 µCP ink does not elucidate the underlying mechanisms during angiogenesis nor controlled sprouting

To investigate the possible differences between exposure of Jag1 µCP ink and Dll4 µCP ink on a gene level, we performed qPCR on samples that were exposed to homogenous coatings of Jag1-Bead ink, Dll4- Bead ink and Fc-Bead ink. These samples consisted of unconfined HUVECs exposed to the µCP coatings, that could sprout for 24h in Matrigel.

We looked at genes of the VEGFR family, the Notch signaling family and the ligand specific target genes EFNB2 and PTEN[233] (Figure 14). While Dll4 ink induced expression of VEGFR3 (FLT4, p= 0.0353) and inhibited expression of VEGFR1 (FLT1, p= 0.0255) in the neighboring cells, the influence of Jag1 in the ink was very modest for all genes (Figure 14). Although no significant differences could be found, Dll4 appeared to have a more pronounced effect on Notch signaling target genes such as the VEGFR family, EFBN2, and Hey2, than Jag1. Jag1 appeared to induce the expression of Dll4 and Hey1 more efficiently than Dll4, though this could not be statically confirmed.

In comparison with previous data as presented earlier in this thesis, we observed the same induction of VEGFR3 upon stimulation with the Dll4 containing ink, which indicated that VEGFR3 was involved in the Notch signaling crosstalk with VEGF signaling in our system. As the boxplots corresponding to Dll4 induction appeared to be broader than those corresponding to Jag1 induction, this might suggest that Dll4 is involved in a signaling feedback loop operating at 24h after the first exposure to the ligand. Additionally, we do want to note that in our data the changes in gene expression overall were relatively small.

To place our data into perspective, we again need to consider the same conditions as were considered for the data from Study 1, Figure 3 and Figure 13, as the cells were seeded homogenously on top of homogenous coating with the ink, and the time period of 24 hours, might balance out gene expression patterns. However, our main objective was if we could see a difference in gene expression upon stimulation between our µCP ink with Dll4 or Jag1 to explain a possible difference in their sprouting patterning potential. For clear understanding of the underlying mechanisms, the difference in gene expression in ECs upon stimulation with Jag1 or Dll4 in single cell analysis might be needed, to filter out any signaling feedback loops or communal signaling responses.

From literature we know, that Jag1/Notch1 signaling suppresses soluble VEGFR1[61], and that Jag1 may act as a antagonist on Dll4/Notch1 signaling, thereby increasing VEGFR2 expression in uterine decidual capillaries[99]. We did not observe these effects in our setup.

Taken together, the obtained data was not able to clearly define the underlying genetic processes in our experimental setup, nor elucidate the mechanisms behind the different roles of Jag1 and Dll4 in angiogenesis. Therefore, we decided to resort to other methods to obtain answers.

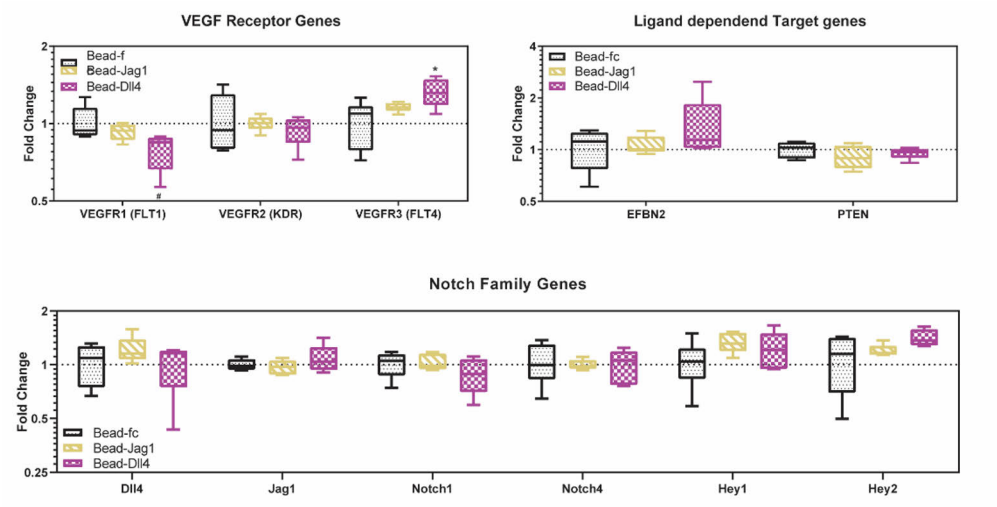

Figure 14 The gene expression profile of endothelial cells exposed to the printing ink containing the ligand functionalized beads after 24h. Comparison between the Fc, Jag1, and Dll4 gene expression induction. For the VEGFR family there is a difference between Fc and Dll4 for VEGFR1 (p = 0.0255) and VEGFR3 (p = 0.0353), but none for VEGFR2. Conversely, no difference between Fc, Jag1 and Dll4 is observed for the target genes EFBN2 and PTEN or any of the Notch family genes. N=6 for all conditions.

3.2 Motivation for the use of μCP lines of Jag1 as a possible tool for positive endothelial patterning

Though the gene expression profile of genes involved in endothelial sprouting upon Jag1-ink exposure did not provide clear trends to elucidate mechanisms of Jag1 induced sprouting, we continued with the curiosity towards Jag1-pattern induced sprouting. From literature we know that Jag1 may act as modulator or antagonist of the Dll4/Notch1 regulation of tip-stalk cells specification[95,99,113]. Additionally, in absence of Dll4/Notch1 signaling, Jag1/Notch1 signaling increases the number of tip cells (Figure 6). Furthermore, from studies done by our research group, we know that the addition of Jag1 ligands to vimentin-impaired ECs, can rescue their defective sprouting, both *ex vivo* in vimentin knock-out arterial ring assays, as *in vitro* in 3D angiogenesis assays with vimentin knock-down HUVECs[225]. Together with the mechanism of signaling of Jag1 in the endothelial wall during recruitment and differentiation of VSMCs via lateral induction[74,78,79], there are strong indicators that extracellular Jag1 might induce positive stimulation of endothelial sprouting. Therefore, we hypothesized that the use of Jag1 in μCP lines might induce endothelial sprouting on top of the μCP lines instead of sprouting restricted to the area in between the lines, as we observed with Dll4 μCP lines in Study I. This would enable positive patterning of endothelial sprouting, which we envision is easier to incorporate in biomaterial applications for the vascularization of TE constructs.

In preliminary screenings and concept development, we explored the idea of combining Jag1 and Dll4 patterns. Additionally, to fairly compare the patterning potential of the ligands, we wanted to exclude potential unequal proliferative effects. To elucidate a potential effect of Jag1 on EC proliferation we exposed homogenously seeded HUVECs to a homogenous coating of beads functionalized with different concentrations of ligand for both Jag1 and Dll4, and combinations of both ligands. We used ratios of 25-100% of ligand (for either Jag1 or Dll4) to beads, and fully immobilized beads with a ratio of 25% Dll4/75% Jag1, vice versa and 50/50% Dll4 and Jag1. The same amount of HUVECs was seeded for every sample, and after 24h the number of nuclei was counted for every condition. Although no significant differences were found, we did observe slight trends where more nuclei were observed on higher concentrations of Dll4 ligands whereas less nuclei were observed on lower concentrations of less Jag1, with an exemption for the lowest Jag1 amount present on the beads (data not shown). Additionally, we observed that the beads themselves also increased the number of nuclei. Hence, a potential proliferative effect of the Dll4 or Jag1 ligands should be taken in consideration when interpreting our data.

To study the patterning role of Jag1 in μCP lines, we seeded ECs homogenously on different ligand patterns (Section 1.1.3 of the results, Figure 11). Here, we did not observe a clear difference in behavior between the ECs seeded on top of Dll4 μCP lines and ECs seeded on top of Jag1 μCP lines. However, homogenously seeded ECs on Dll4 μCP lines did not show any directional sprouting, while we did observe this for ECs seeded with the micro fluidic channels in Study I. Therefore, we needed to explore the experimental setup used in Study I with Jag1 ligands, for fair comparison of the possible spatial control over endothelial sprouting exerted by Jag1 or Dll4. The findings of that comparisons is described in Study II and section 4 of the Results.

4 Spatial patterns of Jag1 and Dll4 elicit different spatial control over endothelial sprouting

In study II, we investigated the difference between μCP lines of Jag1 and Dll4 in exerting spatial control over endothelial sprouting. Additionally, we wanted to investigate the potential of Jag1 patterns to elicit spatial control over endothelial sprouting. We wanted to know, whether the use of Jag1 lines could lead to positive patterning of endothelial sprouts (Study II, Figure 1E), opposed to the induced negative patterning we observed when using Dll4 lines[173].

We employed the same method and used microfluidic channels to seed the ECs in a confined manner. Images were captured by fluorescent microscopy at 24h of sprouting, and further analyzed by image analysis as described above. As expected, we observed no effect of the Fc-IgG lines on the sprouts (Study II, Figure 2). Endothelial sprouts in the Fc-IgG lines samples could cross the lines without problem. However, we observed a similar behavior of the endothelial spouts in the Jag1 lines samples, as cells could be seen on top and in between the lines and crossing them as well. Therefore, indicating that by visual assessment of the samples, we could not observe positive patterning induced by the Jag1 lines. In contrast, we observed endothelial sprouts in the Dll4 line samples confining to the areas in between the Dll4 lines, consistent with negative patterning, thereby confirming our previous findings.

4.1 Dll4 and Jag1 lines induce distinct sprout orientations

To analyze the samples more quantitively, we selected ROIs by the same criteria as defined earlier in this thesis. To assess the direction of the endothelial sprouts within every ROI, we used the directionality plugin of Image J, to produce a histogram of average directions (Study II, Figure 3A). We then normalized the received orientation angles to the direction of the lines in that sample, so that sprouts directed completely in the direction of the μCP lines would have a direction angle of 0 degrees, while directions could vary between -90 and +90 degrees. We observed visually different patterns of directions between the sample groups of Fc-IgG, Dll4 and Jag1 lines (Study II, Supplementary Figure 1), though the resulting dispersion of the graph fitted to the histograms was not significantly different between samples (Study II, Figure 3B).

We assumed the observed lack of difference was due to the symmetry of the system, as we normalized the directions to the direction of the μCP lines and therefore sprouts could deviate from the lines either to the right or to the left, balancing out any differences. Therefore, we computed a different parameter, named “the deviation angle”, where we used only the absolute

value of the orientation angles. The deviation angle would then describe the amount of deviation of the lines the sprout would orient itself. The deviation angles of sprouts exposed to Jag1 μCP lines were found to be significantly larger than the deviation angles of sprouts exposed to Dll4 μCP lines (Study II, Figure 3C).

In summary, we observed a similar general direction for endothelial sprouts in all groups, namely 0 degrees. However, endothelial sprouts exposed to lines of Jag1, deviate more from this general direction and could therefore not be hindered in sprouting, when reaching another Jag1 line. This is in contrast with endothelial sprouts exposed to Dll4 lines where the sprouts are dictated to follow the direction of the Dll4 lines.

4.2 Jag1 lines cannot dictate sprout location, in contrast to Dll4 lines.

Next, we used the parameter Efficiency of controlled sprouting (Ef_{cs}), to quantify the amount of spatial control, similar as in Study I. Briefly, the Ef_{cs} describes the number of cells that are located in between the μCP lines, as a percentage of the total amount of cells per ROI (Study II, Figure 4A). Here, we also linked the value of the Ef_{cs} to different modes of patterning (Study II, Figure 1E). Meaning, that $Ef_{cs} \approx 50\%$ correspond to random patterning, and values of $Ef_{cs} > 50$ %, and $Ef_{cs} < 50\%$ correspond to negative and positive patterning respectively. Again, Ef_{cs} values closer to the extreme percentages (0% and 100%) correspond to a higher spatial control.

We observed Ef_{cs} value of around 50% for the Jag1 line samples, which was not much different from the Ef_{cs} for the control Fc Lines (Study II, Figure 4B). This was in contrast with the Ef_{cs} value, $Ef_{cs} = 70.17 \pm 28.59$ mean ± SD for the samples with Dll4 lines, which was increased compared to both Fc and Jag1 lines samples (Fc: $Ef_{cs} = 42 \pm 38.57$ and Jag1: $Ef_{cs} = 47.77 \pm 30.69$ mean ± SD). To exclude differences based on the number of cells per ROI, we compared the average amount of cells per ROI for the different groups and found no significant differences (Study II, Figure 4C).

Taken together, we must conclude that spatial lines of external Dll4 are more potent in dictating sprout location than lines with external Jag1. Though, what mechanism lies beneath is still unclear.

5 Jag1 and Dll4 elicit different spatial control over endothelial sprouting due to differential activation potential

As our gene expression data, based on the experimental setup, did not fully explain the difference between Dll4 and Jag1 lines in terms of exerted spatial control over endothelial sprouting, we employed computational modeling of signaling crosstalk in angiogenesis to provide possible answers to our outstanding questions.

5.1 A computational model to simulate endothelial sprouting on spatial patterns of Notch ligands

In Study II, we extended the computational model based on Boareto *et al.*[123], to include spatial patterns of ligands and simulate our experiments. The original model includes Notch signaling crosstalk with the VEGF pathway and considers both Dll4 and Jag1 signaling. Additionally it includes the difference in signaling efficacy between Dll4-Notch1 and Jag1-Notch1 as described in previous studies[60].

The adjusted model consists of a set of differential equations describing the dynamics of VEGF and Notch signaling for each cell (Study II, Equations 2-7). The differential equations describe the change of protein content of Notch1, NICD, Jag1, Dll4, and (activated) VEGFR over time. The equations take into account production and degradation rates, cis-inhibition and trans-activation and protein content of the patterns among others (Study II, Supplementary Table 1). Additionally, a set of 3 equations is used to define the summation of Notch1, Dll4, and Jag1 content on the patterned lines and on neighboring cells (Study II, Equations 8-10).- 77 -

As initial conditions, the cells are assigned a random protein content and phenotype, to mimic the experiments *in vitro* where cells are influenced by VEGF in the culture media. In the model, the endothelial phenotype is assigned on the level of VEGFR activity which influences Notch-driven phenotype decisions. Relatively high VEGFR activity results in a migrating tip cell phenotype, relatively low VEGFR activity results in a proliferating stalk cell phenotype and moderate VEGFR activity results in a modelled tip/stalk hybrid type, which can slowly migrate.

The model implementation takes advantage of the spatial periodicity of our experimental setup and focused only on a limited area of the culture. Namely, the model considers only cells located in between the patterned lines and on top of half of the patterned lines at both ends (Study II, Figure 5A and Figure 15). The lines were considered by assuming that the Notch receptors of the cells on top of the lines were bound to the corresponding ligands, similar to Notch signaling ligands of neighboring cells. The simulation of cell-cell signaling was done for 12 cells on a row, with the first

three cells on top of the patterned lines, and then 6 cells in between lines, with the last three cells again on top of the lines (Figure 15). The modelled time of signaling was 12 hours. This time point was chosen based on the fact that by this time, the cells would have changed phenotype and started sprouting from their original positions.

In Study II, Figure 5B we show representative images of ECs on top of patterns of different ligands (Dll4 and Jag1), with different amounts of molecules of ligand in the patterns. The patterns where zero molecules of the ligand are used can be interpreted as no patterns. We observe a clear increase in the stalk cell phenotype on the Dll4 lines patterns when increasing the number of molecules, inhibiting other phenotypes on the lines. Simultaneously we see only few cells in between the Dll4 line patterns that have a definite tip or stalk cell phenotype.

The simulation is in agreement with the experimental results on Dll4 in Study I and Study II, where we only observe sprouts in between the Dll4-patterned lines. The data indicates that the initiation of the sprouts, e.g., the first tip cell, emerges from the area in between the lines of Dll4. In contrast, we observe no such pattern for an increasing number of molecules on Jag1 patterns, which is in agreement with our experimental data on Jag1 in Study II.

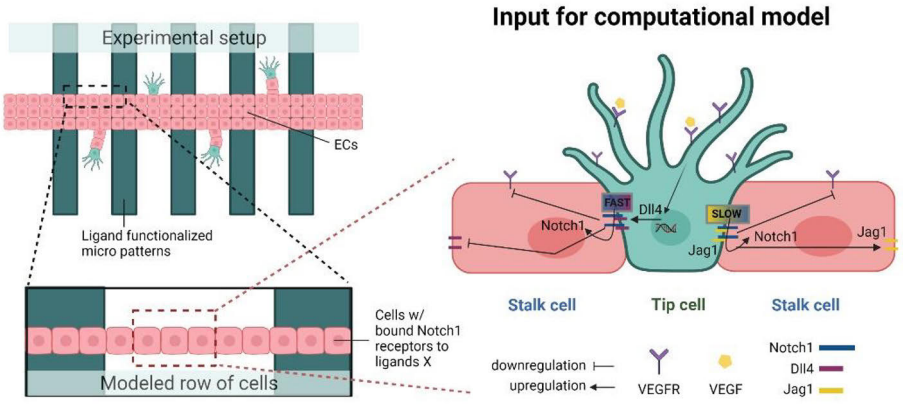

Figure 15 Scheme of the conceptual input of the computational model. Due to the symmetry of the experiment system, a row of 12 cells was simulated in the model. Here. 3 cells are exposed to the lines of ligand (either Dline or Jline), followed by 6 cells that are not on the lines, and end with 3 cells again exposed to the lines of ligand. The computational model incorporates the following relationships as numerical functions; upregulation of Dll4 upon VEGF/VEGFR signaling, downregulation of VEGFR and Dll4 upon increased levels of NICD. Fast increase of NICD upon Dll4/Notch1 signaling. Slower increase of NICD upon Jag1/Notch1 signaling, and upregulation of Jag1 upon increased NICD.

5.2 Simulated efficiencies of controlled sprouting mimic the experimental results

In order to better link the computational model to the experimental results, we calibrated the number of molecules in the line patterns, D_{line} and $J_{line.}$ To this aim, we obtained the Jag1 gene expression of HUVECs exposed to homogenously coated ligands for 6 hours, via qPCR (Study II, Figure 5C), and compared the outcomes of the gene expression to the simulated results with different ligand densities caused by the number of molecules in the patterns (Study II, Figure 5D). We observed the same increased gene expression of Jag1 caused by the Dll4 coating, in relation to the Jag1 coating, for both experimental and computational results (Study II, Figure 5C and D). Therefore, we chose $D_{line} = J_{line} = 3000$ molecules to be the representative value for the ligand density in the simulations, as this parameter value led to a higher level of Jag1 expression caused by Dll4 lines compared to a relative lower levels caused by Jag1 lines in the computational model.

Using this calibration, we quantitively compared the results of the experimental sprouting experiments and the simulations by calculating the Ef_{cs} for 10000 simulations, using the representative value of 3000 molecules for D_{line} and J_{line}. As shown in Study II, Figure 5F, the Ef_{cs} difference observed in the sprouting experiments between Jag1 and Dll4 is also present in the simulations. Here, Dll4 lines again elicited a high Ef_{cs}, while Jag1 lines did not clearly differ from the control. Furthermore, we simulated the Ef_{cs} for different pattern densities (Study II, Figure 5E) and observed that the increase of the Dll4 pattern density further increased the value of the Ef_{cs}. The Ef_{cs} value induced by Jag1 patterns slowly increased as well upon pattern density, though this was still significantly lower than the Dll4 pattern.

Together, the data shows that the computational model was able to replicate the experimentally observed response of endothelial cells to the exposure of spatial lines of different ligands. Additionally, the model includes the assumption that Dll4-Noch1 signaling activation occurs at a higher rate than Jag1-Notch1 signaling activation, and the simulated results highlight a possible role for the temporal dynamics in Dll4-Jag1-Notch1 signaling differences.

5.3 Temporal dynamics is a key factor in determining endothelial sprouting response to Notch ligand-functionalized lines

Additional simulations were performed to explore the influence of signaling temporal dynamics compared to the influence of other parameters. The influence of the width of the lines (Study II, Figure 6B), the end time of the simulations (Study II, Figure 6A) and other model parameters which

describe cell signaling dynamics (Study II, Figure 6 C-D) was explored. Interestingly, the end time of the simulations greatly influence the Ef_{cs} outcomes.

In our model, the phenotype decision to tip, stalk or hybrid EC at the end time of the simulation, relates to the migration of the EC and it is also used to calculate the Ef_{cs}. This indicates that the timing of cell migration from the original configuration (or confined seeding in the experiments) is a major determinant of the effect on spatial control Dll4 and Jag1 have. As in the *in vitro* situation the cells migrate away from the spatial ligand lines, leaving them no longer influenced by the ligands. As seen in Study II, Figure 6A, Dll4 lines already affect the simulated Ef_{cs} after 12 and 24 hours of exposure, while for Jag1 this can only be seen for the 24-hour end time and to a lower degree. This indicates that Jag1 lines might have control over sprouting, were it not that ECs would have already migrated away from the Jag1 lines by the 24-hour time point. Prolonged and persistent exposure to Jag1 lines might therefore have a different effect than what we observe in our *in vitro* experiments. In the other model parameters, no large variations could be observed other than switching ligand type (Dll4 to Jag1 and vice versa) (Study II, Figure 6B-D).

We therefore conclude that the choice of ligand and the temporal dynamics are key factors in determining the endothelial sprouting response of the ECs to the Notch ligand functionalized lines.

5.4 The implications of temporal dynamics-based difference in potential to spatially control endothelial sprouting between Jag1 and Dll4

In order to capture the experimental results with the simulations, the affinity assumption of the computational model is key. The assumption is that there is a lower affinity of Jag1 to Notch1, compared to Dll4, which causes a slower rate of Jag1-mediated Notch1 activation. This assumption is based on experimental data of Luca *et al.*[60]. They additionally found that cellular tension on the catch bond between either Dll4 or Jag1 with Notch1 is important. Dll4 requires lower cellular tensions in order to activate Notch1 signaling, compared to Jag1. This also indicates that in our experimental system, where the ligands are bound to fluorescent beads containing IgG with the recombinant Fc domain, the strength of the bonding, and the fixation of the beads to the surface may influence the signaling potential. Jag1/Notch1 signaling would be more influenced by these parameters than Dll4.

When relating the slower rate of Jag1 mediated Notch1 activation to both our simulations and our experiments, we can deduct that µCP Dll4 lines rapidly activate Notch1, driving the EC on top of the lines to a stalk cell phenotype and allowing sprout formation initiated by EC tip cells for EC in

between the μCP Dll4. Jag1 mediated Notch1 activation and induction of the stalk cell phenotype is slower, leaving time for the ECs to migrate away from the μCP lines of Jag1 before the cellular fate is determined.

Our findings highlight the temporal dynamics of Notch, in agreement with other studies, and emphasize the importance of ligand-receptor binding and activation rates for spatial control of angiogenesis exerted by ligand micropatterns. In order to achieve better spatial control using Jag1 patterns, a more controlled timing of cell migration is needed, or the use of engineered ligands with a higher affinity to Notch1[60] to limit the time required for inducing a stalk cell phenotype. Since the first option is biologically unrealistic and the second would require additional control conditions and verifications while adding another degree of uncertainty, our preferred Notch ligand for spatial control over endothelial cell fate and sprouting is therefore Dll4.

It must be noted that both in our experimental setup, and in our computational model, we do not expose the ECs to gradients of VEGF, which contrasts with native angiogenesis. In the experimental setups, we use VEGF in the cell culture medium. The computational model does not consider VEGF gradients, in line with the *in vitro experiments*, for ease of translation and validation of the experiments. However, the computational model could be extended with the inclusion of filopodia formation[126], cell shape changes and cell movement[125], which are all affected by gradients of VEGF[31], to investigate the role of the gradients to the EC responses to Dll4 and Jag1 line patterns. Here, we were satisfied with not including them, as we look at the initial phenotype switch and migration from the seeded area, though the absence of VEGF gradients in our computational model could explain the lack of alternating tip-stalk phenotypes for EC on control substrates (Study II, Figure 5B). Without a VEGF gradient, the main determinant of tip-stalk cell patterns are multiple VEGF-Notch signaling feedback loops at the gene level, which generally take 4-6 hours[224]. Additionally, the lack of alternating tip stalk cell patterns has been shown previously and was caused by the end time of the simulations for native angiogenesis[123].

Together, we deduct that our chosen end time of 12 hours might be too short for the development of a clear tip-stalk cell pattern in the control situation, but this is justified when considering the time period needed for the EC to start migrating away from the seeded area, which we chose to mimic from the *in vitro* setup with the computational model. Therefore, as we do not deem it biologically realistic to expect cells to remain still for longer than 12 hours, we feel we mimic the experimental setup as realistically as possible.

Further considerations of temporal-based dynamics of spatial control over endothelial sprouting and its potential in context of TE applications or approaches are discussed in section 7.

6 Alternative patterning techniques for spatial patterning of Notch ligands

The successful spatial control exerted by µCP lines of Dll4, accommodate for experimental designs with more complex geometry than a pattern of lines. To achieve full spatial control over endothelial sprouting, non-linear patterns and geometries must be explored, as in biology rarely anything is based on straight lines. Additionally, the application of different geometries could elucidate further the potential and the limitations of Notch ligand based spatial control of endothelial sprouting, and even shed more light on the underlying mechanisms.

Questions such as would Dll4 also dictate location and direction of the sprouts with geometries that leave less freedom, such as zigzag patterns or circular patterns, would the sprouts adopt these geometries as well, or just adjust to their surroundings? These experiments could shed light on how instructive Dll4 is, e.g. is Dll4 instructive or just extorts an inhibitory effect. Additionally, the obtained knowledge of such experiments could facilitate and increase control over the creation of more complex vasculature structures. However, to investigate multiple different geometries, the method of µCP is not ideal, as for different geometries different masks and master wavers need to be designed and produced. This could be a time consuming and labor-intensive practice.

Therefore, we looked for alternative patterning techniques in order to investigate different geometries and their influence on the spatial control exerted by patterns of Notch signaling ligands.

6.1 Photo patterning with the Alvéole PRIMO

One promising alternative technique for patterning is a photo patterning technique based on precise UV light to remove anti-fouling agents, to later add the required protein or patterning agent of choice as published in 2016, by Strale *et al.*[203].

Based on this technology the authors created a product for easy use of the technique, the Alvéole PRIMO, which has since been used by several research groups to pattern proteins for *in vitro* experiments. The general use has been to pattern ECM proteins[234,235], or more specifically fibronectin[203,236–239], collagen[240] and E-cadherin[241] within a confined or non-adhering environment. However, the device is also capable of patterning 2.5D[238] and 3D structures[235,236] and can be used in combination with different techniques such as traction force microscopy[239,242]. Additionally the technique can also be used to pattern hydrogels within PDMS chips after assembly[243].

The design of patterns can be easily adjusted, as no masks need to be made in advance[203], and therefore the technique appears ideal for patterns

that are more complex than just lines. However, as the technique and precision revolve around initial anti-fouling of the surface, this could prove troublesome for applications that require the cells to actually migrate out of their original seeded area and remain unhindered. As we ultimately investigate the influence of Notch ligand lines or other geometries on sprouting/migrating behavior, any hinderance by the culture surface should be avoided.

6.1.1 Lack of adherence of HUVECs after anti-fouling treatment required for photo-patterning hinders controlled sprouting applications

For the protein patterning of the Alvéole PRIMO to work, the patterning surface needs to be treated with an antifouling (PEG-PLL) barrier, that can be removed with patterned UV light in the shape of the desired pattern. However, after patterning this barrier is not removed. Therefore, in order to implement the technique of the PRIMO to HUVECs migrating and sprouting over the treated surface, we needed to verify that the behavior of the EC is not influenced by the antifouling barrier.

To this end, we tested several concentrations of PEG-PLL coating for HUVEC adherence, with untreated glass. We generically used 0.1% gelatin coating as controls. Figure 16A-E shows representative images for all conditions (scale bare represents 100 μm). Figure 16F-I shows the quantitative analysis of 3 representative images per sample (n=3 per condition). The coating treatment with the higher 0.5 w/v% PEG-PLL clearly showed a negative effect on the number of cells found on the treated coverslips. While there appeared to be no decrease in cell number for the lower concentrations of PEG-PLL, these coatings increased the number of cell aggregates, indicating that the cells did not properly adhere to coated surfaces. This was confirmed by the decreased number of healthy cells for all the coatings with PEG-PLL.

This indicates that a PEG-PLL barrier inhibits or disrupts the adherence of the HUVECs, unless the barrier is removed. To achieve this, a negative patterning design could be proposed for the UV light to remove the remaining PEG-PLL, after patterning of the desired geometry with Notch ligands immobilized to fluorescent beads. Importantly, the fluorescence of the beads should not be altered by treatment with the UV light in order to be able to visualize the patterns. Therefore, the fluorescent spectra of the beads should ideally not overlap by with the UV light used and the choice of beads may need to be reconsidered for use with the PRIMO.

6.1.2 Photo patterning optimization; a pilot study

To further explore whether photo patterning with the Alvéole PRIMO can be used to obtain more complex patterns, we set up a pilot, where we first wanted to replicate the experiments from Study I and II with patterns made with the PRIMO. Therefore, we used patterns of the same dimensions,

namely 100 µm lines with 100 µm spacing in between, and used the same fluorescent bead-ligand mixture for the patterns as before. As the UV light of the PRIMO is only able to pattern its field of view, multiple patterns needed to align side by side. Therefore, the patterning of one sample took 4 hours alone, and this limited the number of samples that could be produced within a reasonable timeframe.

Figure 17A-E shows representative images of the experiments using the photo patterning of the PRIMO. In Figure 17A some directed sprouts can be observed, which are guided by a Dll4 pattern (red). The pattern was not clearly visible directly next or under the seeded HUVECs, but an image of higher magnification (Figure 17B) showed clear lines and sufficient contrast between photo patterned and un-patterned areas. However, some fluorescence, and thus fluorescent beads containing ligands, was still observed in the unpatterned areas. Figure 17C-E shows a sample with Jag1 pattern (C, red) with HUVECs seeded on top (D, actin cytoskeleton in green) and the merged image (E). Here, we observed less defined lines, and more fluorescent background signaling, indicating that the Bead-Jag1 was not confined to the pattern, but also present at the anti-fouling sites. Additionally, the lines of Jag1 appeared to be most visible at the area where the HUVECs were seeded, although the lines were less clear underneath healthy cells, opposed to lines underneath dead cells. This indicated that the line patterns were either removed by the cells, or removed at the same time of the removing of the micro fluidic channel or were not correctly patterned due to suboptimal contrast with the UV light, or by adherence of the Bead-Jag1 outside the pattern.

Regarding the effect of the anti-fouling agents on the sprouting behavior, we did observe less sprouting in Figure 17A than what we observed in Dll4 samples of Study I and II. Additionally, most sprouts could be seen to orient themselves towards the area on the sample where the lines were more prominent, however, the red fluorescence was also more prominent there, which could indicate a suboptimal effect of the anti-fouling agent at that site. Therefore, we could not exclude the effect of the anti-fouling on the endothelial sprouting behavior in these samples.

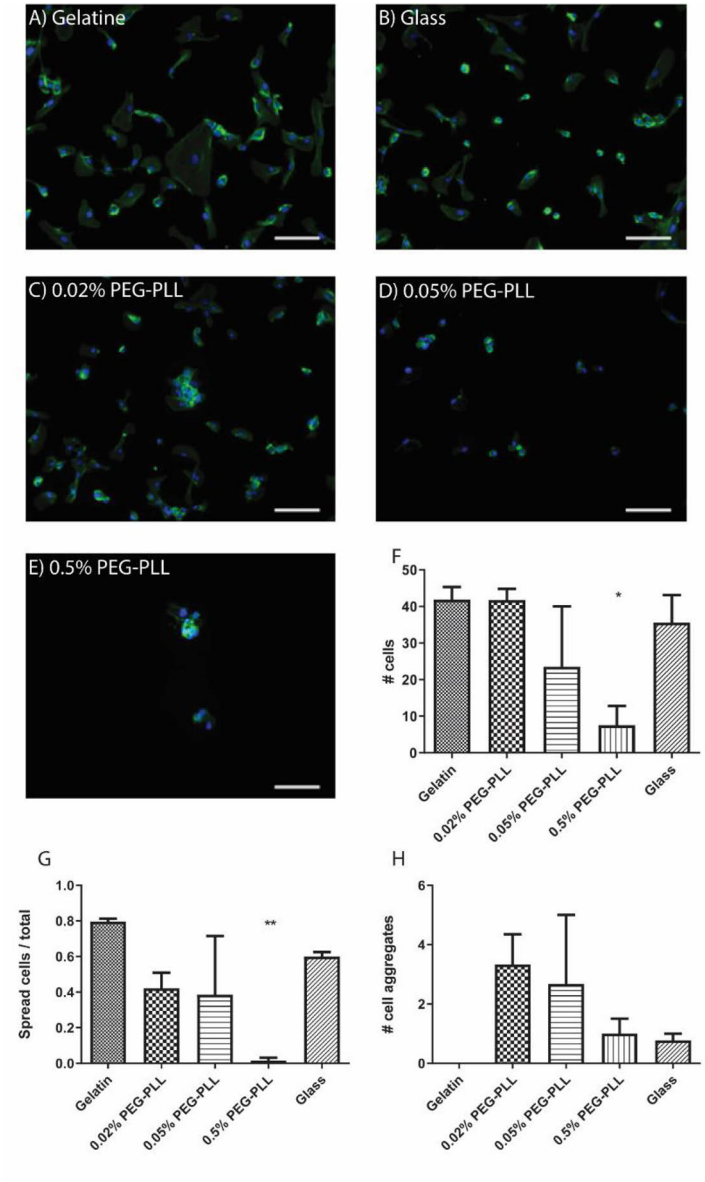

Figure 16 Fluorescent stainings of HUVECs seeded on coverslips coated with varying concentrations of PEG-PLL (C-E), the exact concentration is mentioned in the images. As controls, the generically used gelatin coating (A) and untreated coverslips (B) were included. The actin cytoskeleton can be seen in green and the nuclei in blue. Higher concentrations of PEG-PLL show less (functional) of HUVECs. Scale bars represent 100µm. (F-H) Analysis of PEG-PLL coatings in terms of amount and visual assessment of HUVECs shown in the representative images, (n=3 per sample, 3 samples per condition). The total

amount of cells adhered to the coating is severely decreased with 0.5% PEG-PLL (p=0.02345) and those there are mostly rounded up. (** p=0.0042)*

Next, we explored whether more complex patterns could be obtained using the PRIMO photo patterning technique. We designed a simple line pattern, where we alternated lines of Dll4 and Jag1 to explore the possibility of dual patterning (Figure 17F). The underlying mechanistic research question of this pattern design was whether the ECs seeded perpendicularly on top of these alternating lines, would take their spatial guiding cues from Dll4 or Jag1. Would they be repulsed by the Dll4 lines and attracted by the Jag1 lines, or would the endothelial sprouts conduct themselves completely differently?

The protocol used was based on Strale *et al*.[203], and was indented to be combined with seeding of the ECs through micro fluidic channels. However, both the beads linked to Dll4 (Red) (Figure 17G) as those of Jag1 (Green) (Figure 17H) co-localized (Figure 17I), suggesting that both ligand solutions remained at the same location after washing, possibly even bound to each other, which indicated that there was insufficient blocking in between the adsorption of the first bead-ligand and the removal of the antifouling for the second bead-mixture.

As dual patterning with the PRIMO has been successfully achieved before[203,236], it should be possible to optimize this process for our applications. However, the setup of the microscope-PRIMO combination with the Leica DMi8 TIRF in our department, has challenged optimization to ensure sufficient contrast and substrate passivation for PDMS chips in the past[238]. This suggests that in our specific situation, where we need well-defined patterns by using anti-fouling agents, in addition to ensure anti-fouling removal afterwards for correct interpretation of EC behavior in response to the ligand lines, optimization of the system for dual patterns is needed and is likely to be time consuming.

In sum, this alternative mask-less UV patterning technique could provide more complex spatial patterns for exploring the spatial guiding properties of Notch ligands, but significant optimization would be needed. Therefore, the gain in complexity and the research questions backing it, should be balanced with the amount of optimization as well as with the lessened throughput compared to the current system used.

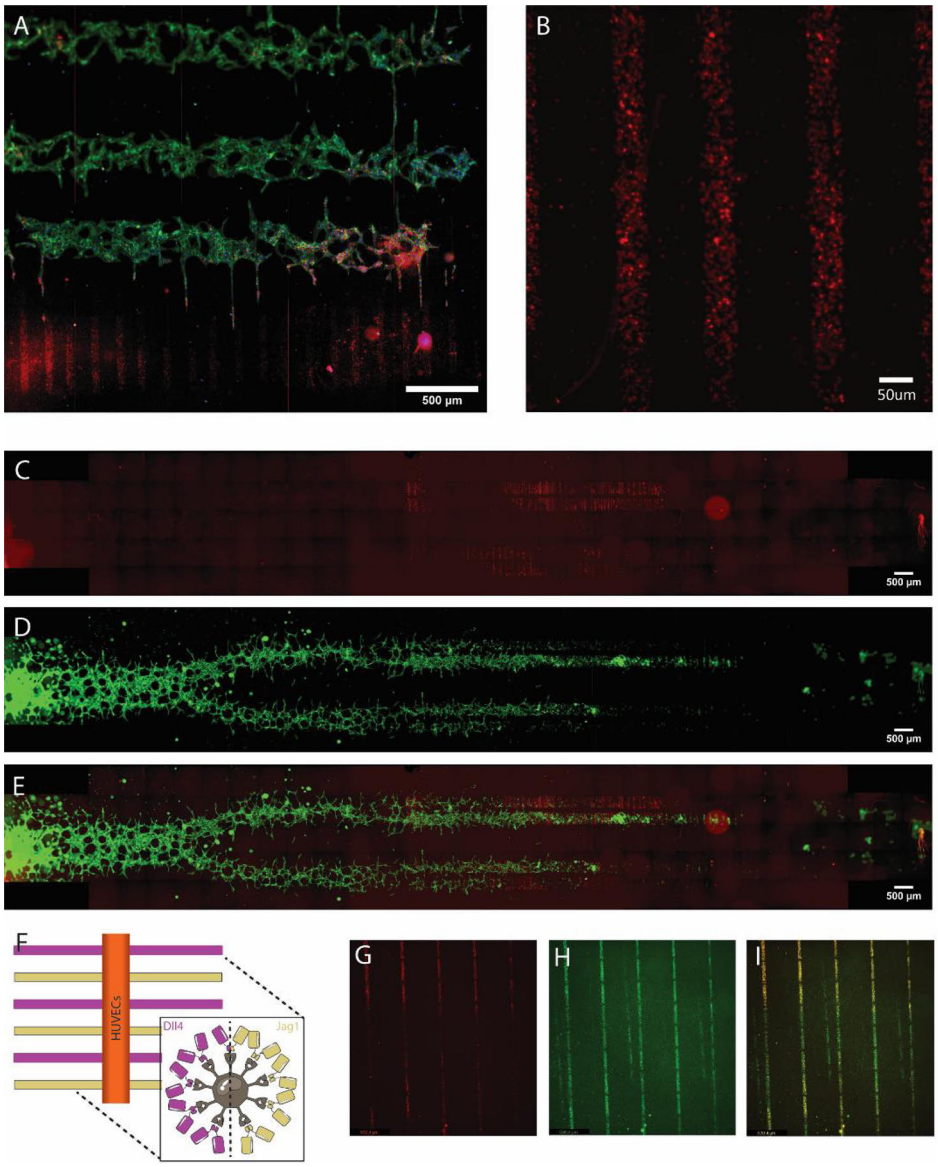

Figure 17 Trials with photo patterning of Bead-Ligand mixture using the Alvéole PRIMO. A) Endothelial sprouting of HUVECs seeded on top of Dll4 patterns. Some directed sprouting can be observed, though the pattern is not consistent throughout the samples Actin cytoskeleton in Green, Bead-Dll4 in Red, Nuclei in Blue. Scale bar represents 500 µm. B) Pattern of Dll4-beads as patterned with the PRIMO (Red). Scale bare represents 50 µm. C-E) Sample with endothelial sprouting on top of Jag1 Patterns Scale bar represent 500 µm. C) Pattern of Jag1-beads (red). D) Endothelial cells sprouting, represented by the actin cytoskeleton in green. E) merged image. F) Design of the dual

patterning experiment, with alternating lines of Dll4 (purple) and Jag1 (yellow). G) Dual patterning; Dll4 pattern (red). H) Dual patterning; Jag1 pattern (green). I) Dual patterning; merged image.

6.2 Other patterning techniques

In this thesis, we addressed two patterning techniques: µCP and photo patterning using the Alvéole PRIMO. While µCP results in precise and defined patterns with resolutions as small as 1 µm[214], reliable resolutions lie upwards of 20 µm. Patterning with the PRIMO has an advantage over µCP in terms of independency of masks to pattern and pattern designs can be swiftly adjusted.
Recently, patterning of VEGF via confined adsorption has been investigated for the purpose of vascularization of TE constructs[191]. Here, while they did not use µCP, masks were still required for confined pouring of the solution which limits the adjustability of the patterns. 3D bioprinting has also been investigated for engineering of vasculature[5], though mostly for direct printing of cells. Bioprinting of proteins and ligands, has the advantage of swift adjustment of the pattern design and capability to print more complex structures. However, while geometric dimension of around 100 µm wide is feasible with bioprinting, the definition of the geometries increases with larger width, mainly to up to 1 mm, which is too large for our setup[244,245]. Therefore, these patterning techniques were not considered for the experiments in this thesis.

7 Relevance of patterns of Notch ligands for revealing disease phenotypes, and for therapeutics, biomaterials and TE

With the findings of this thesis, we have demonstrated the *in vitro* potential of spatially distributed Notch ligands as an engineering tool to guide and control endothelial sprouting. In this section we discuss how this new knowledge can be applied to engineer vasculature for TE applications and discuss the spatial incorporation of Notch ligands in biomaterials for that purpose. Next, we discuss how the assay used in this thesis can aid in the discovery of disease phenotypes and aid the development of therapeutics.

7.1 Translation of spatially patterned Notch ligands for therapeutics, biomaterials and TE

In this thesis, we have demonstrated by engineering spatial patterns of Notch ligands it is possible to control the spatial location and direction of budding endothelial sprouts. We have proven that spatial patterns of Dll4 are a potent tool to control endothelial sprouting. We have found that spatial patterns of Jag1 have a lower potential to control the location and direction of endothelial sprouts compared to spatial patterns of Dll4, which likely arises from the lower affinity of Jag1 to Notch1 compared with the affinity of Dll4 to Notch1, resulting in a slower Jag1-mediated Notch1 activation (Figure 18A).

Therefore, for future studies towards application of spatial patterns of Notch ligands in biomaterials for TE, we should focus on Dll4 rather than Jag1 or utilize high affinity forms of Jag1 ligands obtained by directed evolution and synthetic biology approaches (Figure 18B). However, the temporal aspects of Notch signaling via prolonged Jag1 exposure in patterns could be investigated further and might be used as a tool towards negative of positive patterning of endothelial sprouts.

While Dll4 serves as a guiding cue in 2D by the inhibitory and confining effect and negative patterning of the spatial Dll4 lines, this might raise challenges for applications in 3D, as an additional degree of freedom (in the Z direction) for the cells to sprout to comes into the picture. Dll4 functionalization in 3D might still be of use, possibly to avoid sprouting through or towards some areas in a 3D construct (Figure 18C).

For now, we do not know whether engineered Jag1 with increased affinity to Notch1 could lead to positive or negative patterning. However, if after further research these engineered Jag1 would induce positive patterning, this could be applied as local confined pro-angiogenic stimulus. A combination of locally confined patterns of restrictive Dll4 and sprout inducing Jag1 in a 3D construct could be used as a fairly precise, vascularization inducing blueprint for organized engineered vasculature.

Additional adaption of the computational model described in section 5 of the Results could be used to predict the feasibility of such 3D construct design.

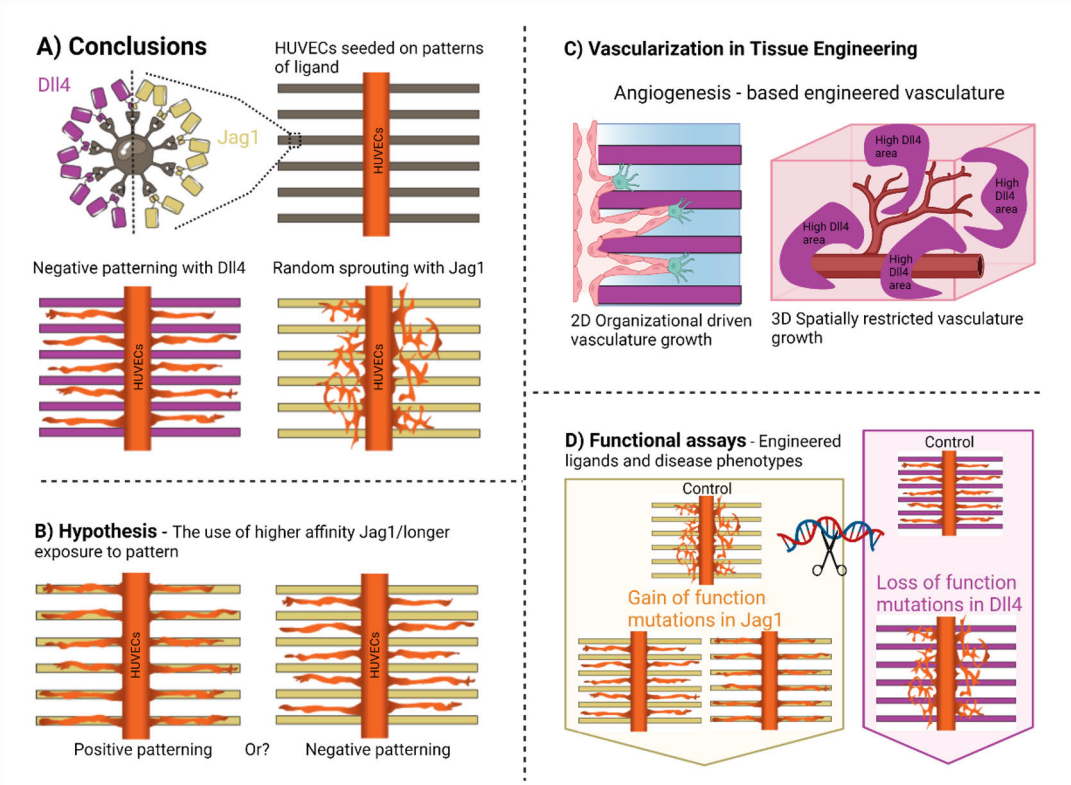

Figure 18 Schematic overview of the results and conclusions of this thesis (A), the hypothesis it raised (B), the potential the findings of this thesis could have for vascularization in TE (C) and the screening of engineered ligands and disease phenotypes (D).

From preliminary data in section 1.1.3 of the Results, we deduct that it is probable that re-orienting an existing vascular bed is too ambitious for our approach. However, to irrevocably exclude this possibility, further research is needed. Options to study this could include a 2D biomaterial surface functionalized with the patterns of Notch ligand upon chorioallantoic membranes of fertilized chicken embryos *in vivo* or outgrown endothelial sprouts of aortic ring assays *ex vivo*. Chick embryos have long been established as an model system for studying and targeting angiogenesis and includes the complex systemic signaling that may occur, though results cannot be directly translated to human angiogenesis[205,210,225].

Options to study this *in vitro* could consist of an *in vitro* engineered vascular bed in 3D, similar to the vasculogenesis-based bottom-up approaches mentioned in the literature section of this thesis, in combination with a 2D Notch ligand patterned surface on top to induce vascular remodeling. This approach would allow for the use of human cells, for better translation. However, the throughput and efficiency of the method would be hindered by the requirement of first establishing vascular beds *in vitro* and would require optimization.

Results of these studies could clarify the feasibility of re-orientating the vascular bed with patterns of Notch ligands, which consequently could be of use for developing biomaterial patches for efficient re-vascularization for the regeneration of injured and ischemic tissues, such as in MI.

7.1.1 Patterning of biomaterials for spatial presentation of Notch ligands

In this thesis, we highlight the spatial control over Notch signaling as an important tool in inducing cell fate and discover a role for temporal dynamics in inducing cell fate in the endothelium. Therefore, the incorporation of spatial and temporal control of ligand presentation in biomaterial could prove key for the development of materials that could dictate organization of vasculature and other tissues.

With the rapid development of Notch functionalization of biomaterials, as discussed in the literature section 4 in this thesis and in the study by Tiemeijer and Sanlidag *et al.* [130], not included in this thesis, options for the inclusion of spatial patterns of Notch ligands in biomaterials are expanding. Via reversible photopatterning, spatio-temporal control of the presentation of Notch ligands in 3D hydrogel matrices was achieved[174]. Here, PEG-based hydrogels were functionalized with alkoxyamine sites that could be cleaved upon UV irradiation, which then could be used for covalent immobilization of aldehyde-functionalized proteins, among which Delta. Via photo-scissible linkers, the proteins could again be removed by UV irradiation as well. Additionally, Jag1 functionalization has been studied in hyaluronate hydrogels, where photo-sissible cages were used to timely and locally uncage the Jag1 ligand and induce Notch signaling in hepatoblasts[140]. These two studies show the feasibility of both spatial and temporal control exerted by biomaterials functionalized with Notch ligands. Which could aid the development of a 3D spatial patterned construct for TE.

Light-based patterning of several different ligands and proteins in hydrogels has been extensively researched[246,247], and light might even be used to induce pulling forces at the site of the hydrogel to mimic mechanotransduction[248]. As the induction of Notch signaling is depended on pulling forces[15,60] and mechanotransduction[82], this could add another dimension of control over cell fate via ligand functionalized biomaterials.

As the ECM stiffness plays a role in the regulation of neo vessel growth and branching[49], stiffness gradients in biomaterials could be deployed for additional control over endothelial sprouting. The combination of spatial Notch ligand patterns and stiffness gradients could be complementary. The initial organizational control during the start of endothelial sprouting would come from the ligand patterns, the continued stimulation for vascularization into one direction would come from the stiffness gradient. This combinatorial approach could prolong the organizational control for larger constructs, where it is not feasible to have patterns of Notch ligands distributed throughout the constructs.

7.2 Functional assays of engineered ligands to reveal disease phenotypes and underlining molecular and cellular mechanisms

The method presented in this thesis can also be used as a functional assay to reveal disease phenotypes and mechanisms of action. Regarding the method as a functional assay, it could be used to screen the functionality of engineered Notch ligands (Figure 18D). Spatial control of endothelial sprouting by lines of the ligand is limited to unaltered Dll4/Notch1 signaling.

Engineered Dll4 ligands altered to incorporate disease mutations or to increase affinity to the Notch1 receptor etc. require confirmation of the increased or decreased functioning of the engineered Dll4 ligand, to prove the alteration of the ligand is as designed.

Therefore, we hypothesize that if engineered Dll4 ligands are functional and able to induce Notch signaling, they should exert a similar control over sprouting location and direction as we have observed in Study I and II. This could be measured quantitively by calculating the Ef_{cs} values for the engineered ligands. Here, the higher the value of Ef_{cs}, the more control is exerted, the more functional the engineered Dll4 ligand is. In contrast, if the engineered Dll4 ligand does not exert control over sprouting location and direction, represented by a Ef_{cs} value closer to or lower than 50%, they could be deemed non-functional. However, as this reasoning could work for Dll4, for Jag1 this would not work in the same fashion, as Jag1 does not exert control over sprouting location and direction. However, it could be used to investigate engineered Jag1 that has a higher affinity for the Notch1 receptor.

Based on the simulations in Study II, we hypothesize that with an increased duration of exposure to Jag1 the cells would adopt a stalk cell phenotype. Therefore, we believe that engineered Jag1 with increased affinity for the Notch1 receptor might equally induce stalk cell phenotypes, and might exert more control over sprouting location and direction resulting in a higher Ef_{cs} or significantly lower Ef_{cs} than 50%, corresponding to negative or positive patterning.

The advantage that this system has compared to regular protein and gene analysis is that the readout of the induced manipulation is correlated to tissue organization, and indirectly captures a change in cell behavior and possible phenotype, while analyzing change in tissue organization. Therefore, it is possible to directly relate cell outcome and tissue organization to the mutation of the ligand, omitting the interpretation step necessary for gene and protein expression read-outs. However, as mentioned earlier in the thesis, it is not a quick protocol, and efficiency and through put is limited.

As a functional assay, the method could be beneficial for testing disease mutations in engineered ligands. Here, it could be used to reveal mutations that would lead to decreased functionality of the Dll4 ligand or mutations that increase the affinity of Jag1. This is relevant as in several cardiovascular diseases the pathology is directly related to mutations in the components of the Notch signaling pathway [19]. Therefore, our method could be used to reveal disease phenotypes and the underlying mutations.

As a first step to explore this idea, we performed experiments with two bio-engineered protein constructs containing disease mutations, in collaboration with the lab of Prof. Handsford of the University of Oxford. We received two protein constructs hDLL4-Fc Construct WT (F195A) & hDLL4-fc Construct Negative Control (Y216A) which we bound to the fluorescent beads as μCP ink. We included an additional control for the fluorescent beads, functionalized with Fc, and performed experiments similar to those in Study I and II. With this example, we want to highlight the versatility of the method described in this thesis, and the possibility of using it to reveal possible target sites for therapeutics targeting angiogenesis or reveal any other underlying molecular and cellular mechanisms in Notch signaling based endothelial sprouting during angiogenesis.

Concluding Remarks

The crux for engineering micro vasculature for tissue engineering and regenerative medicine is to control the organization of the vascular bed. Current strategies rely either on dictating the location of cell seeding, often via synthetic scaffolds of microchips which limited possibility of integration with native tissue, or on the self-assembly of vascular components that is not easily spatially controlled. In our opinion, the missing link is the spatial control of self-assembled vasculature.

In vivo, new micro vasculature is generated via endothelial sprouting from existing vessels through the process of angiogenesis. This process is regulated by several cell signaling pathways, such as Notch signaling. Notch is also involved in several (cardio) vascular pathologies and cancer angiogenesis. In angiogenesis, Notch signaling is a critical regulator of tip or stalk cell specification of endothelial cells. This specification marks the initiation of endothelial sprout development.

In this thesis we explored the possibilities of using patterns of Notch ligands to provide spatial control over endothelial sprouting and elucidated the underlying mechanisms of ligand-mediated control of sprouting angiogenesis. The obtained knowledge might aid in the design of biomaterials for engineered vasculature and regenerative medicine and increase knowledge for future therapeutic strategies for cancer angiogenesis and cardiovascular pathologies.

Here, for the first time, we have developed method to create spatial patterns of ligands and exposed ECs to these patterns. We showed that the ligands in the patterns were able to induce the Notch signaling pathway *in vitro* and demonstrated that spatial patterns of Dll4 are able to control the location and the direction of endothelial sprouting in a negative pattern-fashion. The sprouting was restricted to areas in between line patterns of Dll4, which allowed us to control the location of sprouting. We hypothesized that the lateral inhibition of Dll4/Notch1 signaling is responsible for the local direction of endothelial cell fate into a tip or stalk cell phenotype, and thereby controlling the local initiation of endothelial sprouting.

In contrast to Dll4, Jag1 did not control the location and direction of endothelial sprouting. To further investigate the mechanisms behind this difference, we developed a computational model that included patterns of ligands. This model represented the signaling cascade after the induction of spatially restricted Notch signaling and was able to simulate our experimental data. Based on the parameter analysis, we discovered that the ligand patterns and the time the ECs were exposed to the line determined the outcome. Based on our data, we concluded that the temporal dynamics of the signaling control sprouting via the ligand patterns. This is mostly

likely due to the difference in affinity for the Notch1 receptor for Dll4 and Jag1.

The data indicated that longer exposure to the Jag1 patterns without migration from the patterns could have induced the ECs as well to sprout in a spatially controlled fashion. However, Dll4 required a shorter time to induce phenotype specification. Therefore, Dll4 is the preferred choice for controlling endothelial sprouting location and direction during angiogenesis.

Our data showed that confined seeding of the ECs was necessary to control endothelial sprouting with ligand patterns, indicating that spatial control by ligand patterns over remodeling of established vascular beds is improbable, though further investigation to prove or disprove this assumption might be worthwhile. The creation of complex geometric ligand patterns would further unravel the potential of controlled sprouting, as well as shed more light on the molecular mechanisms behind this control. However, extensive optimization is required for use of the alternative patterning strategies described in this thesis.

The findings in this thesis contribute to the mechanistic knowledge and applicability of the spatial activation of Notch signaling for controlling angiogenesis. The resulting spatial control over endothelial sprouting during angiogenesis could be applied to design methods and biomaterials for engineering vasculature. The incorporation of spatially distributed Notch ligands in biomaterials may increase spatial control in 2D, but this could be extended to 3D materials with spatio-temporal regulation of the ligand mediated Notch activation in the future. The benefit of incorporation of patterns of Notch ligands for this purpose would be that structural and organizational control over the vascular bed that forms is not dependent on pre-formed inorganic structures such as microchips and this would increase integration with the native or engineered tissue.

Additionally, the method developed in this thesis can be used as a functional assay for the screening of engineered ligands and disease phenotypes. As we study the direct relation between local activation of Notch signaling and the patterned sprouts, any loss of function mutations would result in changes in the patterning profile of the endothelial sprouts, for example from negative to random patterning when investigating Dll4. This way, disease mutations can be quickly identified, and the functionality of engineered ligands tested. Therefore, the method shows the potential of spatial presentation of Notch ligands as a therapeutic handle and as an engineering tool. Further exploration of the spatial and temporal control of Notch signaling is needed for fine tuning biomaterial design for vascular engineering, especially in 3D constructs. Recent light-depended spatial and temporal functionalization of hydrogels could progress this research further.

In conclusion, this study reveals the potential of spatial patterns of Notch signaling ligands for controlling endothelial sprouting during angiogenesis, and thereby highlights spatial Notch activation as an important engineering tool for vascular tissue engineering, as well as a promising therapeutic handle.

Acknowledgements

Het laatste, het dankwoord, omdat je een Phd natuurlijk nooit alleen doet. Ik zwoer dat ik het niet lang ging maken, maar daar heb ik me er niet aan kunnen houden. Ik hoop dat ik niemand vergeet, maar naar zo veel jaren rondgelopen te hebben op de TUe kan ik geen garanties geven..

Dear **Cecilia,** Queen of (the) Notch(ies), thank you for your trust-in and support-of this crazy project, which started with a picture of a microscopy image of some directed endothelial cells and a simple "YESS!" from a still naive master student. This continued in a jump in the deep waters of cell biology and of international PhD (and tax, health and pension) regulations. I have never been much interested the latter, however, when you have to deal with it- you have to deal with it. I am still convinced you have an unclaimed fortune somewhere waiting on you. Thank you for being a positive reinforcer and guiding light even when we were treading with baby-steps. Progress! I am very grateful to you for giving me this opportunity to research the subject of my own choosing and your trust that it came from solid (research) grounds. Thank you for not only focusing the research work, but also on teambuilding and participating in the Notch drinks, whenever you were in town. After being used to just barge in your office during my student years, sending meeting requests for video calls was a bit of a change, but luckily we almost always got hold of you within a day or so. Thank you for your detailed correctness of the biological terms and pathways, when my engineering brain thought only about function. A true collaboration between biology and engineering! I am truly grateful for your support and guidance while being my promotor and now also when acting as the custos during the defense.

Beste **Carlijn**, dankjewel dat je mijn co-promotor en co-supervisor wilde zijn. Bedankt ook voor je steun tijdens het bedenken van mijn onderwerp, het 'iets te ambitieuze' masterproject. Ik kan me nog goed herinneren dat ik mijn idee pitchte aan jou en Cecilia en ik meteen te horen kreeg dat het project te groot zou zijn voor een master, en dat het eerder op een PhD project leek. Ik heb het heel fijn gevonden dat ik meteen na mijn master als onderzoeksassistent al een paar maanden het project kon ontwikkelen tot een PhD project. Ook vond ik het fijn dat ik alle support kreeg om het project hier in Eindhoven te blijven doen. Hoewel we meerdere lobby's hadden lopen en meer situaties uitgeschetst hadden, bleek alleen de huidige situatie bureaucratisch te kunnen. Gelukkig heb ik altijd het gevoel gehad dat ik welkom was binnen de groep en er helemaal bij hoorde. Daarbij kon ik ook je engineers-pet tijdens het schrijven van het review erg waarderen en voelde ik me gesterkt wanneer we tegengeluid moesten geven aan al die

biologie. Aan het delen van krukken tips (hoe neem je dan je wijntje mee?) en een luisterend oor voor zorgen omtrent knieën en (internationale) logistiek en aan de gezelligheid tijdens STEM en andere werk-uitjes heb ik fijne herinneringen!

I would like express my gratitude to **Lorenzo Moroni** and **Ana Teixeira** for taking the time to read and review my thesis ahead of the defense. I am grateful for all the kind words of praise for this thesis. **Stephan Huveneers**, bedankt dat je de rol van opponent in de defense ceremony op je wilt nemen en voor je enthousiasme betreffende het onderwerp van mijn proefschrift.

Dank aan alle leden van de **STEM groep** voor het warme bad, groepsuitjes en het delen van onze onderzoeken. En natuurlijk aan een belangrijk sub-onderdeel van de STEM groep: **de Notchies** in Eindhoven. Zonder jullie was mijn Phd veel minder interessant en veel saaier geweest. Bedankt **Rob, Oscar, Nicole, Jelle, Janine, Tommaso, Jordy, Cansu** en **Hetty**, voor alle jullie gezelligheid, de Notchbiertjes, het sparren over de cellen, de rest van ons onderzoek, de biologie en de engineers aanpak, de meetings, het gezelschap tijdens conferenties, het luisterend oor voor de (onderzoeks) frustraties en de verbondenheid. Als "Finse" promovenda was ik deel van zowel de Finse Notchies als de Eindhovense. Thanks to the (pre corona) yearly fun visits between the FI group and NL group we still felt connected as Notchies. Special thanks to **Daniel, Rasmus, Sebastian, Christian** and **Marika** for their company during the Notch conferences, **Sami** for his contribution as co-author (and fun!) and **Kati** for all project related logistics.

Speaking of logistics, and especially for international logistics between two universities (and governments), I needed some help to navigate all this. Thank you to **Christel** and **Andrea** for your willingness to answers all my questions and listening to my worries. Dankjewel voor **Yvon** en **Moniek** voor het verfrissend pragmatisch regelen van de Eindhovense praktische zaken zodat ik niet teveel over pasjes, gastenverklaringen, bestellingen en laptops hoefde na te denken.

Onderzoek doe je niet alleen en zonder de input van anderen had ik nooit de artikelen die er nu liggen af kunnen krijgen. **Rob**, dankjewel dat je me als halve master begeleider de wondere wereld van de HUVECs en Notch heb laten zien. Met jou is het altijd gezellig in het lab en je wilt altijd mee denken of helpen. Dropjes zijn alleen nooit veilig bij jou, maar gelukkig geheimen wel, al liggen we vaak samen onder dezelfde steen. **Oscar**, dankjewel dat ik altijd bij je kon komen met vragen over de biologie, sparren over analyses en andere hersenkronkels. Je open instelling heeft er altijd voor gezorgd dat ik bij jou terecht kon voor alles, zowel onderzoek, universiteitspolitiek, NL-

FI relaties en persoonlijke zorgen. Dankjewel dat je zo'n geweldige collega was. **Jelle** dank voor je hulp bij al mijn micro fabrication vragen, gezelligheid en "is het altijd voor bier" mailtjes! Very big thanks to the co-authors of my papers, and in particular, **Sami, Tommaso, Oscar** and **Jean-Phillipe**. **Sami**, thank you for your patience and drive through our periods of writing, mostly during lockdown or medical downs that prevented us (but mostly me) from physically performing experiments. **Tommaso**, thank you for all your hard work and computational knowledge and gut to take on this weird project of directing angiogenesis. I am confident you will make sure the knowledge we gained will be used in the future. **Oscar**, thank you for your creative mind and out of the box analysis idea's. And **JP** thank you very much for taking on this weird project and giving us the mechanical tools to actually investigate and developing the method with me. Without your continued enthusiasm, I doubt we could have made it possible. And, I'll promise I won't change my "succes" surname in the near future. Professionally, that is!

Tijdens mijn promoveren heb ik ook een aantal studenten mogen begeleiden. **Matthijs, Jonne,** en **Mark**, "mijn" BEP-pers, dankjewel voor jullie interesse in het onderwerp en voor jullie projecten. Jonne, jouw enthousiasme voor het model heeft de basis gelegd voor de samenwerking met Tommaso en het eruitvolgende artikel. Mark, helaas heb ik je verloren aan mijn broer voor je master project, maar gelukkig ben je door gegaan met onderzoek en nu ook aan het promoveren! Special thanks to my international Master student **Jaakko** who brought a bit of Finland to Eindhoven, and helped developing our method further with more complexity. Though the pandemic short cutted your stay here, I am grateful for the amount of pilots you were able to run!

Mijn onderzoek had ik nooit kunnen doen zonder een goed lab, gelukkig was het celllab niet alleen een goed lab maar ook een heel gezellige! Dankjewel aan **Moniek, Marloes, Marina, Mark, Sylvia** en **Yuana** voor het regelen van het reilen en zeilen in het lab. Dankjewel aan **Noortje,** voor je gezelligheid, lekkere baksels en goede cel-culture tips! Jouw advies was altijd goud waard! Dankjewel aan **Ronald, Sergio, DJ, Johnick, Mathilde, Tamar, Cas, Meike, Rienk, Inge, Nikita, Nidhi** en **Bart** voor jullie praatjes, tips en grappen tussen wachtstappen door!

Helaas ben ik de afgelopen tijd niet meer vaak op kantoor geweest, mede door corona. Maar de eerste paar jaar van mijn promotie traject (en daarvoor het research assistentschap) werd gemarkeerd door het gezellige kantoor waar ik in zat. Bedankt voor alle uitjes, etentjes, biertjes, borrels, lunches, koffie, woorden-kots en gezelligheid (en het snaaien uit de koe) **Bente, Dina, Dylan, Elias, Hetty, Janne, Maike, Maaike, Marc, Marjan,**

Mathieu, Nicole, Pim, Ronald, Sana, Suzanne, Stefan, Stefan en **Willeke**! Ik draai nog altijd met heel veel plezier onze 4.12 playlisten waarbij we allemaal hebben bijgedragen, van hardstyle tot duitse slagers, en van Britney Spears tot Rammstein en George Micheal. Dank ook aan onze gast-kantoor genoten; **Rodrigo, Talitha, Valentine** en **Valery**. Voor de aanvullende gezelligheid op donderdag middag en andere feestjes ook dank aan de leden van 4.11; **Emiel, Eline, Kuijtim, Louis, Nicole, Niels** en **Stefan**.

En dan nu, mijn paranimfen **Suup** en **Nicole**, ondanks dat volgens jullie dat niet officieel zijn in deze buitenlandse ceremonie wil ik jullie er toch heel graag bij hebben en lekker dwars zijn. **Suup,** tegelijk begonnen, jij aan je PhD en ik aan mijn research assistentschap, en tegelijk terecht gekomen in 4.12. Dat betekende samen een welkom-in-kantoor uitje regelen! 11 stokbroden (n+1), 10 liter soep, 20+ speciaalbier, een rondleiding en een heleboel woorden-kots verder kreeg ik wel in de gaten dat wij het wel eens goed met elkaar zouden kunnen vinden! Daarbij was het ook altijd super gezellig met je in het lab, strooide je rond met twixen, deelde je poetsdoekjes uit bij de vleet (vanwege dat on-opgeruimde bureau van mij) en was je altijd te porren voor een donderdag middag drankje (ook zonder saldo!). Je openheid, oprechte enthousiasme en uitvloeiende positiviteit kan ik erg waarderen. Net als je dansmoves onder de invloed van duitse dextro. Helaas lijkt het erop dat bij dit schrijven de defense datum ergens in October is, dus hopelijk, hopelijk, met fingers (en tenen) crossed kan je er bij zijn. (Maar een nieuw leven op de wereld zetten heeft voorrang natuurlijk) **Nicole**, partner in Notch, niemand begreep de FI-NL situatie zo goed als jij! Dankjewel dat je alles al had uitgezocht, je checklist voor het afronden en mentale support voor wanneer de ik door de regeltjes het bos niet meer zag. Daarnaast ben je natuurlijk een top wijf, die aan de kleinste dingen denkt, waar je geweldig mee kan kletsen, klagen en sparren en je stond altijd voor me klaar. Jouw "niet-lullen-maar-poetsen" mentaliteit pas precies wat ik als twijfel-kont soms nodig had. We hebben samen de grootste lol gemaakt, de meeste krukken verloren en de chillste hotelkamers uitgezocht. Bij jou kon ik altijd met mijn gedachten, gevoelens en ideeën terecht en hierdoor was het helemaal geen straf om samen een hotelkamer te delen of de wondere wereld van Notch te betreden. Dankjewel dat je met mijn rare kronkels kon dealen en me schone kleren wilde brengen. Ik ben heel blij jou als collega te hebben gehad en nog blijer dat je zo'n fijne vriendin bent!

Omdat ik tijdens mijn PhD niet alleen aan dit onderzoek heb gewerkt, maar ook mijn eigen tissue heb ge-reengineered, wil ik graag iedereen die mij heeft geholpen om niet alleen één knie, maar 2 knieën werkend te krijgen bedanken. Veel dank aan het medische team; **dr. Bos** en **dr. Sander**

Koëter, en het team van **B&SIS fysiotherapie** en dan met name **Franske, Bernice, Anne, Susanne** die mijn de afgelopen jaren (op)nieuw hebben leren lopen, buigen, strekken, en fysiek gepusht hebben om weer kracht in mijn benen te krijgen en fit genoeg te worden voor een stukje rennen op de loopband. Dank aan **Dirk** voor het lenen van de hometrainer, om tussen het (thuis)werken door ook die knieën even los te draaien. En dank ook aan **Teun** om te leren luisteren naar mijn lichaam en om te leren trots op mezelf te mogen zijn. Dankzij jullie kreeg ik de fysieke en mentale kracht die nodig was dit traject tot een succes te brengen.

Ook een bedankje aan mijn huidige collega's uit het CP gebouw van Organon in Oss. Dank voor jullie begrip en vertrouwen dat ik naast de laatste loodjes van dit promotie traject "gewoon" mijn werk kon doen als Pharmaceutisch Specialist. Dank voor het geduld tijdens het inleren van dit groentje in de industrie, en jullie interesse en support tijdens het afronden van dit traject!

Voor afleiding of stoom afblazen heb ik gelukkig hulp gekregen van mijn lieve vrienden**, Marieke, Marieke, Dorien, Evi, Renske, Saskia** en **Benjamin**, **Nicole, Suup, Willeke, Evelien, Lisette** en **Lars, Anniek** en **Zita** en **Sophie**. Dank voor jullie geduld tijdens mijn soms wat afwezigheid, jullie luisterend oor voor de mooie en minder mooie momenten, gezelligheid tijdens de etentjes, lunches, en feestjes, tips en hulp voor de grote stappen in het leven, de relativering momenten en het sparren over kaften en opmaak strategiën. Ik vind het heel fijn dat jullie nog steeds zijn blijven aanhaken!

Een groot bedankje aan mijn familie. Waaronder mijn schoonfamile **Els, Eric** en **Merel**, dank voor jullie aanhoudende belangstelling, begrip, support en interesse naar de voortgang van dit traject. Dank aan al de "extended" en bijna-familie voor jullie belangstelling! Ik wil in het speciaal mijn oudtantes **Rita** en **Ans** noemen voor de moeite die jullie gestopt hebben in het willen begrijpen van dit complexe onderwerp en het toesturen van een erfstuk, het proefschrift uit 1927. Dank aan **Opa Tiemeijer** die altijd op de hoogte wilde zijn van de voortgang van mijn PhD, ik weet zeker dat je trots op me zou zijn!

Liefste broertje **Bart**, dank dat jij er bent, om me stevig te knuffelen wanneer dat nodig is (en voor de gezelligheid), voor de knieen-knuffels, voor de gezelligheidsbubbel tijdens corona, voor de etentjes en de (zelfgemaakte) drankjes, voor het volgen van deze onbegrijpbare, lastige, tot-het-uiterste-drijvende onderneming: de Phd in de Biomedische Technologie. Dank voor je gulheid, je opbeurend enthousiasme, (bijna) altijd blijvende optimisme en je goede keus in vriendinnen. **Noa**, dank voor

je scherpe blik, je belangstelling, je sport-steuntje-in-de-rug, je attendheid, je gezelligheid, je psychologische inzichten, je etentjes-smaak en de gin-tonics!

Pap en **Mam**, zonder jullie had ik dit niet kunnen doen. Het stimuleren van uitdagende doelen, maar met de garantie dat alles op je eigen tempo mag en moet kunnen is van ontzettend belang geweest tijdens dit onderzoek. Dank voor jullie belangstelling, zorgen, support, onvoorwaardelijke steun en knuffels.

Het allergrootste bedankje gaat natuurlijk naar jou, **Bastiaan**, de voorzitter van mijn fan-club. Dankjewel voor alle peptalks, support, mantelzorg, lekker eten, afleiding, rationale, knuffels, liefde en nog heel veel meer. Ik ben heel dankbaar dat je het al zo lang met mij uithoud. Ik heb heel veel zin in de toekomst waar we beide die dr. titel mogen dragen en ons gaan storten op het volgende project, het nieuwe huis met paradijstuin.

Curriculum Vitae

Laura Angeline Tiemeijer was born on September 11th, 1991 in Eindhoven, the Netherlands. She went to the Van Maerlant Lyceum (then; Pleincollege Van Maerlant) in Eindhoven to obtain her pre-university degree, where she chose for the Nature/Technology and Nature/Health specialization. She enrolled in Biomedical Engineering at the Eindhoven University of Technology and obtained her Bachelor of Science degree in 2013. During her Bachelor's she followed courses at the department of Pharmacology at Utrecht University for her minor. She continued with the Master Biomedical Engineering at Eindhoven University of Technology, specializing in the Regenerative Medicine and Technology track in collaboration with Utrecht University. Her Master's thesis was supervised by Prof. Carlijn Bouten and Prof. Cecilia Sahlgren and during the Master's thesis studies she lay the groundwork for spatial use of Notch ligands. Her externship was performed at the satellite group of Prof. Molly Stevens at the Karolinska Institutet in Stockholm, Sweden. Here she studied the development of polymeric drugs based on RAFT chemistry under the supervision of Dr. Adam Gormley. She obtained her Master of Science degree in 2016. After returning to the Netherlands, she worked as a research assistant for 4 months at the Soft Tissue Engineering and Mechanobiology group of Prof. Carlijn Bouten. In 2017 she started as a joint supervision PhD candidate at the faculty of Science and Engineering, department of Cell Biology of Åbo Akademi in Turku, Finland under supervision of Prof. Cecilia Sahlgren, together with the co-supervision of Prof. Carlijn Bouten at the Eindhoven University of Technology. The findings of her PhD studies are presented in this thesis.

References

1. WHO. Cardiovascular diseases (CVDs). 1–6 (2021). Available at: https://www.who.int/en/news-room/fact-sheets/detail/cardiovascular-diseases-(cvds). (Accessed: 20th July 2021)
2. Mendis, S., Puska, P. & Norrving, B. Global atlas on cardiovascular disease prevention and control. *World Heal. Organ.* 2–14 (2011). doi:NLM classification: WG 120
3. Bouten, C. V. C. *et al.* Substrates for cardiovascular tissue engineering. *Adv. Drug Deliv. Rev.* **63**, 221–241 (2011).
4. Vacanti, J. P. & Langer, R. Tissue engineering: The design and fabrication of living replacement devices for surgical reconstruction and transplantation. *Lancet* **354**, 32–34 (1999).
5. Song, H. H. G., Rumma, R. T., Ozaki, C. K., Edelman, E. R. & Chen, C. S. Vascular Tissue Engineering: Progress, Challenges, and Clinical Promise. *Cell Stem Cell* **22**, 340–354 (2018).
6. Rouwkema, J. & Khademhosseini, A. Vascularization and Angiogenesis in Tissue Engineering: Beyond Creating Static Networks. *Trends Biotechnol.* **34**, 733–745 (2016).
7. Jain, R. K., Au, P., Tam, J., Duda, D. G. & Fukumura, D. Engineering vascularized tissue. *Nat. Biotechnol.* **23**, 821–823 (2005).
8. Malheiro, A., Wieringa, P., Mota, C., Baker, M. & Moroni, L. Patterning Vasculature: The Role of Biofabrication to Achieve an Integrated Multicellular Ecosystem. *ACS Biomater. Sci. Eng.* **2**, 1694–1709 (2016).
9. Martino, M. M. *et al.* Extracellular matrix and growth factor engineering for controlled angiogenesis in regenerative medicine. *Front. Bioeng. Biotechnol.* **3**, 45 (2015).
10. Kant, R. J. & Coulombe, K. L. K. Integrated approaches to spatiotemporally directing angiogenesis in host and engineered tissues. *Acta Biomater.* **69**, 42–62 (2018).
11. Carmeliet, P. Angiogenesis in life, disease and medicine. *Nature* **438**, 932–936 (2005).
12. Phng, L. K. & Gerhardt, H. Angiogenesis: A Team Effort Coordinated by

Notch. *Dev. Cell* **16**, 196–208 (2009).

13. Holderfield, M. T. & Hughes, C. C. W. Crosstalk between vascular endothelial growth factor, notch, and transforming growth factor-β in vascular morphogenesis. *Circ. Res.* **102**, 637–652 (2008).
14. Sjöqvist, M. & Andersson, E. R. Do as I say, Not(ch) as I do: Lateral control of cell fate. *Dev. Biol.* **447**, 58–70 (2019).
15. Bray, S. J. Notch signalling: a simple pathway becomes complex. *Nat. Rev. Mol. Cell Biol.* **7**, 678–689 (2006).
16. Benedito, R. & Hellström, M. Notch as a hub for signaling in angiogenesis. *Exp. Cell Res.* **319**, 1281–1288 (2013).
17. Hellström, M. *et al.* Dll4 signalling through Notch1 regulates formation of tip cells during angiogenesis. *Nature* **445**, 776–780 (2007).
18. Benedito, R. *et al.* The Notch Ligands Dll4 and Jagged1 Have Opposing Effects on Angiogenesis. *Cell* **137**, 1124–1135 (2009).
19. Mašek, J. & Andersson, E. R. The developmental biology of genetic notch disorders. *Dev.* **144**, 1743–1763 (2017).
20. Andersson, E. R. & Lendahl, U. Therapeutic modulation of Notch signalling-are we there yet? *Nat. Rev. Drug Discov.* **13**, 357–378 (2014).
21. Couch, J. A. *et al.* Balancing Efficacy and Safety of an Anti-DLL4 Antibody through Pharmacokinetic Modulation. *Clin. Cancer Res.* **22**, 1469–1479 (2016).
22. Varnum-Finney, B. *et al.* Immobilization of Notch ligand, Delta-1, is required for induction of notch signaling. *J. Cell Sci.* **113 Pt 23**, 4313–4318 (2000).
23. Delaney, C. *et al.* Notch-mediated expansion of human cord blood progenitor cells capable of rapid myeloid reconstitution. *Nat. Med.* **16**, 232–236 (2010).
24. Osathanon, T. *et al.* Surface-bound orientated Jagged-1 enhances osteogenic differentiation of human periodontal ligament-derived mesenchymal stem cells. *J. Biomed. Mater. Res. Part A* **101A**, 358–367 (2013).
25. Marieb, E. N. & Hoehn, K. Chapter 19 The Cardiovascular system: Blood Vessels. in *Human Anatomy & Physiology* (ed. Beauparlant, S.) 695–745 (Pearson Benjamin Cummings, 2010).
26. Atkins, G. B., Jain, M. K. & Hamik, A. Endothelial differentiation: Molecular

mechanisms of specification and heterogeneity. *Arterioscler. Thromb. Vasc. Biol.* **31**, 1476–1484 (2011).

27. Bazzoni, G. & Dejana, E. Endothelial cell-to-cell junctions: Molecular organization and role in vascular homeostasis. *Physiol. Rev.* **84**, 869–901 (2004).
28. Simionescu, M., Simionescu, N. & Palade, G. E. Morphometric data on the endothelium of blood capillaries. *J. Cell Biol.* **60**, 128–152 (1974).
29. Braet, F. & Wisse, E. Structural and functional aspects of liver sinusoidal endothelial cells fenestrae: a review. *Comp. Hepatol.* **1**, (2002).
30. Potente, M., Gerhardt, H. & Carmeliet, P. Basic and therapeutic aspects of angiogenesis. *Cell* **146**, 873–887 (2011).
31. Gerhardt, H. & Betsholtz, C. Endothelial-pericyte interactions in angiogenesis. *Cell Tissue Res.* **314**, 15–23 (2003).
32. Potente, M. & Carmeliet, P. The Link Between Angiogenesis and Endothelial Metabolism. *Annu. Rev. Physiol.* **79**, 43–66 (2017).
33. Chang, W. G. & Niklason, L. E. A short discourse on vascular tissue engineering. *npj Regen. Med.* **2**, 7 (2017).
34. Laurent, J. *et al.* Convergence of microengineering and cellular self-organization towards functional tissue manufacturing. *Nat. Biomed. Eng.* **1**, 939–956 (2017).
35. Bogorad, M. I. *et al.* Review: in vitro microvessel models. *Lab Chip* **15**, 4242–4255 (2015).
36. Ngo, M. T. & Harley, B. A. C. Angiogenic biomaterials to promote therapeutic regeneration and investigate disease progression. *Biomaterials* **255**, 120207 (2020).
37. Zheng, Y. *et al.* Notch signaling in regulating angiogenesis in a 3D biomimetic environment. *Lab Chip* 18–22 (2017). doi:10.1039/C7LC00186J
38. Raghavan, S., Nelson, C. M., Baranski, J. D., Lim, E. & Chen, C. S. Geometrically controlled endothelial tubulogenesis in micropatterned gels. *Tissue Eng. Part A* **16**, 2255–2263 (2010).
39. Miller, J. S. *et al.* Rapid casting of patterned vascular networks for perfusable engineered three-dimensional tissues. *Nat. Mater.* **11**, 768–774 (2012).

40. Nishiguchi, A., Matsusaki, M., Asano, Y., Shimoda, H. & Akashi, M. Effects of angiogenic factors and 3D-microenvironments on vascularization within sandwich cultures. *Biomaterials* **35**, 4739–4748 (2014).
41. Fang, Y., Zhang, T., Zhang, L., Gong, W. & Sun, W. Biomimetic design and fabrication of scaffolds integrating oriented micro-pores with branched channel networks for myocardial tissue engineering. *Biofabrication* (2019). doi:10.1088/1758-5090/ab0fd3
42. Zheng, Y. *et al.* In vitro microvessels for the study of angiogenesis and thrombosis. *Proc. Natl. Acad. Sci.* **109**, 9342–9347 (2012).
43. Song, H. H. G., Park, K. M. & Gerecht, S. Hydrogels to model 3D in vitro microenvironment of tumor vascularization. *Adv. Drug Deliv. Rev.* **79**, 19–29 (2014).
44. Morgan, J. T., Shirazi, J., Comber, E. M., Eschenburg, C. & Gleghorn, J. P. Fabrication of centimeter-scale and geometrically arbitrary vascular networks using in vitro self-assembly. *Biomaterials* **189**, 37–47 (2018).
45. Kim, S., Lee, H., Chung, M. & Jeon, N. L. Engineering of functional, perfusable 3D microvascular networks on a chip. *Lab Chip* **13**, 1489 (2013).
46. Moya, M. L., Hsu, Y.-H., Lee, A. P., Hughes, C. C. W. & George, S. C. In Vitro Perfused Human Capillary Networks. *Tissue Eng. Part C Methods* **19**, 730–737 (2013).
47. Devolder, R. J., Bae, H., Lee, J. & Kong, H. Directed blood vessel growth using an angiogenic microfiber/microparticle composite patch. *Adv. Mater.* **23**, 3139–3143 (2011).
48. Lee, V. K. *et al.* Generation of multi-scale vascular network system within 3D hydrogel using 3D bio-printing technology. *Cell. Mol. Bioeng.* **7**, 460–472 (2014).
49. Edgar, L. T., Underwood, C. J., Guilkey, J. E., Hoying, J. B. & Weiss, J. A. Extracellular matrix density regulates the rate of neovessel growth and branching in sprouting angiogenesis. *PLoS One* **9**, 1–10 (2014).
50. Silva, E. A., Eseonu, C. & Mooney, D. J. Endothelial cells expressing low levels of CD143 (ACE) exhibit enhanced sprouting and potency in relieving tissue ischemia. *Angiogenesis* **17**, 617–630 (2014).

51. Yuen, W. W. *et al.* Statistical platform to discern spatial and temporal coordination of endothelial sprouting. *Integr. Biol. (Camb).* **4**, 292–300 (2012).
52. Cao, L. & Mooney, D. J. Spatiotemporal control over growth factor signaling for therapeutic neovascularization. *Adv. Drug Deliv. Rev.* **59**, 1340–1350 (2007).
53. Anderson, E. M. & Mooney, D. J. The Combination of Vascular Endothelial Growth Factor and Stromal Cell-Derived Factor Induces Superior Angiogenic Sprouting by Outgrowth Endothelial Cells. *J. Vasc. Res.* **52**, 62–69 (2015).
54. Cao, L. *et al.* Modulating Notch signaling to enhance neovascularization and reperfusion in diabetic mice. *Biomaterials* **31**, 9048–9056 (2010).
55. Cao, L., Arany, P. R., Wang, Y.-S. & Mooney, D. J. Promoting Angiogenesis via Manipulation of VEGF Responsiveness with Notch Signaling. *Biomaterials* **30**, 4085–4093 (2009).
56. Klose, R. *et al.* Soluble Notch ligand and receptor peptides act antagonistically during angiogenesis. *Cardiovasc. Res.* **107**, 153–163 (2015).
57. Gazave, E. *et al.* Origin and evolution of the Notch signalling pathway: An overview from eukaryotic genomes. *BMC Evol. Biol.* **9**, 1–27 (2009).
58. Siebel, C. & Lendahl, U. Notch signaling in development, tissue homeostasis, and disease. *Physiol. Rev.* **97**, 1235–1294 (2017).
59. Pursglove, S. E. & Mackay, J. P. CSL: A notch above the rest. *Int. J. Biochem. Cell Biol.* **37**, 2472–2477 (2005).
60. Luca, V. C. *et al.* Notch-Jagged complex structure implicates a catch bond in tuning ligand sensitivity. *Science (80-.).* **1324**, 1320–1324 (2017).
61. Kangsamaksin, T. *et al.* NOTCH decoys that selectively block DLL/NOTCH or JAG/NOTCH disrupt angiogenesis by unique mechanisms to inhibit tumor growth. *Cancer Discov.* **5**, 182–197 (2015).
62. Handford, P. A., Korona, B., Suckling, R., Redfield, C. & Lea, S. M. *Structural insights into notch receptor-ligand interactions*. *Molecular Mechanisms of Notch Signaling* **1066**, (Springer International Publishing AG, part of Springer Nature 2018, 2018).

63. Hori, K., Sen, A. & Artavanis-Tsakonas, S. Notch signaling at a glance. *J. Cell Sci.* **126**, 2135–2140 (2013).
64. Felician, G. *et al.* Epigenetic modification at Notch responsive promoters blunts efficacy of inducing Notch pathway reactivation after myocardial infarction. *Circ. Res.* **115**, 636–649 (2014).
65. Ehebauer, M., Hayward, P. & Arias, A. M. Notch, a universal arbiter of cell fate decisions. *Science* **314**, 1414–1415 (2006).
66. Chiba, S. Notch signaling in stem cell systems. *Stem Cells* **24**, 2437–2447 (2006).
67. Androutsellis-Theotokis, A. *et al.* Notch signalling regulates stem cell numbers in vitro and in vivo. *Nature* **442**, 823–826 (2006).
68. Kwon, C. *et al.* Notch post-translationally regulates β-catenin protein in stem and progenitor cells. *Nat. Cell Biol.* **13**, 1244–51 (2011).
69. Andersen, P., Uosaki, H., Shenje, L. T. & Kwon, C. Non-canonical Notch signaling: Emerging role and mechanism. *Trends Cell Biol.* **22**, 257–265 (2012).
70. Polacheck, W. J. *et al.* A non-canonical Notch complex regulates adherens junctions and vascular barrier function. *Nature* **552**, 258–262 (2017).
71. Rostama, B., Peterson, S. M., Vary, C. P. H. & Liaw, L. Notch signal integration in the vasculature during remodeling. *Vascul. Pharmacol.* **63**, 97–104 (2014).
72. De la Pompa, J. L. & Epstein, J. A. Coordinating Tissue Interactions: Notch Signaling in Cardiac Development and Disease. *Dev. Cell* **22**, 244–254 (2012).
73. MacK, J. J. & Luisa Iruela-Arispe, M. NOTCH regulation of the endothelial cell phenotype. *Curr. Opin. Hematol.* **25**, 212–218 (2018).
74. Manderfield, L. J. *et al.* Notch activation of Jagged1 contributes to the assembly of the arterial wall. *Circulation* **125**, 314–323 (2012).
75. Driessen, R. C. H. *et al.* Shear stress induces expression, intracellular reorganization and enhanced Notch activation potential of Jagged1. *Integr. Biol.* (2018). doi:10.1039/C8IB00036K
76. Watson, O. *et al.* Blood flow suppresses vascular Notch signalling via dll4

and is required for angiogenesis in response to hypoxic signalling. *Cardiovasc. Res.* **100**, 252–261 (2013).

77. Mack, J. J. *et al.* NOTCH1 is a mechanosensor in adult arteries. *Nat. Commun.* **8**, 1–18 (2017).
78. High, F. A. *et al.* Endothelial expression of the Notch ligand Jagged1 is required for vascular smooth muscle development. *Proc. Natl. Acad. Sci. U. S. A.* **105**, 1955–1959 (2008).
79. Liu, H., Kennard, S. & Lilly, B. NOTCH3 expression is induced in mural cells through an autoregulatory loop that requires Endothelial-expressed JAGGED1. *Circ. Res.* **104**, 466–475 (2009).
80. Loerakker, S. *et al.* Mechanosensitivity of Jagged–Notch signaling can induce a switch-type behavior in vascular homeostasis. *Proc. Natl. Acad. Sci.* **115**, E3682–E3691 (2018).
81. Engeland, N. C. A. Van *et al.* Vimentin regulates Notch signaling strength and arterial remodeling in response to hemodynamic stress. 1–14 (2019). doi:10.1038/s41598-019-48218-w
82. Stassen, O. M. J. A., Ristori, T. & Sahlgren, C. M. Notch in mechanotransduction – from molecular mechanosensitivity to tissue mechanostasis. *J. Cell Sci.* **133**, (2021).
83. Roca, C. & Adams, R. H. Regulation of vascular morphogenesis by Notch signaling. *Genes Dev.* **21**, 2511–2524 (2007).
84. Sainson, R. C. A. & Harris, A. L. Regulation of angiogenesis by homotypic and heterotypic notch signalling in endothelial cells and pericytes: From basic research to potential therapies. *Angiogenesis* **11**, 41–51 (2008).
85. Hirashima, M. Regulation of endothelial cell differentiation and arterial specification by VEGF and Notch signaling. *Anat. Sci. Int.* **84**, 95–101 (2009).
86. Gaengel, K., Genové, G., Armulik, A. & Betsholtz, C. Endothelial-mural cell signaling in vascular development and angiogenesis. *Arterioscler. Thromb. Vasc. Biol.* **29**, 630–638 (2009).
87. Shawber, C. J. & Kitajewski, J. Notch function in the vasculature: Insights from zebrafish, mouse and man. *BioEssays* **26**, 225–234 (2004).
88. Skuli, N. *et al.* Endothelial HIF-2?? regulates murine pathological

angiogenesis and revascularization processes. *J. Clin. Invest.* **122**, 1427–1443 (2012).

89. Lobov, I. B. *et al.* Delta-like ligand 4 (Dll4) is induced by VEGF as a negative regulator of angiogenic sprouting. *Proc. Natl. Acad. Sci. U. S. A.* **104**, 3219–24 (2007).

90. Scehnet, J. S. *et al.* Inhibition of Dll4-mediated signaling induces proliferation of immature vessels and results in poor tissue perfusion. *Blood* **109**, 4753–4760 (2007).

91. Lu, P. *et al.* Perinatal angiogenesis from pre-existing coronary vessels via DLL4–NOTCH1 signalling. *Nat. Cell Biol.* **23**, 967–977 (2021).

92. Adams, R. H. & Eichmann, A. Axon Guidance Molecules in Vascular Patterning. *Cold Spring Harb. Perspect. Biol.* **2**, a001875 (2010).

93. Blanco, R. & Gerhardt, H. VEGF and Notch in tip and stalk cell selection. *Cold Spring Harb. Perspect. Med.* **3**, 1–20 (2013).

94. Sainson, R. C. & Harris, A. L. Hypoxia-regulated differentiation: let's step it up a Notch. *Trends Mol. Med.* **12**, 141–143 (2006).

95. Benedito, R. *et al.* The Notch Ligands Dll4 and Jagged1 Have Opposing Effects on Angiogenesis. *Cell* **137**, 1124–1135 (2009).

96. Bentley, K., Gerhardt, H. & Bates, P. A. Agent-based simulation of notch-mediated tip cell selection in angiogenic sprout initialisation. *J. Theor. Biol.* **250**, 25–36 (2008).

97. Bentley, K. *et al.* The role of differential VE-cadherin dynamics in cell rearrangement during angiogenesis. *Nat. Cell Biol.* **16**, 309–321 (2014).

98. Jakobsson, L., Bentley, K. & Gerhardt, H. VEGFRs and Notch: a dynamic collaboration in vascular patterning. *Biochem. Soc. Trans.* **37**, 1233–1236 (2009).

99. Marchetto, N. M. *et al.* Endothelial jagged1 antagonizes dll4/notch signaling in decidual angiogenesis during early mouse pregnancy. *Int. J. Mol. Sci.* **21**, 1–20 (2020).

100. Jin, S. *et al.* Notch signaling regulates platelet-derived growth factor receptor-?? expression in vascular smooth muscle cells. *Circ. Res.* **102**, 1483–1491 (2008).

101. Andersson, E. R. *et al.* Mouse Model of Alagille Syndrome and Mechanisms of Jagged1 Missense Mutations. *Gastroenterology* **154**, 1080–1095 (2018).
102. Sega, F. V. D. *et al.* Notch signaling regulates immune responses in atherosclerosis. *Front. Immunol.* **10**, 1–13 (2019).
103. Ferrari, R. & Rizzo, P. The Notch pathway: A novel target formyocardial remodelling therapy? *Eur. Heart J.* **35**, 2140–2145 (2014).
104. Huang, F. *et al.* Mesenchymal stem cells modified with miR-126 release angiogenic factors and activate Notch ligand Delta-like-4, enhancing ischemic angiogenesis and cell survival. *Int. J. Mol. Med.* **31**, 484–492 (2013).
105. Al Haj Zen, A. *et al.* Inhibition of delta-like-4-mediated signaling impairs reparative angiogenesis after ischemia. *Circ. Res.* **107**, 283–293 (2010).
106. Gude, N. & Sussman, M. Notch signaling and cardiac repair. *J. Mol. Cell. Cardiol.* **52**, 1226–1232 (2012).
107. Niessen, K. & Karsan, A. Notch signaling in cardiac development. *Circ. Res.* **102**, 1169–1181 (2008).
108. Meisel, C. T., Porcheri, C. & Mitsiadis, T. A. Cancer Stem Cells, Quo Vadis? The Notch Signaling Pathway in Tumor Initiation and Progression. *Cells* **9**, (2020).
109. Jung, Y. D. *et al.* The role of the microenvironment and intercellular cross-talk in tumor angiogenesis. *Semin. Biol.* **12**, 105–112 (2002).
110. Zeng, Q. *et al.* Crosstalk between tumor and endothelial cells promotes tumor angiogenesis by MAPK activation of Notch signaling. *Cancer Cell* **8**, 13–23 (2005).
111. Hainaud, P. *et al.* The role of the vascular endothelial growth factor-Delta-like 4 ligand/Notch4-Ephrin B2 cascade in tumor vessel remodeling and endothelial cell functions. *Cancer Res.* **66**, 8501–8510 (2006).
112. Ohnuki, H. *et al.* Tumor-infiltrating myeloid cells activate Dll4/Notch/TGF-?? signaling to drive malignant progression. *Cancer Res.* **74**, 2038–2049 (2014).
113. Oon, C. E. *et al.* Role of Delta-like 4 in Jagged1-induced tumour angiogenesis and tumour growth. *Oncotarget* **8**, 40115–40131 (2017).
114. Liu, Z., Fan, F., Wang, A., Zheng, S. & Lu, Y. Dll4-Notch signaling in regulation

of tumor angiogenesis. *J. Cancer Res. Clin. Oncol.* **140**, 525–536 (2014).

115. Wieland, E. *et al.* Endothelial Notch1 Activity Facilitates Metastasis. *Cancer Cell* **31**, 355–367 (2017).
116. Ristori, T., Sjöqvist, M. & Sahlgren, C. M. Ex vivo models to decipher the molecular mechanisms of genetic Notch cardiovascular disorders. *Tissue Eng. Part C Methods* **00**, 1–10 (2021).
117. Boareto, M. *et al.* Jagged–Delta asymmetry in Notch signaling can give rise to a Sender/Receiver hybrid phenotype. *Proc. Natl. Acad. Sci.* **112**, E402–E409 (2015).
118. Ristori, T., Stassen, O. M. J. A., Sahlgren, C. M. & Loerakker, S. Lateral induction limits the impact of cell connectivity on Notch signaling in arterial walls. *Int. j. numer. method. biomed. eng.* **36**, 1–21 (2020).
119. Shaya, O. *et al.* Cell-Cell Contact Area Affects Notch Signaling and Notch-Dependent Patterning. *Dev. Cell* **40**, 505-511.e6 (2017).
120. Heck, T., Vaeyens, M. & Van Oosterwyck, H. Computational models of sprouting angiogenesis and cell migration: towards multiscale mechanochemical models of angiogenesis. *Math. Model. Nat. Phenom.* **xx**, 1–46 (2015).
121. Palm, M. M. *et al.* Computational screening of tip and stalk cell behavior proposes a role for apelin signaling in sprout progression. *PLoS One* **11**, 1–31 (2016).
122. Moreira-Soares, M., Coimbra, R., Rebelo, L., Carvalho, J. & Travasso, R. D. M. Angiogenic Factors produced by Hypoxic Cells are a leading driver of Anastomoses in Sprouting Angiogenesis-a computational study. *Sci. Rep.* **8**, 1–12 (2018).
123. Boareto, M., Kumar, M., Ben-jacob, E. & Onuchic, J. N. Jagged mediates differences in normal and tumor angiogenesis by affecting tip-stalk fate decision. (2015). doi:10.1073/pnas.1511814112
124. Zakirov, B. *et al.* Active perception during angiogenesis: Filopodia speed up Notch selection of tip cells in silico and in vivo. *Philos. Trans. R. Soc. B Biol. Sci.* **376**, (2021).
125. Vega, R., Carretero, M., Travasso, R. D. M. & Bonilla, L. L. *Notch signaling and*

taxis mechanims regulate early stage angiogenesis: A mathematical and computational model. *PLoS Computational Biology* **16**, (2020).

126. Venkatraman, L., Regan, E. R. & Bentley, K. Time to decide? Dynamical analysis predicts partial tip/stalk patterning states arise during angiogenesis. *PLoS One* **11**, 1–23 (2016).
127. Bentley, K. & Chakravartula, S. The temporal basis of angiogenesis. *Philos. Trans. R. Soc. B Biol. Sci.* **372**, (2017).
128. Benedito, R. & Hellström, M. Notch as a hub for signaling in angiogenesis. *Exp. Cell Res.* **319**, 1281–1288 (2013).
129. Andersson, E. R. & Lendahl, U. Therapeutic modulation of Notch signalling — are we there yet? *Nat. Publ. Gr.* **13**, 357–378 (2014).
130. Tiemeijer, L. A., Sanlidag, S., Bouten, C. V. C. & Sahlgren, C. M. Engineering tissue morphogenesis : taking it up a Notch. *Trends Biotechnol.* **xx**, 1–13 (2022).
131. Tung, J. C., Paige, S. L., Ratner, B. D., Murry, C. E. & Giachelli, C. M. Engineered Biomaterials Control Differentiation and Proliferation of Human-Embryonic-Stem-Cell-Derived Cardiomyocytes via Timed Notch Activation. *Stem Cell Reports* **2**, 271–281 (2014).
132. Wu, Y. *et al.* Therapeutic antibody targeting of individual Notch receptors. *Nature* **464**, 1052–1057 (2010).
133. Choy, L. *et al.* Constitutive NOTCH3 signaling promotes the growth of basal breast cancers. *Cancer Res.* **77**, 1439–1452 (2017).
134. Machuca-Parra, A. I. *et al.* Therapeutic antibody targeting of Notch3 signaling prevents mural cell loss in CADASIL. *J. Exp. Med.* **214**, 2271–2282 (2017).
135. Putti, M., Stassen, O. M. J. A., Schotman, M. J. G., Sahlgren, C. M. & Dankers, P. Y. W. Influence of the Assembly State on the Functionality of a Supramolecular Jagged1-Mimicking Peptide Additive. *ACS Omega* **4**, 8178–8187 (2019).
136. Goruganthu, M. U. L., Shanker, A., Dikov, M. M. & Carbone, D. P. Specific Targeting of Notch Ligand-Receptor Interactions to Modulate Immune Responses: A Review of Clinical and Preclinical Findings. *Front. Immunol.*

11, 1–14 (2020).

137. Mamaeva, V. *et al.* Mesoporous silica nanoparticles as drug delivery systems for targeted inhibition of notch signaling in cancer. *Mol. Ther.* **19**, 1538–1546 (2011).
138. Mamaeva, V. *et al.* Inhibiting notch activity in breast cancer stem cells by glucose functionalized nanoparticles carrying γ-secretase inhibitors. *Mol. Ther.* **24**, 926–936 (2016).
139. Nandagopal, N. *et al.* Dynamic Ligand Discrimination in the Notch Signaling Pathway. *Cell* **172**, 869-880.e19 (2018).
140. Rizwan, M. *et al.* Photochemically Activated Notch Signaling Hydrogel Preferentially Differentiates Human Derived Hepatoblasts to Cholangiocytes. *Adv. Funct. Mater.* **31**, 1–15 (2021).
141. Bi, P. *et al.* Stage-specific effects of Notch activation during skeletal myogenesis. *Elife* **5**, 1–22 (2016).
142. Zhang, Y. *et al.* Oscillations of Delta-like1 regulate the balance between differentiation and maintenance of muscle stem cells. *Nat. Commun.* **12**, (2021).
143. Dallas, M. H., Varnum-Finney, B., Delaney, C., Kato, K. & Bernstein, I. D. Density of the Notch ligand Delta1 determines generation of B and T cell precursors from hematopoietic stem cells. *J. Exp. Med.* **201**, 1361–1366 (2005).
144. Gonçalves, R. M., Martins, M. C. L., Almeida-Porada, G. & Barbosa, M. A. Induction of notch signaling by immobilization of jagged-1 on self-assembled monolayers. *Biomaterials* **30**, 6879–6887 (2009).
145. Blache, U. *et al.* Notch-inducing hydrogels reveal a perivascular switch of mesenchymal stem cell fate. *EMBO Rep.* e45964 (2018). doi:10.15252/embr.201845964
146. Delaney, C., Varnum-Finney, B., Aoyama, K., Brashem-Stein, C. & Bernstein, I. D. Dose-dependent effects of the Notch ligand Delta1 on ex vivo differentiation and in vivo marrow repopulating ability of cord blood cells. *Blood* **106**, 2693–2699 (2005).
147. Kim, H. *et al.* Notch ligand Delta-like 1 promotes in vivo vasculogenesis in

human cord blood–derived endothelial colony forming cells. *Cytotherapy* **17**, 579–592 (2015).

148. Winkler, A. L. *et al.* Significance of Nanopatterned and Clustered DLL1 for Hematopoietic Stem Cell Proliferation. *Adv. Funct. Mater.* **27**, 1–13 (2017).
149. Lee, J. & Kotov, N. A. Notch ligand presenting acellular 3d microenvironments for ex vivo human hematopoietic stem-cell culture made by layer-by-layer assembly. *Small* **5**, 1008–1013 (2009).
150. Beckstead, B. L., Santosa, D. M. & Giachelli, C. M. Mimicking cell–cell interactions at the biomaterial–cell interface for control of stem cell differentiation. *J. Biomed. Mater. Res. Part A* **79A**, 94–103 (2006).
151. Taqvi, S., Dixit, L. & Roy, K. Biomaterial-based notch signaling for the differentiation of hematopoietic stem cells into T cells. *J. Biomed. Mater. Res. Part A* **79A**, 689–697 (2006).
152. Shah, N. J. *et al.* An injectable bone marrow–like scaffold enhances T cell immunity after hematopoietic stem cell transplantation. *Nat. Biotechnol.* **37**, 293–302 (2019).
153. Toda, H., Yamamoto, M., Kohara, H. & Tabata, Y. Orientation-regulated immobilization of Jagged1 on glass substrates for ex vivo proliferation of a bone marrow cell population containing hematopoietic stem cells. *Biomaterials* **32**, 6920–6928 (2011).
154. Osathanon, T., Nowwarote, N., Manokawinchoke, J. & Pavasant, P. bFGF and JAGGED1 regulate alkaline phosphatase expression and mineralization in dental tissue-derived mesenchymal stem cells. *J. Cell. Biochem.* **114**, 2551–2561 (2013).
155. Sukarawan, W., Peetiakarawach, K., Pavasant, P. & Osathanon, T. Effect of Jagged-1 and Dll-1 on osteogenic differentiation by stem cells from human exfoliated deciduous teeth. *Arch. Oral Biol.* **65**, 1–8 (2016).
156. Manokawinchoke, J. *et al.* Indirect immobilized Jagged1 suppresses cell cycle progression and induces odonto/osteogenic differentiation in human dental pulp cells. *Sci. Rep.* **7**, 10124 (2017).
157. Nowwarote, N. *et al.* Characterization of a bioactive Jagged1-coated polycaprolactone-based membrane for guided tissue regeneration. *Arch.*

Oral Biol. **88**, 24–33 (2018).

158. Beckstead, B. L. *et al.* Methods to promote Notch signaling at the biomaterial interface and evaluation in a rafted organ culture model. *J. Biomed. Mater. Res. Part A* **91A**, 436–446 (2009).
159. Nickoloff, B. J. *et al.* Jagged-1 mediated activation of notch signaling induces complete maturation of human keratinocytes through NF-κB and PPARγ. *Cell Death Differ.* **9**, 842–855 (2002).
160. Matea, C. T., Mocan, T., Tabaran, F., Iancu, C. & Mocan, L. C. Rational design of gold nanocarrier for the delivery of JAG-1 peptide. *J. Nanobiotechnology* **13**, 1–11 (2015).
161. Gerbin, K. A., Mitzelfelt, K. A., Guan, X., Martinson, A. M. & Murry, C. E. Delta-1 Functionalized Hydrogel Promotes hESC-Cardiomyocyte Graft Proliferation and Maintains Heart Function Post-Injury. *Mol. Ther. - Methods Clin. Dev.* **17**, 986–998 (2020).
162. Wen, F. *et al.* Induction of Myogenic Differentiation of Human Mesenchymal Stem Cells Cultured on Notch Agonist (Jagged-1) Modified Biodegradable Scaffold Surface. *ACS Appl. Mater. Interfaces* **6**, 1652–1661 (2014).
163. Valcourt, D. M., Dang, M. N., Scully, M. A. & Day, E. S. Nanoparticle-Mediated Co-Delivery of Notch-1 Antibodies and ABT-737 as a Potent Treatment Strategy for Triple-Negative Breast Cancer. *ACS Nano* **14**, 3378–3388 (2020).
164. Ndong, J. D. L. C., Stephenson, Y., Davis, M. E., García, A. J. & Goudy, S. Controlled JAGGED1 delivery induces human embryonic palate mesenchymal cells to form osteoblasts. *J. Biomed. Mater. Res. Part A* **106**, 552–560 (2018).
165. Safaee, H. *et al.* Tethered Jagged-1 Synergizes with Culture Substrate Stiffness to Modulate Notch-Induced Myogenic Progenitor Differentiation. *Cell. Mol. Bioeng.* **10**, 501–513 (2017).
166. Kim, H. *et al.* Notch ligand Delta-like 1 promotes in vivo vasculogenesis in human cord blood–derived endothelial colony forming cells. *Cytotherapy* **17**, 579–592 (2015).
167. Winkler, A.-L. *et al.* Bioinstructive Coatings for Hematopoietic Stem Cell

Expansion Based on Chemical Vapor Deposition Copolymerization. *Biomacromolecules* **18**, 3089–3098 (2017).

168. Sukarawan, W., Peetiakarawach, K. & Pavasant, P. Archives of Oral Biology Effect of Jagged-1 and Dll-1 on osteogenic differentiation by stem cells from human exfoliated deciduous teeth. *Arch. Oral Biol.* **65**, 1–8 (2016).
169. Seo, D. *et al.* A mechanogenetic toolkit for interrogating cell signaling in space and time. *Cell* **165**, 1507–1518 (2016).
170. Kaylan, K. B. *et al.* Spatial patterning of liver progenitor cell differentiation mediated by cellular contractility and Notch signaling. *Elife* **7**, 1–23 (2018).
171. Narui, Y. & Salaita, K. Membrane Tethered Delta Activates Notch and Reveals a Role for Spatio-Mechanical Regulation of the Signaling Pathway. *Biophys. J.* **105**, 2655–2665 (2013).
172. Liu, L., Wada, H., Matsubara, N., Hozumi, K. & Itoh, M. Identification of Domains for Efficient Notch Signaling Activity in Immobilized Notch Ligand Proteins. *J. Cell. Biochem.* **118**, 785–796 (2017).
173. Tiemeijer, L. A., Frimat, J., Stassen, O. M. J. A., Bouten, C. V. C. & Sahlgren, C. M. Spatial patterning of the Notch ligand Dll4 controls endothelial sprouting in vitro. *Sci. Rep.* **8**, 6392 (2018).
174. DeForest, C. A. & Tirrell, D. A. A photoreversible protein-patterning approach for guiding stem cell fate in three-dimensional gels. *Nat. Mater.* **14**, 523–531 (2015).
175. Blache, U. *et al.* Notch-inducing hydrogels reveal a perivascular switch of mesenchymal stem cell fate. *EMBO Rep.* **19**, (2018).
176. Putti, M., de Jong, S. M. J., Stassen, O. M. J. A., Sahlgren, C. M. & Dankers, P. Y. W. A Supramolecular Platform for the Introduction of Fc-Fusion Bioactive Proteins on Biomaterial Surfaces. *ACS Appl. Polym. Mater.* **1**, 2044–2054 (2019).
177. Boopathy, A. V. *et al.* The modulation of cardiac progenitor cell function by hydrogel-dependent Notch1 activation. *Biomaterials* **35**, 8103–8112 (2014).
178. Dishowitz, M. I. *et al.* Jagged1 immobilization to an osteoconductive polymer activates the Notch signaling pathway and induces osteogenesis. *J. Biomed. Mater. Res. Part A* **102**, 1558–1567 (2014).

179. Mamaeva, V. *et al.* Inhibiting notch activity in breast cancer stem cells by glucose functionalized nanoparticles carrying γ-secretase inhibitors. *Mol. Ther.* **24**, 926–936 (2016).
180. Richter, L. R. *et al.* Targeted Delivery of Notch Inhibitor Attenuates Obesity-Induced Glucose Intolerance and Liver Fibrosis. *ACS Nano* **14**, 6878–6886 (2020).
181. Kim, M. J. *et al.* Notch1 targeting siRNA delivery nanoparticles for rheumatoid arthritis therapy. *J. Control. Release* **216**, 140–148 (2015).
182. Chillakuri, C. R. *et al.* Structural Analysis Uncovers Lipid-Binding Properties of Notch Ligands. *Cell Rep.* **5**, 861–867 (2013).
183. Kovall, R. A., Gebelein, B., Sprinzak, D. & Kopan, R. The Canonical Notch Signaling Pathway: Structural and Biochemical Insights into Shape, Sugar, and Force. *Dev. Cell* **41**, 228–241 (2017).
184. Deforest, C. A. & Tirrell, D. A. A photoreversible protein-patterning approach for guiding stem cell fate in three-dimensional gels. *Nat. Mater.* **14**, 523–531 (2015).
185. López-Guerra, M. *et al.* Specific NOTCH1 antibody targets DLL4-induced proliferation, migration, and angiogenesis in NOTCH1-mutated CLL cells. *Oncogene* **39**, 1185–1197 (2020).
186. Jenkins, D. W. *et al.* MEDI0639: A novel therapeutic antibody targeting Dll4 modulates endothelial cell function and angiogenesis in vivo. *Mol. Cancer Ther.* **11**, 1650–1660 (2012).
187. McKeage, M. J. *et al.* Phase IB Trial of the Anti-Cancer Stem Cell DLL4-Binding Agent Demcizumab with Pemetrexed and Carboplatin as First-Line Treatment of Metastatic Non-Squamous NSCLC. *Target. Oncol.* **13**, 89–98 (2017).
188. Liu, Y. R. *et al.* Delta-like ligand 4-targeted nanomedicine for antiangiogenic cancer therapy. *Biomaterials* **42**, 161–171 (2015).
189. Liu, P. *et al.* Tazarotene-loaded PLGA nanoparticles potentiate deep tissue pressure injury healing via VEGF-Notch signaling. *Mater. Sci. Eng. C* **114**, 111027 (2020).
190. Boopathy, A. V. *et al.* Intramyocardial Delivery of Notch Ligand-Containing

Hydrogels Improves Cardiac Function and Angiogenesis Following Infarction. *Tissue Eng. - Part A* **21**, 2315–2322 (2015).

191. Casanova, M. R. *et al.* Spatial immobilization of endogenous growth factors to control vascularization in bone tissue engineering. *Biomater. Sci.* **8**, 2577–2589 (2020).
192. Kwee, B. J. & Mooney, D. J. Manipulating the Intersection of Angiogenesis and Inflammation. *Ann. Biomed. Eng.* **43**, 628–640 (2015).
193. Song, H.-H. G., Rumma, R. T., Ozaki, C. K., Edelman, E. R. & Chen, C. S. Review Vascular Tissue Engineering : Progress, Challenges, and Clinical Promise. *Cell Stem Cell* **22**, 340–354 (2018).
194. Blanco, R. & Gerhardt, H. VEGF and Notch in tip and stalk cell selection. *Cold Spring Harb. Perspect. Med.* **3**, 1–20 (2013).
195. Kofler, N. M. *et al.* Notch Signaling in Developmental and Tumor Angiogenesis. *Genes and Cancer* **2**, 1106–1116 (2011).
196. Gale, N. W. *et al.* Haploinsufficiency of delta-like 4 ligand results in embryonic lethality due to major defects in arterial and vascular development. *Proc. Natl. Acad. Sci. U. S. A.* **101**, 15949–15954 (2004).
197. Krebs, L. T. *et al.* Notch signaling is essential for vascular morphogenesis in mice. *Genes Dev.* **14**, 1343–1352 (2000).
198. Jakobsson, L. *et al.* Endothelial cells dynamically compete for the tip cell position during angiogenic sprouting. *Nat. Cell Biol.* **12**, 943–953 (2010).
199. Margadant, C. Positive and negative feedback mechanisms controlling tip/stalk cell identity during sprouting angiogenesis. *Angiogenesis* **18**, 3–5 (2020).
200. Bentley, K. & Chakravartula, S. The temporal basis of angiogenesis. *Philos. Trans. R. Soc. B Biol. Sci.* **372**, (2017).
201. Arima, S. *et al.* Angiogenic morphogenesis driven by dynamic and heterogeneous collective endothelial cell movement. *Development* **138**, 4763–4776 (2011).
202. Melero, C. *et al.* Light-induced molecular adsorption of proteins using the primo system for micro-patterning to study cell responses to extracellular matrix proteins. *J. Vis. Exp.* **2019**, 1–19 (2019).

203. Strale, P. O. *et al.* Multiprotein Printing by Light-Induced Molecular Adsorption. *Adv. Mater.* **28**, 2024–2029 (2016).
204. Cines, B. D. B. *et al.* The Journal of The American Society of Hematology. **91**, 3527–3561 (1998).
205. Staton, C. A., Reed, M. W. R. & Brown, N. J. A critical analysis of current in vitro and in vivo angiogenesis assays. *Int. J. Exp. Pathol.* **90**, 195–221 (2009).
206. Davis, J., Crampton, S. P. & Hughes, C. C. W. Isolation of human umbilical vein endothelial cells (HUVEC). *J. Vis. Exp.* 2–3 (2007). doi:10.3791/183
207. Addis, R. *et al.* Human umbilical endothelial cells (HUVECs) have a sex: Characterisation of the phenotype of male and female cells. *Biol. Sex Differ.* **5**, 1–12 (2014).
208. Tian, D. *et al.* Protective effect of rapamycin on endothelial-to-mesenchymal transition in HUVECs through the Notch signaling pathway. *Vascul. Pharmacol.* **113**, 20–26 (2019).
209. Piera-Velazquez, S. & Jimenez, S. A. Endothelial to mesenchymal transition: Role in physiology and in the pathogenesis of human diseases. *Physiol. Rev.* **99**, 1281–1324 (2019).
210. Park, H. J. *et al.* Human umbilical vein endothelial cells and human dermal microvascular endothelial cells offer new insights into the relationship between lipid metabolism and angiogenesis. *Stem Cell Rev.* **2**, 93–102 (2006).
211. Arnaoutova, I. & Kleinman, H. K. In vitro angiogenesis: endothelial cell tube formation on gelled basement membrane extract. *Nat. Protoc.* **5**, 628–635 (2010).
212. Driessen, R. C. H. *et al.* Shear stress induces expression, intracellular reorganization and enhanced Notch activation potential of Jagged1. *Integr. Biol. (United Kingdom)* **10**, 719–726 (2018).
213. Driessen, R. *et al.* Computational characterization of the dish-in-a-dish, a high yield culture platform for endothelial shear stress studies on the orbital shaker. *Micromachines* **11**, 1–14 (2020).
214. Kane, R. S., Takayama, S., Ostuni, E., Ingber, D. E. & Whitesides, G. M. Patterning proteins and cells using soft lithography. *Biomaterials* **20**, 2363–

2376 (1999).

215. Qin, D., Xia, Y. & Whitesides, G. M. Soft lithography for micro- and nanoscale patterning. *Nat. Protoc.* **5**, 491–502 (2010).

216. Kaji, H., Camci-Unal, G., Langer, R. & Khademhosseini, A. Engineering systems for the generation of patterned co-cultures for controlling cell-cell interactions. *Biochim. Biophys. Acta - Gen. Subj.* **1810**, 239–250 (2011).

217. Neto, A. I., Levkin, P. A. & Mano, J. F. Patterned superhydrophobic surfaces to process and characterize biomaterials and 3D cell culture. *Mater. Horizons* **5**, 379–393 (2018).

218. Chen, C. S., Mrksich, M., Huang, S., Whitesides, G. M. & Ingber, D. E. Geometric control of cell life and death. *Science (80-.).* **276**, 1425–1428 (1997).

219. Chappell, J. C., Mouillesseaux, K. P. & Bautch, V. L. Flt-1 (VEGFR-1) is Essential for the VEGF-Notch Feedback Loop during Angiogenesis HHS Public Access. *Arter. Thromb Vasc Biol* **33**, 1952–1959 (2013).

220. Benedito, R. *et al.* Notch-dependent VEGFR3 upregulation allows angiogenesis without VEGF–VEGFR2 signalling. *Nature* **484**, 110–114 (2012).

221. Tammela, T. *et al.* Blocking VEGFR-3 suppresses angiogenic sprouting and vascular network formation. *Nature* **454**, 656–660 (2008).

222. Shawber, C. J. *et al.* Notch alters VEGF responsiveness in human and murine endothelial cells by direct regulation of VEGFR-3 expression. *J. Clin. Invest.* **117**, 3369–3382 (2007).

223. Wang, Y. *et al.* Ephrin-B2 controls VEGF-induced angiogenesis and lymphangiogenesis. *Nature* **465**, 483–486 (2010).

224. Ubezio, B. *et al.* Synchronization of endothelial Dll4-Notch dynamics switch blood vessels from branching to expansion. *Elife* **5**, 1–32 (2016).

225. Antfolk, D. *et al.* Selective regulation of Notch ligands during angiogenesis is mediated by vimentin. *Proc. Natl. Acad. Sci.* 201703057 (2017). doi:10.1073/PNAS.1703057114

226. Sjöqvist, M. *et al.* PKCζ regulates Notch receptor routing and activity in a Notch signaling-dependent manner. *Cell Res.* **24**, 433–450 (2014).

227. Toda, H., Yamamoto, M., Kohara, H. & Tabata, Y. Orientation-regulated

immobilization of Jagged1 on glass substrates for ex vivo proliferation of a bone marrow cell population containing hematopoietic stem cells. *Biomaterials* **32**, 6920–6928 (2011).

228. Gama-Norton, L. *et al.* Notch signal strength controls cell fate in the haemogenic endothelium. *Nat. Commun.* **6**, (2015).
229. Guisoni, N., Martinez-Corral, R., Garcia-Ojalvo, J. & de Navascués, J. Diversity of fate outcomes in cell pairs under lateral inhibition. *Development* **144**, 1177–1186 (2017).
230. Kakuda, S. & Haltiwanger, R. S. Deciphering the Fringe-Mediated Notch Code: Identification of Activating and Inhibiting Sites Allowing Discrimination between Ligands. *Dev. Cell* **40**, 193–201 (2017).
231. Palano, M. T. *et al.* Jagged ligands enhance the pro-angiogenic activity of multiple myeloma cells. *Cancers (Basel).* **12**, 1–18 (2020).
232. Pedrosa, A. R. *et al.* Endothelial jagged1 antagonizes Dll4 regulation of endothelial branching and promotes vascular maturation downstream of Dll4/Notch1. *Arterioscler. Thromb. Vasc. Biol.* **35**, 1134–1146 (2015).
233. Serra, H. *et al.* PTEN mediates Notch-dependent stalk cell arrest in angiogenesis. *Nat. Commun.* **6**, (2015).
234. Engel, L. *et al.* Extracellular matrix micropatterning technology for whole cell cryogenic electron microscopy studies. *J. Micromechanics Microengineering* **29**, (2019).
235. Stoecklin, C. *et al.* A New Approach to Design Artificial 3D Microniches with Combined Chemical, Topographical, and Rheological Cues. *Adv. Biosyst.* **2**, 1–11 (2018).
236. Pasturel, A., Strale, P. O. & Studer, V. Tailoring Common Hydrogels into 3D Cell Culture Templates. *Adv. Healthc. Mater.* **9**, 1–8 (2020).
237. Jiang, C. *et al.* Mechanochemical control of epidermal stem cell divisions by B-plexins. *Nat. Commun.* **12**, (2021).
238. Van Der Putten, C. *et al.* Protein Micropatterning in 2.5D: An Approach to Investigate Cellular Responses in Multi-Cue Environments. *ACS Appl. Mater. Interfaces* (2021). doi:10.1021/acsami.1c01984
239. Uroz, M. *et al.* Traction forces at the cytokinetic ring regulate cell division

and polyploidy in the migrating zebrafish epicardium. *Nat. Mater.* **18**, 1015–1023 (2019).

240. Khan, E. S. *et al.* Photoactivatable Hsp47: A Tool to Regulate Collagen Secretion and Assembly. *Adv. Sci.* **6**, (2019).
241. Zhang, Y. *et al.* Biomimetic niches reveal the minimal cues to trigger apical lumen formation in single hepatocytes. *Nat. Mater.* **19**, 1026–1035 (2020).
242. Ghagre, A. *et al.* Pattern-Based Contractility Screening, a Reference-Free Alternative to Traction Force Microscopy Methodology. *ACS Appl. Mater. Interfaces* **13**, 19726–19735 (2021).
243. Nguyen, H. T., Massino, M., Keita, C. & Salmon, J. B. Microfluidic dialysis using photo-patterned hydrogel membranes in PDMS chips. *Lab Chip* **20**, 2383–2393 (2020).
244. Kang, H. W. *et al.* A 3D bioprinting system to produce human-scale tissue constructs with structural integrity. *Nat. Biotechnol.* **34**, 312–319 (2016).
245. Guillotin, B. *et al.* Laser assisted bioprinting of engineered tissue with high cell density and microscale organization. *Biomaterials* **31**, 7250–7256 (2010).
246. Hammer, J. A. & West, J. L. Dynamic Ligand Presentation in Biomaterials. *Bioconjug. Chem.* **29**, 2140–2149 (2018).
247. Shadish, J. A., Benuska, G. M. & DeForest, C. A. Bioactive site-specifically modified proteins for 4D patterning of gel biomaterials. *Nat. Mater.* **18**, 1005–1014 (2019).
248. Liu, Z. *et al.* Nanoscale optomechanical actuators for controlling mechanotransduction in living cells. *Nat. Methods* **13**, 143–146 (2016).

Appendix I: Original publication Study I

I

SCIENTIFIC REPORTS

OPEN

Spatial patterning of the Notch ligand Dll4 controls endothelial sprouting *in vitro*

Received: 11 September 2017
Accepted: 5 April 2018
Published online: 23 April 2018

L. A. Tiemeijer[1,2], J-P. Frimat[3], O. M. J. A. Stassen[1], C. V. C. Bouten[1] & C. M. Sahlgren[1,2,4]

Angiogenesis, the formation of new blood vessels, is a vital process for tissue growth and development. The Notch cell-cell signalling pathway plays an important role in endothelial cell specification during angiogenesis. Dll4 - Notch1 signalling directs endothelial cells into migrating tip or proliferating stalk cells. We used the directing properties of Dll4 to spatially control endothelial cell fate and the direction of endothelial sprouts. We created linear arrays of immobilized Dll4 using micro contact printing. HUVECs were seeded perpendicular to these Dll4 patterns using removable microfluidic channels. The Notch activating properties of surface immobilized Dll4 were confirmed by qPCR. After induction of sprouting, microscopic images of fluorescently labelled endothelial sprouts were analysed to determine the direction and the efficiency of controlled sprouting (Ecs). Directionality analysis of the sprouts showed the Dll4 pattern changes sprout direction from random to unidirectional. This was confirmed by the increase of Ecs from 54.5 ± 3.1% for the control, to an average of 84.7 ± 1.86% on the Dll4 patterned surfaces. Our data demonstrates a surface-based method to spatially pattern Dll4 to gain control over endothelial sprout location and direction. This suggests that spatial ligand patterning can be used to provide control over (neo) vascularization.

Since diffusion is not efficient over larger distances, blood vessels are crucial for transport of nutrients, oxygen and elimination of waste to support organ growth and repair of damaged tissue[1]. Inefficient transport leads to tissue hypoxia and a demand for the formation of new blood vessels to restore the blood supply and stabilize local oxygen levels. It is known that under the influence of vascular endothelial growth factor (VEGF) released by hypoxic or injured tissue, new vessels sprout from existing vessels, a process called angiogenesis[2,3]. In angiogenic sprouting, one endothelial cell (tip cell) guides the other (stalk) cells towards the VEGF gradient. Delta like ligand 4 (Dll4) – Notch 1 signalling has an important role in sprouting angiogenesis[2–4]. Dll4 – Notch 1 is involved in the specification of endothelial cells (ECs) into migratory tip or proliferating stalk cells[3,5–7]. The binding of VEGF-A to vascular growth factor receptor 2 (VEGFR2) induces Dll4 expression in all endothelial cells[2]. However, some ECs express more extracellular Dll4 than others, thereby inducing Notch signalling in the neighbouring ECs and a stalk cell phenotype, while the Dll4 expressing EC adopts a tip cell phenotype[2]. Induction of Notch signalling in the neighbouring cells reduces expression of VEGFR2 and induces expression of VEGFR1, which desensitizes the cell for the VEGF-A gradient[8,9]. This interplay of the Dll4 - Notch 1 signalling with the VEGF-A gradient has been suggested to be responsible for a salt and pepper pattern of tip- and stalk endothelial phenotypes[10]. The tip and stalk phenotypes are not stable, but reside in a dynamic state and constantly interchange in response to changing Notch signalling levels within individual cells[11]. The influence of Notch signalling on angiogenesis has been studied mainly from a biology driven perspective by confounding techniques. These include *in vivo* knock-in, knock-out models which are influenced by systemic factors, *in vitro* co-cultures influenced by the other cell source, the usage of non-specific Notch signalling inhibitors like DAPT or ligand specific decoys[5–7,9,12,13].

Here we addressed the question if sprouting angiogenesis can be externally controlled by exposure to patterns of Notch ligands. Such external control is of interest in tissue engineering to control and enhance efficient vascularization of tissue-engineered constructs. Notch signalling is inhibited by soluble ligands, but Notch signalling

[1]Department of Biomedical Engineering, Soft Tissue Engineering and Mechanobiology, ICMS Institute for Complex Molecular Systems, Eindhoven University of Technology, Eindhoven, Netherlands. [2]Faculty for Science and Engineering, Biosciences, Åbo Akademi University, Turku, Finland. [3]Department of Mechanical Engineering, Microsystems Group, Eindhoven University of Technology, Eindhoven, Netherlands. [4]Turku Centre for Biotechnology, University of Turku and Åbo Akademi University, Turku, Finland. Correspondence and requests for materials should be addressed to L.A.T. (email: l.a.tiemeijer@tue.nl) or C.M.S. (email: c.m.sahlgren@tue.nl)

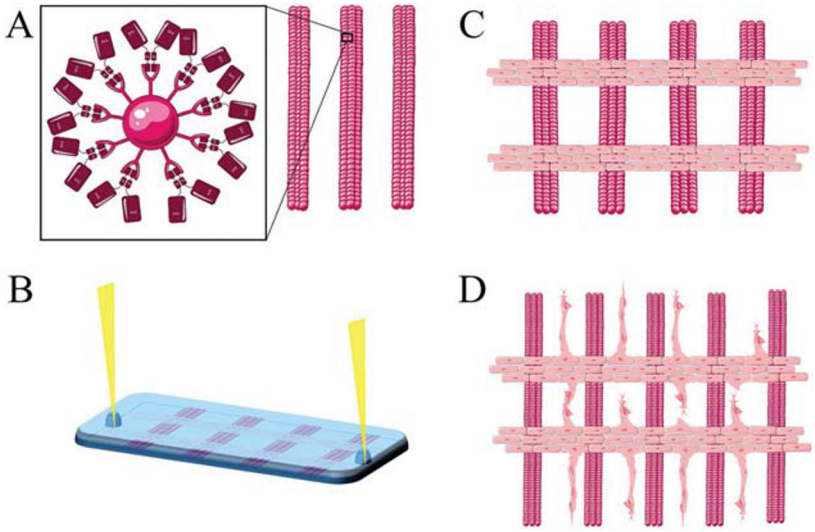

Figure 1. Schematic overview of the method described in this study. In (**A**) patterning of Dll4 by micro contact printing of the Dll4-fc immobilized to pink fluorescent beads in parallel lines with defined width and spacing. In (**B**) seeding of HUVECs through microfluidic channels perpendicular on the patterned Dll4. In (**C**) an overview of the HUVECs in (vessel mimic mimicking) monolayers perpendicular on top of the patterned Dll4 after removal of the microfluidic channels. (**D**) Hypothesized sprouting of the HUVECs after 24 h culture in Matrigel enriched media. Images made with tools from Servier medical art by Servier.

can be activated *in vitro* by immobilization of recombinant Notch ligands[9,14,15]. So far, the induction of Notch signalling *in vitro* using immobilized ligands has been done on homogenously coated (bio)materials[16–19]. Since Notch signalling is cell contact dependent and Dll4 signalling operates through lateral induction e.g. inducing the signal receiving cells to adopt a different fate than the Dll4 expressing signal sending cell, the location of the Dll4 induction should influence the endothelial response[2,4,8]. Therefore, manipulation of Dll4 – Notch 1 signalling to control vascular patterning is of interest. Endothelial cell fate is determined by the local higher concentration of signalling Dll4 originated from the neighbouring cell[2]. To recreate and manipulate this, a surface was created where the high Dll4 signalling neighbour was mimicked by a printed pattern, to see whether we could force the cells on top of this Dll4 pattern to adopt a stalk cell phenotype, leaving the adoption of a tip cell phenotype to the cells in between the high Dll4 sites in the pattern. We expected that this would result in the initiation of endothelial sprouting in between the Dll4 patterned lines, thereby gaining control over the location and direction of sprouting. We used microfabrication techniques (Fig. 1) to produce patterns of immobilized Dll4. We used micro contact printing (μCP) to print a pattern of 100 μm wide lines of immobilized and fluorescent Dll4 on a glass surface. These lines represent a local higher concentration of Dll4 adjacent to a Dll4-free surface area. Thereafter, Human Umbilical Vein Endothelial Cells (HUVECs) were seeded perpendicular to these Dll4 lines, using removable micro channels, which allowed for a control of the initial location of the endothelial cells mimicking a monolayer vessel from which sprouting normally occurs. Following release of the channels the endothelial cells were left to sprout in Matrigel enriched media for 24 h. After fixation, immunofluorescence staining and microscopy, the samples were subdued to image analysis to evaluate if the alternating Dll4 pattern dictated sprouting organization. This proof of concept study is the first to demonstrate the possibility of manipulating angiogenesis by using microfabrication techniques to spatially pattern the Notch ligand Dll4 and control direction of sprouting.

Material and Methods

Fabrication of micro contact printing (μCP) stamps and microfluidic channels. Standard soft photolithography was used to create SU-8 masters (MicroChem) for both the μCP stamps and the microfluidic channels. Briefly, Su-8 2050 was spun at 500 rpm for 10 s, followed by 30 s at 2000 rpm, prebaked 5 min at 65 °C and 15 min at 95 °C. UV exposure was performed with a mask containing the desired features for 35 s at 13mNcm^{-2}. Post baking 5 min at 65 °C and 8 min at 95 °C and finally developed for an hour with SU-8 developer. PDMS consisting of 10:1 w/v parts base to curing agent (Sylgard 184) was degassed by centrifuging and poured onto the SU-8 masters. Secondary degassing under vacuum was followed by curing at 65 °C overnight before PDMS was peeled off to be cut into stamps or channels. μCP stamps were designed to contain straight lines with widths of 100 and 50 μm spaced by 100 μm (Fig. 2A,B). Various microfluidic channels were designed, with channels width of 150 μm and 300 μm, spaced by 300 or 500 μm, with 1.5 mm inlets and outlets (Fig. 2C,D).

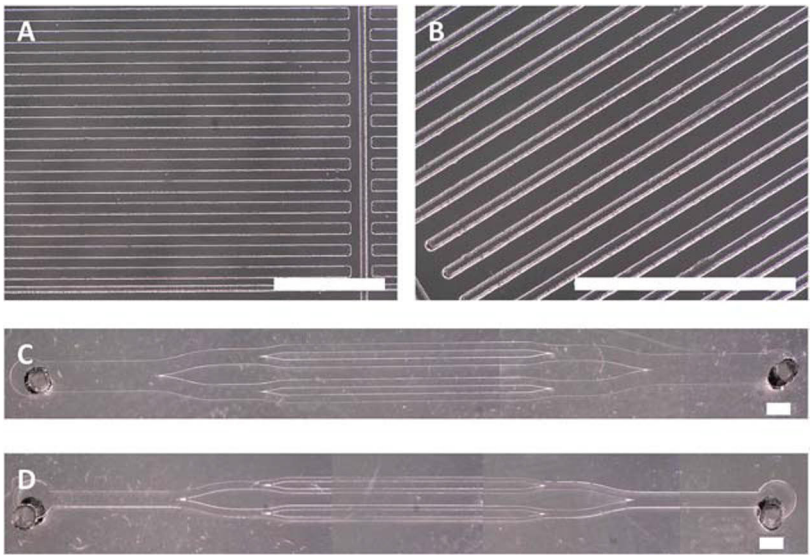

Figure 2. Microscopic images of the different μCP stamps and microfluidic channels. (**A**) Stamps with lines 100 μm wide with 100 μm spacing. (**B**) Stamps with lines 100 μm wide with 50 μm spacing. (**C**) Microfluidic channels with 300 μm wide subchannels. (**D**) Microfluidic channels with 150 μm wide subchannels. Scale bar represents 1 mm.

Cell culture. Human Umbilical Vein Endothelial Cells (HUVECs, Lonza) were cultured in Endothelial Base Medium (EBM-2, Lonza) with additives of 2% FBS, 0.04% Hydrocortisone, 0.4% hFGF-B, 0.1% VEGF, 0.1% R3-IGF-1, 0.1% ascorbic acid, 0.1% hEGF, 0.1% GA-1000, and 0.1% heparin (Lonza) supplemented with 1% penicillin/streptomycin in cell culture flasks coated with 0.1% gelatin (porcine, Sigma) at 37 °C, 5% CO_2. Passage numbers 3–6 were used in these experiments.

Patterning of Dll4 ligands by μCP. 50 μl (10 μg/ml) of active human Dll4 protein fragment ab108557 (Abcam) was incubated with 100 μl (0.1% w/v) protein G fluorescent particles (Spherotech, purple, 0.4–0.6 μm) for 1 h at RT, resulting in a maximum of 0.5 μg of Dll4 ligand immobilized to the beads per sample. Before inking the μCP stamps with 150 μl of the Bead-Dll4 mixture, the stamps were made hydrophilic by treatment with atmospheric plasma for 9 s (Corona Discharge Generator, Tantec HF). In control experiments the stamps were inked with 100 μl of fluorescent beads, without the Dll4 ligands. μCP stamps and ink were incubated for 30 min and dried using N_2 gas prior to printing on glass slides, which were sterilized with 70% ethanol prior to printing. The μCP stamps were left to adhere to the glass for 30 min at RT before removal.

Microfluidic patterning. Microfluidic channels were deposited perpendicular to the patterned glass slides by hand (microchannels face down) and gently pressed to form a contact with the substrate to seal the microchannels. P200 pipette tips (without filter) were placed in the inlets of the channels to act as fluidic reservoirs that allowed feeding of the system by gravity (Fig. 1B). The channels were coated with 1% gelatin in PBS, pipetted in one of the tips, for 5 min at 37 °C, 5% CO_2, followed by careful flushing out of the gelatin solution with preconditioned media (18 h at 37 °C, 5% CO_2). HUVECs in preconditioned media ($9*10^6$ cells/ml) were seeded directly in the pipette tips. The HUVECs were left to adhere for 3 h at 37 °C, 5% CO_2 while being monitored for cell aggregates and sufficient media flow through the channels. After adherence the channels were gently flushed to wash unattached HUVECS away and media was deposited around the channels before the microchannels were taken off, and was then enriched with Matrigel (15% in total amount of media, Corning, lotnr. 4321005) on top of the HUVECs. The HUVECs were left to sprout for 24 h in 37 °C, 5% CO_2.

Fluorescent microscopy and image analysis. The cell samples were fixated for 30 min at RT with 3.7% formaldehyde in PBS. The fixed samples were permeabilised with 0.5% triton X-100 in PBS for 15 min. Netgel (50 mM Tris pH 7.5, 150 mM NaCl, 1 mM EDTA, 0.1% NP-40 (Non-idet) and 0.25% gelatin, in milliQ water) was used as washing buffer. After blocking (30 min, 4% horse serum), the samples were incubated with Dll4 goat anti-human (Santa Cruz) primary antibody at 4 °C overnight. Incubation with IgG donkey anti-goat Alexa555 (Invitrogen) secondary antibody was done for 1 h at RT. Phalloidin (Atto488) and DAPI were used as markers for the actin cytoskeleton and the nuclei respectively. Image acquisition was done using a confocal, two-photon laser scanning Leica TCS SP5X microscope.

The efficiency of patterning the sprouts in the hypothesized area in between the Dll4 lines was quantified by using equation 1 (adjusted from Frimat *et al.*[20]);

$$Ecs = \frac{Coff}{(Coff + Con)}100\% \quad (1)$$

where Ecs is the efficiency of the control over the sprouting of the endothelial cells in percentage, C_{off} is the number of cells that has sprouted from the HUVEC monolayer to the area in between the lines of bead-Dll4 and the C_{on} is the number of cells that have sprouted to the area where they are exposed to the bead-Dll4 complexes. One region of interest (ROI) contains both areas. The direction analysis was done with the image J plugin 'Directionality' on multiple ROI's at once.

qPCR. Activation of the Notch pathway by the μCP ink was verified with qPCR. Culture plates with $2.5*10^4$ cells/cm^2 were subjected to different conditions; mimicking the experimental setup μCP ink coated with gelatin and topped with HUVECs in Matrigel enriched media, a control condition where Dll4 was not attached to the beads, and a control where no μCP ink was present. Additionally all conditions were subdued to the Notch signalling inhibitor DAPT (2.5 mg/ml in media, DMSO as vehicle), and its vehicle DMSO as well. After 24 h at 37 °C, 5% CO_2 RNA was isolated using RNeasy mini kit (Qiagen) according to manufacturer's instructions. RNA was stored at −30 °C before cDNA synthesis. 200ng RNA per sample was used to synthesize cDNA. cDNA (1ng/μl, 2.5 μl volumes) was amplified using primers for FLT1 (VEGFR1) (Forward (Fw): CAAATAAGCACACCACGCCC, Reverse (Rv); CGCCTTACGGAAGCTCTCTT) KDR (VEGFR2) (Fw: CGGTCAACAAAGTCGGGAGA, Rv: CAGTGCACCACAAAGACACG), FLT4 (VEGFR3) (Fw: TGAGAGACGGCACAAGGATG, Rv: CTCCACCAGCTCCGAGAATG), EFNB2 (Fw: CTGCTGGGGTGTTTTGATGG, Rv: GTACCAGTCCTTGTCCAGGTAG), and references genes B2M and ACTB (Primerdesign) using the iQ Thermal cycler (BioRad). iQ SYBR Green (BioRad) was used as fluorescent dye. The number of experimental repetitions was 3 and the PCR was performed 3 times in total.

Statistical analysis. Data was presented as mean ± standard error of the mean (SEM). A one way non-parametric ANOVA Kruskal-Wallis with a Dunn's multiple comparison post hoc test was done to analyse the directionality data, and some of the Ecs data. A non-parametric student-t Mann-Whitney test was used to compare one data set of the Ecs data. A parametric ANOVA with a Bonferoni multiple comparison post hoc test for selected columns was used for the qPCR data. All statistics were done using the GraphPad Prism software. A difference with a p-value less than 0.05 was considered significant.

- The datasets generated during and/or analysed during the current study are available from the corresponding author upon request.

Results and Discussion

Immobilized Dll4 activates endothelial Notch signalling. We generated a homogenously Dll4 functionalized surface on regular plastic culture plates to verify that the immobilized bead-Dll4 complexes were able to activate Notch signalling. Expression of endothelial specific Dll4 – Notch 1 induced target genes was analysed by qPCR on samples of all the experimental conditions and controls. In addition to verifying if the bead Dll4 complex can sustain Dll4 – Notch 1 signalling (Fig. 3), the experiment assessed if induction of Notch signalling by Dll4 through a gelatin coat is possible, as well as investigated the impact of the naked IgG beads on Notch target gene expression. The interaction of Dll4 – Notch 1 and activation of Notch signalling in the receiving (stalk) cell leads to a feedback loop where the expression of VEGF-receptors (VEGFR) are either induced or reduced depending on the receptor[8]. Dll4 induced activation of Notch is thought to repress FLT1 (VEGFR1) expression and promote expression of FLT4 (VEGFR3). KDR (VEGFR2) as a Dll4 – Notch 1 signalling target gene is still debated[21]. We also included the Notch target gene Ephrin B2 in the analyses[22]. Dll4 – Notch 1 signalling was pharmacologically inhibited by the Notch inhibitor DAPT.

The expression of Ephrin B2 and FLT4 (VEGFR3) in HUVECs cultured on top of empty beads, bead-Dll4 complexes and control, was significantly decreased upon treatment with DAPT, indicating that active (basal) Dll4 – Notch 1 signalling is present in the endothelial cell layer. Additionally, Ephrin expression was increased upon the addition of Dll4 to the beads, indicating the immobilization of Dll4 to the fluorescent beads enhances Dll4 – Notch 1 signalling of the cells exposed to the bead-Dll4 complexes. A similar trend can be observed in the expression of VEGFR3, however this was not found significant. It must be noted that the basal Notch activity in these cultures are high, as the cells are grown at high confluency and are in contact with each other, resulting in a constant Dll4 - Notch 1 signalling feedback loop which involves the VEGF receptors. This might explain why a trend of increased VEGFR3 expression can be observed as a result of the bead-Dll4 complexes, but cannot be found to make a significant difference for this particular target gene. Importantly, the beads alone did not induce the expression of key angiogenic target genes and immobilized bead - Dll4 was still able to activate Notch 1 signalling after gelatin coating as seen in the data of Ephrin gene expression.

Patterning recombinant Dll4 ligands by microfabrication techniques. A microfabrication based platform to control endothelial sprouting was designed using μCP to pattern immobilized Dll4 (bead-Dll4) and microfluidic channels to control the seeding and alignment of HUVECs on the patterned Dll4. This approach enabled us to exclude anti-fouling agents to allow free cellular movement after release of the microfluidic channels. This way, endothelial sprouts were constrained and influenced by the experimental conditions alone, and all resulting control over migration, proliferation or sprouting was induced by the micro contact printed bead-Dll4 pattern. During data analyses, regions of interest (ROIs) were defined as regions containing a clearly visible line of patterned fluorescent beads (either linked to Dll4 or not) and the same area in between two lines, alongside a proper endothelial cell monolayer mimicking the endothelial lining in (micro) vessels. Matrigel provided an extracellular matrix (ECM) mimicking structure, which together with additional growth factors in the media,

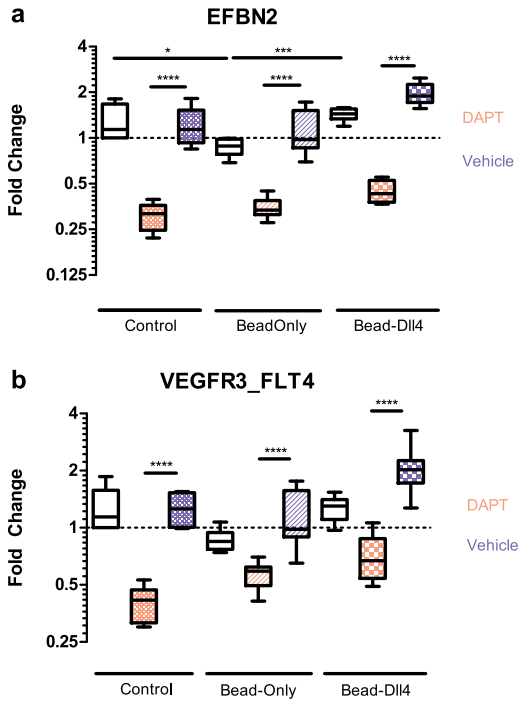

Figure 3. Fold change in gene expression of Ephrin B2 en Flt4 (VEGFR3). The experimental conditions are indicated below the graphs and in the legend adjacent. The condition of Beads with or without attached Dll4 underneath a gelatin coating is used here as well as the rest of this study. DMSO was used as a vehicle control for DAPT. Experiment in triple, qPCR was repeated 3 times. *$p < 0.05$, **$p < 0.01$, ***$p < 0.001$, ****$p < 0.0001$.

supported endothelial sprouting[23]. μCP as used in this study relies on manual reproducibility. Therefore, a maximum of 0.5 μg of Dll4 ligand immobilized to fluorescent beads per sample could be reached. This amount of ligand corresponds to the range used in previous experiments in our group[24,25]. Notch signalling is inhibited by soluble ligands[9,14], and immobilization of ligands has been previously been proven to be necessary to induce Notch signalling in cells and tissue[14,15]. Therefore, we believe this *in vitro* surface based Dll4 – Notch 1 inducing patterning method might mimic cell-cell signalling, and could be used to override natural cell-fate deciding signalling.

Printed bead-Dll4 patterns lead to patterned endothelial sprouts. Figure 4 shows the comparison of the immunofluorescent microscopy images for the control conditions with the patterned bead-Dll4 ink condition. In the absence of patterned bead-Dll4 or fluorescent beads, the endothelial sprouts were shorter and had no clear direction or preference in the location of the origin of the sprouts. In the presence of patterned fluorescent beads with no Dll4 attached, the sprouts were slightly longer and less furcate, but still showed no preference in direction or location of the origin of the sprouts. When exposed to a pattern of bead-Dll4 ligands, the endothelial cells responded to the bead-Dll4 ink and formed significantly longer sprouts, directly parallel to the patterned immobilized Dll4 and demonstrated a clear preference in location of the origin of the sprouts, resulting in a pattern of endothelial sprouts in between the Dll4 ligands. These sprouts anastomosed with sprouts originating from the endothelial cells of neighbouring channels (Supplementary data Fig. 1), demonstrating the possibility of creating a spatially controlled vessel bed using patterned Dll4 ligands.

Endothelial sprouting is spatially restricted by the bead-Dll4 pattern. To quantify the level of control over the location of growing endothelial sprouts, the efficiency of controlled sprouting (Ecs) was calculated for every ROI. Equation (1) was used to determine the Ecs in percentage, with C_{off} being the number of cells not on the line of patterned bead-Dll4 (off) and C_{on} the number of cells on the line of patterned bead-Dll4 (on). Using this formula, the Ecs is equal to 100% if all the sprouting cells are located in between the patterned bead-Dll4 (off). With an Ecs of 0% negative patterning is observed, meaning the cells are located only on the patterned bead-Dll4. When the cells have no particular preference in location regarding to the bead-Dll4 pattern, the Ecs is 50%. As expected, no significant preference of the sprouts could be observed in the bead-only condition, as demonstrated by the mean Ecs of $54.5 \pm 3.1\%$ (Fig. 5a). The patterned bead-Dll4 significantly increased the Ecs to $95 \pm 0.9\%$. These results demonstrate that the Dll4 in the printed ink pattern is the determining parameter for the

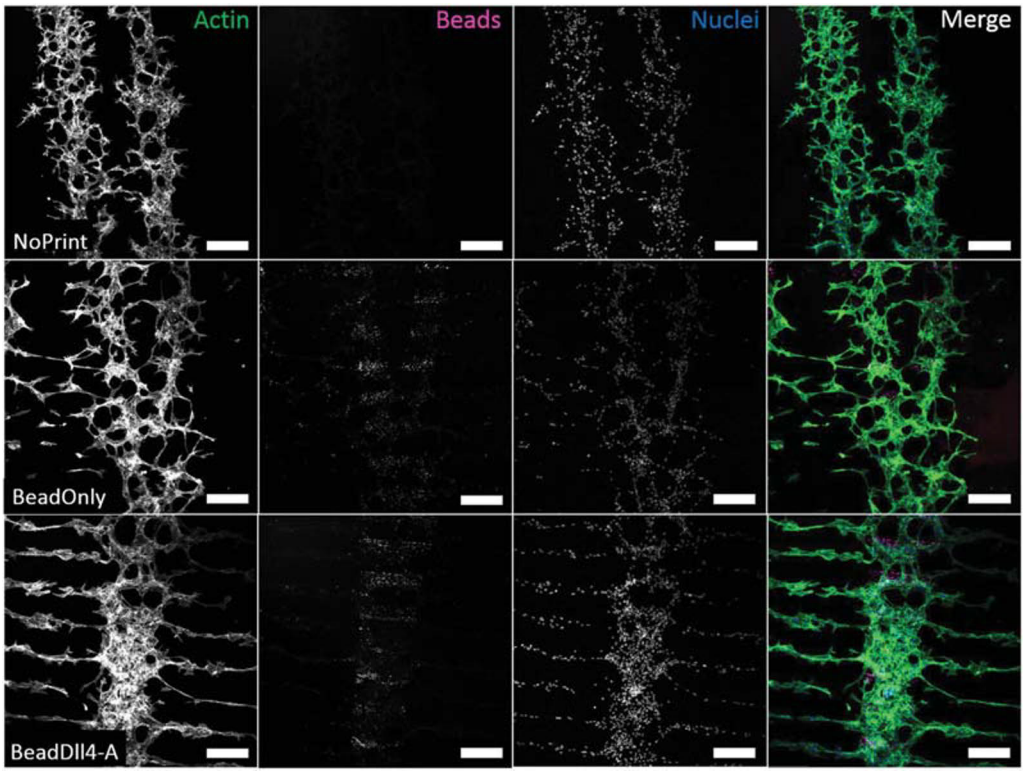

Figure 4. Microscopic immunofluorescent images of labelled sprouting HUVECs, in Matrigel enriched media, on top of gelatin coated glass (NoPrint, top row). Sprouting HUVECS in Matrigel enriched media on top of a line pattern of fluorescent IgG beads coated with gelatin (BeadOnly, middle row) or on a Dll4 ligand immobilized with fluorescent IgG beads line pattern coated with gelatin (BeadDll4, bottom row). First three columns contain intensity values separately. The last column contains the merged image with in green; actin stained with phalloidin, in pink; fluorescent IgG beads, and in blue; nuclei stained with DAPI. Scale bar represents 250 µm.

spatial control over endothelial sprouting, and not the fluorescent IgG particles. It was further confirmed that the number of cells in the two areas of the ROI was similar prior to induction of sprouting and therefore any potential effect of Dll4 on proliferation did not influence the patterning of the sprouts (Supplementary data Fig. 2).

Two other chips were created and analysed in the same fashion to investigate reproducibility of the design. Again a significant difference between Ecs of the bead-Dll4 patterned chips and the bead-only control was found (Fig. 5b), with Ecs values of $81.2 \pm 2.4\%$ and $74.9 \pm 2.6\%$ observed for bead-Dll4 chips B and C respectively, leading to an average Ecs of $84.7 \pm 1.86\%$. The data confirms that the control exerted by the pattern of bead-Dll4 over the spatial localization of the endothelial sprouting is robust and significant. The data clearly demonstrated the ability of the Dll4 ligand to locally inhibit angiogenic sprouting on the printed bead-Dll4 lines and Dll4 patterning can therefore be used to control the location of sprouting.

Dll4 patterning increases unidirectional sprouting. The direction of the endothelial sprouts emerging from the vessel mimicking monolayer was investigated using the image J 'Directionality' plugin software (Fig. 6c–g). The fit dispersion of the software model was used as a parameter for the unidirectionality of the endothelial sprouting from either sides of the monolayer per immunofluorescent image. The dispersion was significantly reduced using patterned Dll4 compared to the controls, demonstrating that the control conditions had a more randomly orientated sprouting (Fig. 6a). Moreover, the correctness of the fitted direction model is increased for the patterned Dll4 condition (Fig. 6b), corroborating the significance of the dispersion data. The general direction of the sprouting however, did not differ between the controls and the patterned Dll4 condition (Supplementary data Fig. 4). As the direction perpendicular to the vessel mimicking monolayer was defined as zero degrees, the average direction of the sprouts in the patterned Dll4 condition was expected to be zero, with a small deviation. Controls were expected to have a larger dispersion. Surprisingly, the average direction was not zero for all the chips, though the average direction remained between an -5 degree and $+8$ degree angle (Supplementary data Fig. 4). This can be explained by the manual placement of the micro fluidic channels on top of the pattern, which

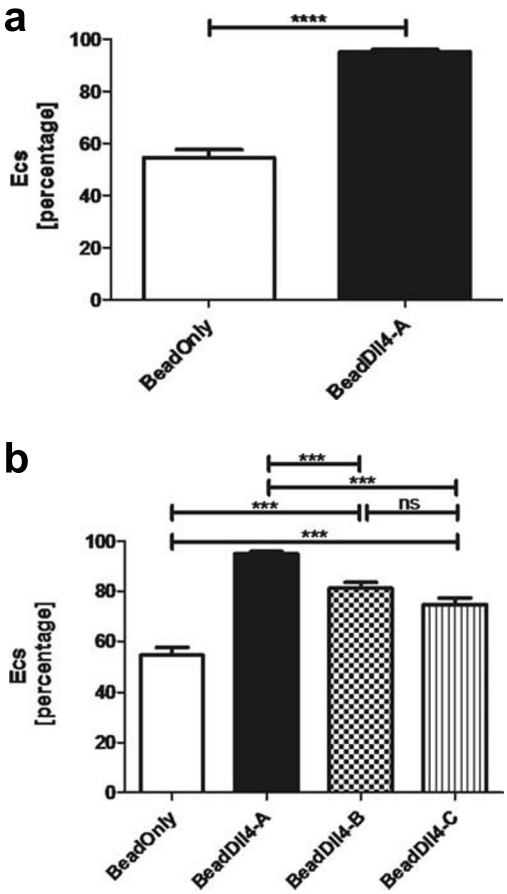

Figure 5. Efficiency of controlled sprouting analysed with (**a**) 89 ROIs of bead-only condition and 98 ROIs of bead-Dll4 condition. (**b**) The reproducibility of the bead-Dll4 chips resulting from the Ecs calculated with 60 ROIs of Bead-Dll4 sample B and 71 ROIs of bead-Dll4 sample (c). *$p < 0.05$, **$p < 0.01$, ***$p < 0.001$, ****$p < 0.0001$.

might have led to a slight deviation of the supposed 90 degree angle between the channels and the pattern, resulting in different sprouting directions. It must be noted that one image analysed by the plugin contained multiple ROIs, resulting in a lower n than the number of ROIs.

Immobilization of Notch ligands to surfaces as a means to activate Notch has been done before, yet focused mostly on the influence of the Jagged ligand[14,16–19]. Dll4 has been immobilized on beads[26] as well as been incorporated in 3D hydrogels[27], however, here we describe the first attempt to immobilize the ligands in a spatial fashion to achieve control over vascular tissue patterning, which may be caused by our interference in the Dll4- mediated lateral inhibition process. The data in this study suggests that there is a clear difference between conditions in sprouting direction and we observe a change from random spouting to unidirectional sprouting, supporting the hypothesis that Dll4 patterning leads to more spatially controlled sprouting. This unidirectional sprouting is a direct result of the restrictions set by the patterned Dll4 beads. Recent data on Notch dose sensitivity in cell fate determination[28] and the finding that cell-cell contact area influences the Notch pathway's signalling strength[29,30] support our idea that the controlled dose and location of the Dll4 ligand is responsible of forcing the endothelial phenotype. Additionally, lateral inhibition has previously been pointed out to be a possible tool for the control over cell to cell patterning[31].

To build on the findings of our study's, it might be suggested that engineering principles can be used to spatially control angiogenesis and vascular patterning in 2D and possibly 3D by changing the design of the Dll4 pattern. Further investigation using different geometric patterns will shed more light on the limits of the patterned Dll4 induced control. In this context, the effects of spatially patterned Jagged1 should be investigated as well, as Jagged1 and Dll4 have opposite effects on sprouting[7]. Additionally, VEGF is an interesting target for controlled angiogenesis. For example, the investigations of hydrogels containing both VEGF and Notch inhibitors in hind limb ischemia, demonstrated the important interplay between the two pathways and their contribution

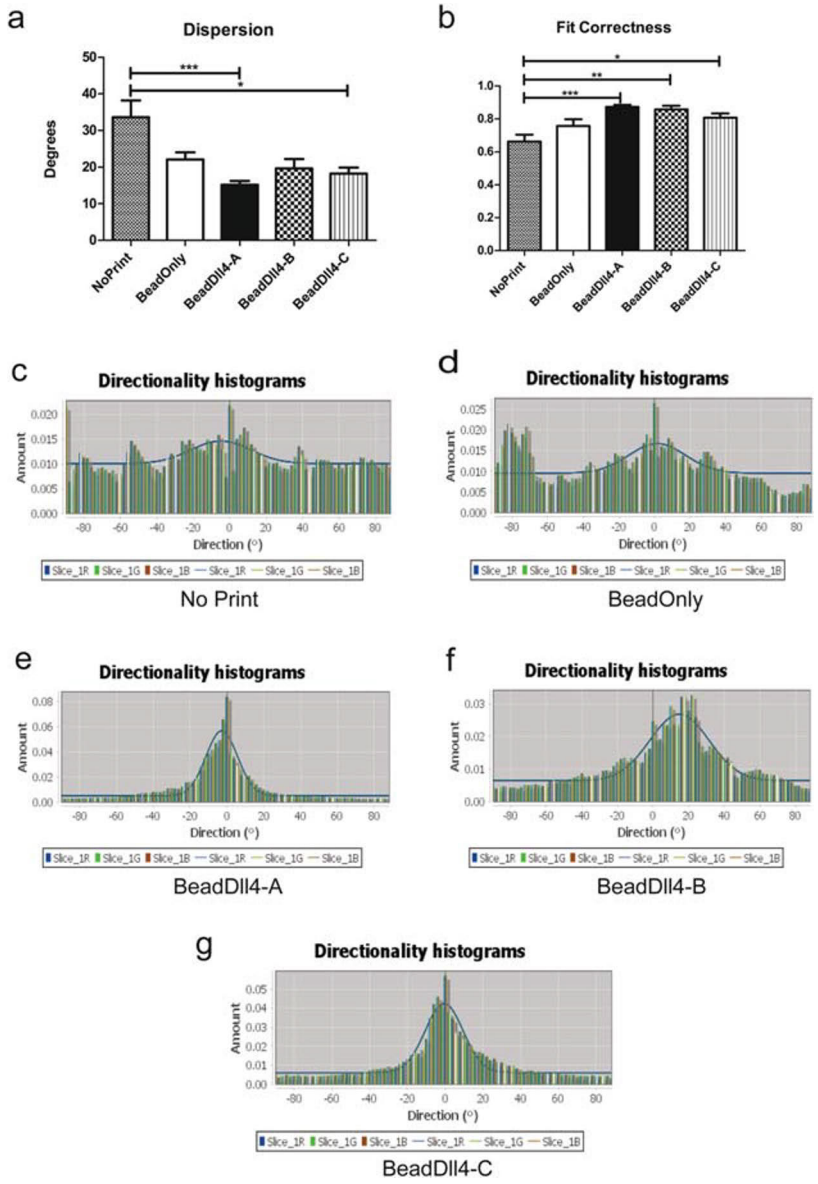

Figure 6. Patterned Dll4 lines result in unidirectional endothelial sprouting. Direction of 5×5 pixel matrices was calculated for all ROI of either side of the vessel mimicking monolayer in one microscopy image, using the Image J plugin 'Directionality'. (**a**) The dispersion of the fitted graph through the histograms in degrees. (**b**) The correctness of this fit through the direction histograms. *$p < 0.05$, **$p < 0.01$ ***$p < 0.001$, ****$p < 0.0001$. NP $n = 15$, BO $n = 21$, BD-A $n = 23$, BD-B $n = 13$, BD-C $= 22$. (**c**) Histogram of the directions found in the no print condition (**d**) for the bead-only control condition and (**e**) for the patterned Dll4 condition, with similar chips BeadDll4-B and C (**f** and **g**).

to neovascularization[32]. However, *in vivo* targeting of angiogenesis by these pro-angiogenic proteins and drugs does not exert control over spatial placement- and guidance of neovessels. This induces random angiogenesis in contrast with our study's results. Research that has moved away from random vascular networks has previously relied on microfabrication techniques to create patterned (micro)vessels[33–37]. However, these approaches rely on material-, or structure induced patterning or direct cell patterning and not on biological cues[34]. Furthermore, templated micro vessels are limited by the use of 3D molds[34,37]. Our approach is unique in utilizing a patterned

bio activated surface to achieve spatial control over vascularization. This implies convenient use- and application of Notch ligand patterned surfaces for direct presentation to (native) (diseased) vascular tissues to stimulate controlled sprouting in the future.

Conclusion

In this paper we describe the development of a unique surface based method to control angiogenic sprouting. We demonstrate that μCP of Notch ligand Dll4 in patterns enables control of the location and direction of endothelial sprouting. By presenting the cells to a pre-existing alternating line pattern of micro contact printed Dll4 we obtained spatial control of angiogenesis. We show that the patterned bead-Dll4 lines are able to locally inhibit angiogenic sprouting and direct the formation- and location of new sprouts. This straight forward and surface based method of endothelial cell fate manipulation provides a stepping stone for future developments of spatial presentation of ligands on (bio)material surfaces for more controlled (neo)vascularization for tissue engineering and/or regenerative medicine applications.

References

1. Carmeliet, P. Angiogenesis in life, disease and medicine. *Nature* **438**, 932–936 (2005).
2. Phng, L. K. & Gerhardt, H. Angiogenesis: A Team Effort Coordinated by Notch. *Dev. Cell* **16**, 196–208 (2009).
3. Adams, R. H. & Eichmann, A. Axon Guidance Molecules in Vascular Patterning. *Cold Spring Harb. Perspect. Biol.* **2**, a001875 (2010).
4. Holderfield, M. T. & Hughes, C. C. W. Crosstalk between vascular endothelial growth factor, notch, and transforming growth factor-β in vascular morphogenesis. *Circ. Res.* **102**, 637–652 (2008).
5. Hellström, M. *et al*. Dll4 signalling through Notch1 regulates formation of tip cells during angiogenesis. *Nature* **445**, 776–780 (2007).
6. Lobov, I. B. *et al*. Delta-like ligand 4 (Dll4) is induced by VEGF as a negative regulator of angiogenic sprouting. *Proc. Natl. Acad. Sci. USA* **104**, 3219–24 (2007).
7. Benedito, R. *et al*. The Notch Ligands Dll4 and Jagged1 Have Opposing Effects on Angiogenesis. *Cell* **137**, 1124–1135 (2009).
8. Sainson, R. C. A. & Harris, A. L. Regulation of angiogenesis by homotypic and heterotypic notch signalling in endothelial cells and pericytes: From basic research to potential therapies. *Angiogenesis* **11**, 41–51 (2008).
9. Kangsamaksin, T. *et al*. NOTCH decoys that selectively block DLL/NOTCH or JAG/NOTCH disrupt angiogenesis by unique mechanisms to inhibit tumor growth. *Cancer Discov.* **5**, 182–197 (2015).
10. Bentley, K., Gerhardt, H. & Bates, P. A. Agent-based simulation of notch-mediated tip cell selection in angiogenic sprout initialisation. *J. Theor. Biol.* **250**, 25–36 (2008).
11. Bentley, K. *et al*. The role of differential VE-cadherin dynamics in cell rearrangement during angiogenesis. *Nat. Cell Biol.* **16**, 309–321 (2014).
12. Scehnet, J. S. *et al*. Inhibition of Dll4-mediated signaling induces proliferation of immature vessels and results in poor tissue perfusion. *Blood* **109**, 4753–4760 (2007).
13. Staton, C. A., Reed, M. W. R. & Brown, N. J. A critical analysis of current *in vitro* and *in vivo* angiogenesis assays. *Int. J. Exp. Pathol.* **90**, 195–221 (2009).
14. Beckstead, B. L., Santosa, D. M. & Giachelli, C. M. Mimicking cell-cell interactions at the biomaterial-cell interface for control of stem cell differentiation. *J. Biomed. Mater. Res. - Part A* **79**, 94–103 (2006).
15. Varnum-Finney, B. *et al*. Immobilization of Notch ligand, Delta-1, is required for induction of notch signaling. *J. Cell Sci.* **113**(Pt 23), 4313–4318 (2000).
16. Gonçalves, R. M., Martins, M. C. L., Almeida-Porada, G. & Barbosa, M. A. Induction of notch signaling by immobilization of jagged-1 on self-assembled monolayers. *Biomaterials* **30**, 6879–6887 (2009).
17. Beckstead, B. L. *et al*. Methods to promote Notch signaling at the biomaterial interface and evaluation in a rafted organ culture model. *J. Biomed. Mater. Res. - Part A* **91**, 436–446 (2009).
18. Toda, H., Yamamoto, M., Kohara, H. & Tabata, Y. Orientation-regulated immobilization of Jagged1 on glass substrates for *ex vivo* proliferation of a bone marrow cell population containing hematopoietic stem cells. *Biomaterials* **32**, 6920–6928 (2011).
19. Tung, J. C., Paige, S. L., Ratner, B. D., Murry, C. E. & Giachelli, C. M. Engineered biomaterials control differentiation and proliferation of human-embryonic-stem-cell-derived cardiomyocytes via timed notch activation. *Stem Cell Reports* **2**, 271–281 (2014).
20. Frimat, J. P. *et al*. Plasma stencilling methods for cell patterning. *Anal. Bioanal. Chem.* **395**, 601–609 (2009).
21. Benedito, R. *et al*. Notch-dependent VEGFR3 upregulation allows angiogenesis without VEGF–VEGFR2 signalling. *Nature* **484**, 110–114 (2012).
22. Shawber, C. J. & Kitajewski, J. Notch function in the vasculature: Insights from zebrafish, mouse and man. *BioEssays* **26**, 225–234 (2004).
23. Nicosia, R. F. & Ottinetti, A. Modulation of microvascular growth and morphogenesis by reconstituted basement membrane gel in three-dimensional cultures or rat aorta: A comperative study of angiogenesis in matrigel, collagen, fibrin and plasma clot. *Vitr. Cell. Dev. Biol.* **26**, 119–128 (1990).
24. Antfolk, D. *et al*. Selective regulation of Notch ligands during angiogenesis is mediated by vimentin. *Proc. Natl. Acad. Sci.* **2017**, 03057, https://doi.org/10.1073/PNAS.1703057114 (2017).
25. Sjöqvist, M. *et al*. PKCζ regulates Notch receptor routing and activity in a Notch signaling-dependent manner. *Cell Res.* **24**, 433–450 (2014).
26. Tagvi, S., Dixit, L. & Roy, K. Biomaterial-based notch signaling for the differentiation of hematopoietic stem cells into Tcells. *J. Biomed. Mater. Res. - Part A* 689–697, https://doi.org/10.1002/jbm.a30916 (2006).
27. DeForest, C. A. & Tirrell, D. A. A photoreversible protein-patterning approach for guiding stem cell fate in three-dimensional gels. *Nat. Mater.* **14**, 523–531 (2015).
28. Gama-Norton, L. *et al*. Notch signal strength controls cell fate in the haemogenic endothelium. *Nat. Commun.* **6** (2015).
29. Shaya, O. *et al*. Cell-Cell Contact Area Affects Notch Signaling and Notch-Dependent Patterning. *Dev. Cell* **40**, 505–511.e6 (2017).
30. Guisoni, N., Martinez-Corral, R., Garcia-Ojalvo, J. & de Navascués, J. Diversity of fate outcomes in cell pairs under lateral inhibition. *Development* **144**, 1177–1186 (2017).
31. Sjöqvist, M. & Andersson, E. R. Do as I say, Not(ch) as I do: Lateral control of cell fate. *Dev. Biol.* 1–13, https://doi.org/10.1016/j.ydbio.2017.09.032 (2017).
32. Cao, L. *et al*. Modulating Notch signaling to enhance neovascularization and reperfusion in diabetic mice. *Biomaterials* **31**, 9048–9056 (2010).
33. Zheng, Y. *et al*. *In vitro* microvessels for the study of angiogenesis and thrombosis. *Proc. Natl. Acad. Sci.* **109**, 9342–9347 (2012).
34. Malheiro, A., Wieringa, P., Mota, C., Baker, M. & Moroni, L. Patterning Vasculature: The Role of Biofabrication to Achieve an Integrated Multicellular Ecosystem. *ACS Biomater. Sci. Eng.* **2**, 1694–1709 (2016).
35. Rouwkema, J. & Khademhosseini, A. Vascularization and Angiogenesis in Tissue Engineering: Beyond Creating Static Networks. *Trends Biotechnol.* **34**, 733–745 (2016).
36. Raghavan, S., Nelson, C. M., Baranski, J. D., Lim, E. & Chen, C. S. Geometrically controlled endothelial tubulogenesis in micropatterned gels. *Tissue Eng. Part A* **16**, 2255–2263 (2010).
37. Bogorad, M. I. *et al*. Review: *in vitro* microvessel models. *Lab Chip* **15**, 4242–4255 (2015).

Acknowledgements
The authors acknowledge the financial support from Academy of Finland (grant number 307133) and the Jane & Aatos Erkko foundation. This work has received funding (O.S.) from the European Union's Seventh Framework Programme for research, technological development and demonstration under grant agreement no. 604514 (ImaValve). Rob Driessen is kindly acknowledged for his help on the HUVEC cell culture.

Author Contributions
L.T., J-P.F. and C.S. wrote the main manuscript text, L.T., J-P.F., C.B. and C.S. designed experiments, L.T. and O.S. performed experiments, J-P.F. provided microfabrication masters, L.T. and C.S. analysed data, all authors reviewed the manuscript.

Additional Information
Supplementary information accompanies this paper at https://doi.org/10.1038/s41598-018-24646-y.

Competing Interests: The authors declare no competing interests.

Publisher's note: Springer Nature remains neutral with regard to jurisdictional claims in published maps and institutional affiliations.

Spatial patterning of the Notch ligand Dll4 controls endothelial sprouting in *vitro*

L. A. Tiemeijer,[ab*] J-P. M. S. Frimat,[c] O. M. J. A. Stassen,[a] C. V. C. Bouten,[a] and C. M. Sahlgren[abd]

a) Department of Biomedical Engineering, Soft Tissue Engineering and Mechanobiology, ICMS Institute for Complex Molecular Systems, Eindhoven University of Technology, Eindhoven, Netherlands.

b) Faculty of Cellbiology, Åbo Akademi University, Turku, Finland

c) Department of Mechanical Engineering, Microsystems Group, ICMS Institute for Complex Molecular Systems, Eindhoven University of Technology, Eindhoven, Netherlands

d) Turku Centre for Biotechnology, University of Turku and Åbo Akademi University, Turku, Finland

Correspondence: L.A. Tiemeijer, Department of Biomedical Engineering, Eindhoven University of Technology, P.O. Box 513, 5600 MB Eindhoven, The Netherlands, +31(0)40-2475415, Email: l.a.tiemeijer@tue.nl

Supplementary information

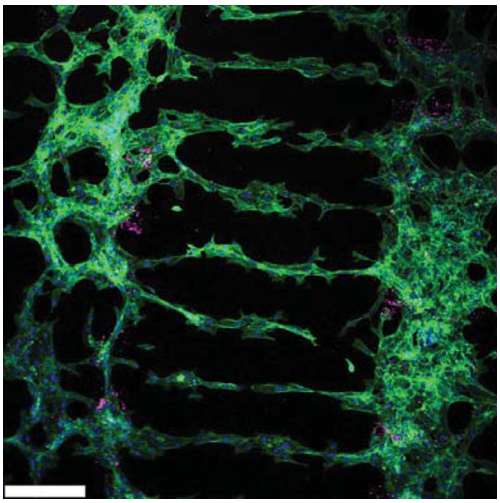

Supplementary figure 1 - Microscopic Immunofluorescent image of stained sprouting HUVECs in Matrigel enriched media on top of a Dll4 ligand immobilized with fluorescent IgG beads line pattern coated with gelatin. Endothelial sprouts originating from two (vessel mimicking) monolayers find one another in between the bead-Dll4 lines and anastomose. In green, actin stained with phalloidin. In pink, fluorescent IgG beads. In blue, nuclei stained using DAPI. Scale bar represents 250µm.

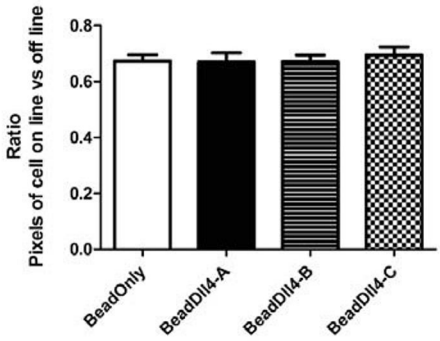

Supplementary figure 2 – To ascertain that Dll4 induced proliferation within the (vessel mimicking) monolayers prior to Matrigel induced sprouting,has no effect on the sprouting control, the amount of cells in both the area's (in between and on the bead-Dll4 lines) were counted. No difference between controls and chips were found.

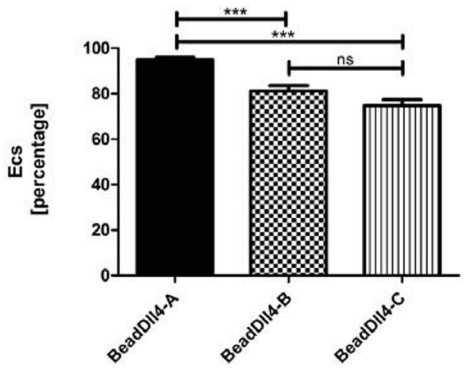

Supplementary figure 3 - Efficiency of controlled sprouting comparison between the different bead-Dll4 chips. Ecs = 81.2±2.4% and 74.9±2.6% for bead-Dll4 B and C respectively differ significantly from the Ecs = 95±0.9% of Bead-Dll4 A, but there is no difference between B and C. Bead-Dll4 A can be interpreted as the most successful chip, though B and C still show significantly more controlled sprouting than the bead-only control (Fig 5B). Data based on 98 ROIs of Bead-Dll4 sample A, 60 ROIs of Bead-Dll4 sample B and 71 ROIs of bead-Dll4 sample C. *** = $p < 0.001$.

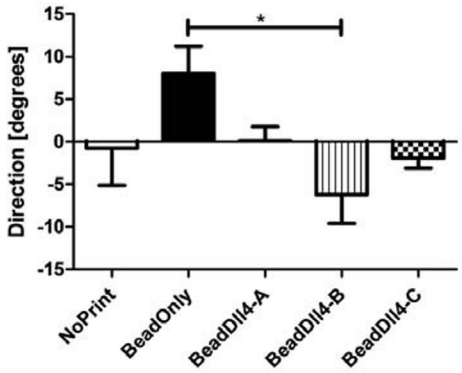

Supplementary figure 4 – Directions of the endothelial sprouts calculated for all experimental conditions using Directionality plugin of Image J. Expected direction of all the samples is around 0 degrees (horizontal). Difference in standard error of the mean is expected be decreased for bead-Dll4 conditions. * = $p < 0.05$, NP n=15, BO n=21, BD n=23.

Appendix II: Orginal publication Study II

II

iScience

CellPress
OPEN ACCESS

Article

Engineered patterns of Notch ligands Jag1 and Dll4 elicit differential spatial control of endothelial sprouting

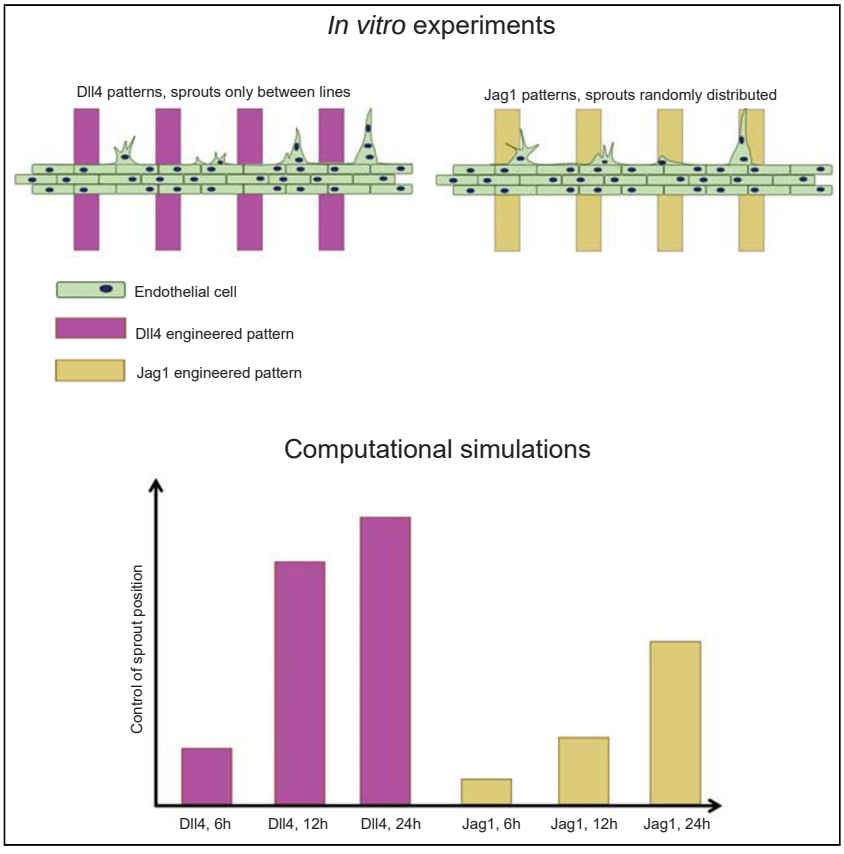

Laura A. Tiemeijer, Tommaso Ristori, Oscar M.J. A. Stassen, ..., Katie Bentley, Carlijn V.C. Bouten, Cecilia M. Sahlgren

l.a.tiemeijer@tue.nl (L.A.T.)
t.ristori@tue.nl (T.R.)
cecilia.sahlgren@abo.fi (C.M.S.)

Highlights

Dll4-functionalized patterns guide direction and location of angiogenic sprouts

Jag1-functionalized patterns do not have relevant effects on angiogenic sprouts

Modeling predicts that differences are due to distinct signaling temporal dynamics

Tiemeijer et al., iScience 25, 104306
May 20, 2022
https://doi.org/10.1016/j.isci.2022.104306

iScience

CellPress
OPEN ACCESS

Article

Engineered patterns of Notch ligands Jag1 and Dll4 elicit differential spatial control of endothelial sprouting

Laura A. Tiemeijer,[1,2,3,10,*] Tommaso Ristori,[2,3,4,10,*] Oscar M.J. A. Stassen,[1,2,5] Jaakko J. Ahlberg,[1] Jonne J.J. de Bijl,[2] Christopher S. Chen,[4,6] Katie Bentley,[4,7,8] Carlijn V.C. Bouten,[2,3] and Cecilia M. Sahlgren[1,2,3,5,9,*]

SUMMARY

Spatial regulation of angiogenesis is important for the generation of functional engineered vasculature in regenerative medicine. The Notch ligands Jag1 and Dll4 show distinct expression patterns in endothelial cells and, respectively, promote and inhibit endothelial sprouting. Therefore, patterns of Notch ligands may be utilized to spatially control sprouting, but their potential and the underlying mechanisms of action are unclear. Here, we coupled *in vitro* and *in silico* models to analyze the ability of micropatterned Jag1 and Dll4 ligands to spatially control endothelial sprouting. Dll4 patterns, but not Jag1 patterns, elicited spatial control. Computational simulations of the underlying signaling dynamics suggest that different timing of Notch activation by Jag1 and Dll4 underlie their distinct ability to spatially control sprouting. Hence, Dll4 patterns efficiently direct the sprouts, whereas longer exposure to Jag1 patterns is required to achieve spatial control. These insights in sprouting regulation offer therapeutic handles for spatial regulation of angiogenesis.

INTRODUCTION

The formation of new blood vessels through angiogenesis is a combination of processes, starting with an endothelial sprout and ending with vascular tube maturation and vessel quiescence (Potente and Carmeliet, 2017). These processes need to be spatially guided to ensure the establishment of a functional vasculature. Proper vascularization of tissues (Carmeliet, 2005) is imperative for regenerative medicine and tissue engineering (TE) (Jain et al., 2005; Rouwkema and Khademhosseini, 2016; Kant and Coulombe, 2018).

The Notch signaling pathway is a key regulator of angiogenesis (Holderfield and Hughes, 2008; Phng and Gerhardt, 2009) and may offer a therapeutic handle for spatial control of endothelial sprouting. Genetic removal of Notch ligands and receptors results in disorganized and nonfunctional vasculature and embryonic lethality (Xue et al., 1999; Krebs et al., 2000; Gale et al., 2004; Limbourg et al., 2005). In addition, deregulated Notch activity is linked to pathological angiogenesis (Kofler et al., 2011; Lobov and Mikhailova, 2018). The Notch ligands Delta-like ligand 4 (Dll4) and Jagged1 (Jag1) have distinct roles during angiogenesis (Benedito et al., 2009; Marchetto et al., 2020). Dll4- and Jag1-mediated activation of the receptor Notch1 regulates tip cell versus stalk cell selection and the formation of new branching points during sprouting angiogenesis. This regulation occurs via a crosstalk with Vascular Endothelial Growth Factor (VEGF) signaling, a key driver of angiogenesis (Holderfield and Hughes, 2008; Phng and Gerhardt, 2009; Potente et al., 2011; Blanco and Gerhardt, 2013), and includes Dll4-mediated lateral inhibition. VEGF-VEGFR2 signaling induces Dll4 expression in endothelial cells (Hellström et al., 2007; Phng and Gerhardt, 2009) and the adoption of a migratory tip cell phenotype. Dll4-mediated Notch1 activation in neighboring cells reduces their expression of VEGFR2, causing a lateral inhibition of the tip cell phenotype in these cells, which are thus induced to retain a stalk cell phenotype (Hellström et al., 2007; Lobov et al., 2007; Sainson and Harris, 2008; Benedito et al., 2009). Therefore, the crosstalk between VEGF and Dll4-mediated Notch signaling enhances the differentiation between two adjacent tip and stalk cells. Jag1 competes with Dll4 for Notch binding, thereby counteracting the Dll4-mediated lateral inhibition process and indirectly

[1]Faculty for Science and Engineering, Biosciences, Åbo Akademi University, Turku, 20500, Finland

[2]Department of Biomedical Engineering, Eindhoven University of Technology, Eindhoven, 5612 AZ, the Netherlands

[3]Institute for Complex Molecular Systems (ICMS), Eindhoven University of Technology, Eindhoven, 5612 AZ, the Netherlands

[4]The Biological Design Center and Department of Biomedical Engineering, Boston University, Boston, MA 02215, USA

[5]Turku Bioscience Centre, Åbo Akademi University and University of Turku, Turku, 20500, Finland

[6]The Wyss Institute for Biologically Inspired Engineering, Harvard University, Boston, MA 02115, USA

[7]The Francis Crick Institute, London, NW1 1AT, UK

[8]Department of Informatics, King's College London, London, WC2B 4BG, UK

[9]Lead contact

[10]These authors contributed equally

*Correspondence: l.a.tiemeijer@tue.nl (L.A.T.), t.ristori@tue.nl (T.R.), cecilia.sahlgren@abo.fi (C.M.S.)

https://doi.org/10.1016/j.isci.2022.104306

promoting the tip cell phenotype (Benedito et al., 2009; Marchetto et al., 2020). This Dll4-Jag1 competition needs to be tightly balanced to obtain physiological angiogenesis, characterized by a characteristic pattern of tip cells alternated by stalk cells. This underlies a dose-dependent effect of the ligands. For example, although deletion of Jag1 decreases sprouting, also excessive and unbalanced expression of Jag1 can counteract the formation of the characteristic tip-and-stalk pattern and lead to pathological sprouting (Kang et al., 2019). How this competition between ligands is balanced and how ligand-receptor signaling specificity is achieved is under intense investigation (Benedito et al., 2009; Kakuda and Haltiwanger, 2017; Luca et al., 2017). Despite numerous studies on the role of Notch in angiogenesis, how the spatial organization of Jag1 and Dll4 ligands affect endothelial sprouting still needs to be elucidated.

External patterns of these ligands may provide novel strategies to spatially control and direct endothelial sprouting for regenerative medicine and TE. Several *in vitro* techniques have been proposed to engineer organized vascular networks (Raghavan et al., 2010; Kim et al., 2013; Moya et al., 2013; Malheiro et al., 2016; Rouwkema and Khademhosseini, 2016; Kant and Coulombe, 2018). These methods mainly rely on bioengineering approaches such as PDMS scaffolds, 3D (bio)printing, and microchips, which provide the structural layout of the microvasculature *ex vivo*, but have limited potential to integrate with native or engineered tissues. Direct targeting and stimulation of angiogenesis *in vivo* and *in vitro* have been extensively investigated; examples include injectable biomaterials enriched with Notch signaling components and VEGF (Cao et al., 2010), 3D collagen and Matrigel gels incorporating Notch ligands (Antfolk et al., 2017; van Engeland et al., 2019), and decoy-based targeting of Notch ligands (Kangsamaksin et al., 2015). Although these approaches effectively induce growth of the vasculature, they do not exert control over the location and direction of the blood vessels. We believe that spatially controlled initiation of endothelial sprouting may be an essential first step toward the engineering of functional (micro)vasculature.

Computational models simulating the crosstalk between VEGF and Notch signaling have contributed to our understanding of angiogenesis. Simulations from agent-based models have resulted in a wide range of experimentally validated predictions of sprouting angiogenesis, highlighting the strongly dynamic nature of the tip-stalk phenotypic competition (Bentley et al., 2008; Bentley et al., 2009, 2014; Jakobsson et al., 2010; Ubezio et al., 2016; Zakirov et al., 2021) and the importance of the temporal dynamics of Dll4-Notch1 signaling in defining vascular density (Bentley and Chakravartula, 2017). The role of Jag1 in the VEGF-Notch crosstalk was computationally investigated by Boareto et al. (2015b), who obtained simulations in agreement with previous *in vivo* experiments with Notch1-Jag1 signaling dysregulation (Benedito et al., 2009). Further simulations based on this model could thus help to elucidate the impact of ligand organization on the spatial control of angiogenesis.

Here, we compared the potential of patterns of external Dll4 and Jag1 to spatially control the location and direction of endothelial sprouts (Figure 1). Dll4 micropatterned lines directed the sprout initiation and location in between the lines. These data are in agreement with our previous results, demonstrating that spatial patterns of externally presented Dll4 ligands inhibit angiogenic sprouting (Tiemeijer et al., 2018). Interestingly, spatial patterns of external Jag1 had no evident impact on the location of sprouts. We adapted a previous *in silico* model (Boareto et al., 2015b) to simulate our experimental setting and elucidate the mechanisms behind the ligand-specific effects on angiogenic patterning. The simulations suggest that the lower spatial control of Jag1 compared with Dll4 derives from different timing of Notch activation, which results from the different affinity of Notch1 to the distinct ligands (Luca et al., 2017). The data show that Dll4 is a more potent spatial regulator of endothelial sprouting compared with Jagged1, and its unique ability to exert spatial control could be exploited as a tool for vascular patterning and engineering.

RESULTS

A tailored *in vitro* system enabled a controlled comparison of the effect of Notch ligands on endothelial sprouting

The effect of Jag1 and Dll4 patterns in spatially controlling endothelial sprouting was investigated in a tightly controlled platform that we previously developed (Tiemeijer et al., 2018) (Figure 1). Briefly, microcontact printing (μCP) was adopted to print 100-μm wide fluorescent lines, functionalized with either Jag1 or Dll4, alternated with 100 μm spacing, on glass slides (Figures 1A and 1B). Line functionalization with Fc fragments was used as a control. Microfluidic channels placed on top of the micropatterned lines enabled spatially confined seeding of human umbilical vein endothelial cells (HUVECs) in 150-μm and

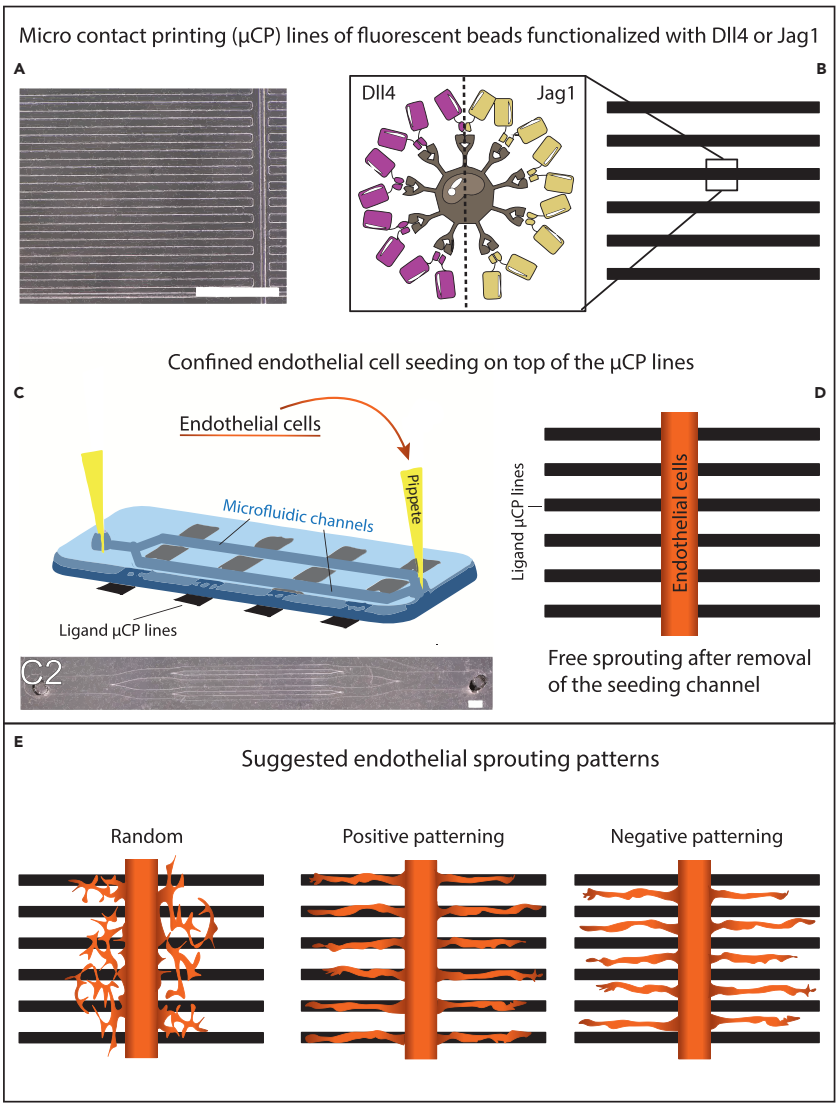

Figure 1. Schematic overview of experimental approach

To compare possible different influences of Dll4 vs Jag1 patterns on endothelial sprouting, the method previously described in Tiemeijer et al. (2018) was adapted.

(A–C and E) In short, microcontact printing (μCP) stamps (A) were inked with fluorescent beads functionalized with either Dll4 or Jagged1, and lines of 100 μm with 100 μm spacing were printed on glass slides (B). (D) In addition, endothelial cells were seeded on top, via microfluidic channels (C and C2) perpendicular to the lines. After channel removal, Matrigel was added, and the endothelial cells were left to sprout freely for 24 h. With respect to the ligand-functionalized lines, we envision the possibility of three different spatial sprouting patterns (E), random, positive, and negative patterning. Scale bar represents 1mm.

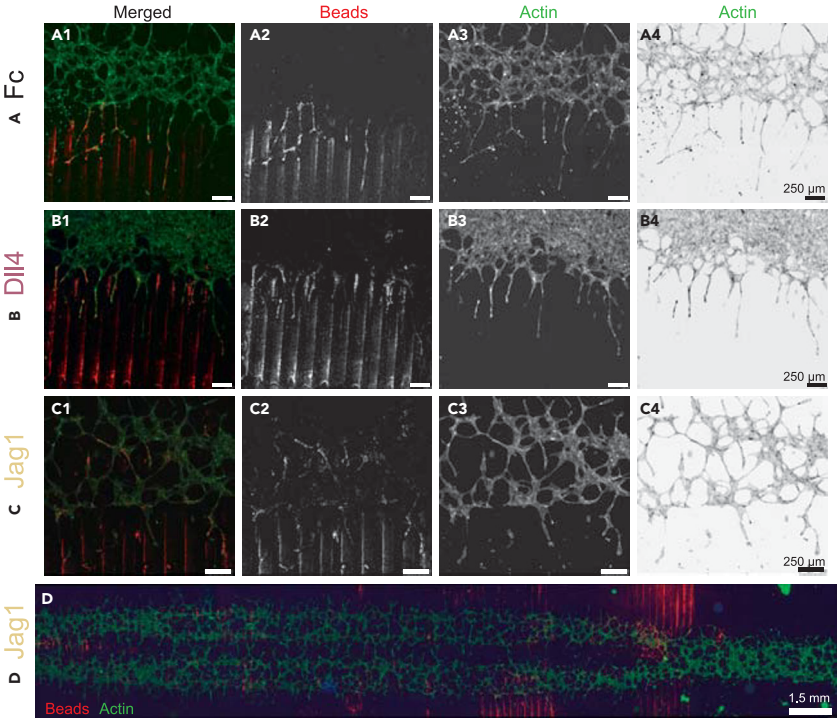

Figure 2. Endothelial sprouting on substrates with different ligand lines after 24 h

(A–D) The top rows (A–C) show zoomed-in sections of representative samples with Jag1, Dll4, and Fc lines, highlighting the fluorescent beads (red) used in the μCP ink (column 2), and the actin skeleton (green) of the endothelial cells, shown as normal and inverted for clearer visual assessment (column 3 and 4, respectively). The bottom row (D) shows a representative image of a whole Jag1 sample, from which ROIs were taken for analysis. As expected, Fc lines did not seem to affect the sprouts, and sprouting did seem to be confined to space between Dll4 lines. However, Jag1 lines did not seem to affect endothelial sprouts, and a similar crossing behavior as in Fc samples could be observed. Scale bars in A–C represent 250 μm. Scale bar in D represents approximately 1.5 mm.

300-μm wide lines perpendicular to the ligand patterns (Figures 1C and 1D). This confined seeding was important to control and study the initiation of sprouting from a restricted area, to mimic sprouting from a native vessel *in vivo*, here represented by a confined endothelial monolayer *in vitro*. Immediately after cell adherence, the channels were removed. After channel removal, Matrigel was placed on top of the cells and the patterned substrate, to allow free cellular sprouting for a period of 24 h, after which cells were fixated for analysis. At the onset of sprouting, the endothelial cells were in contact with the ligand-functionalized lines beneath them, which was expected to influence their tip-stalk cell fate. Moreover, the path of the sprouts during sprouting could be expected to be influenced by ligand-functionalized lines encountered at the sprouting front. To determine the effects of the lines on the sprout location and direction (Figure 1E), fluorescent microcopy was adopted to visualize the actin cytoskeleton, the cell nuclei, and the fluorescent beads in the functionalized lines (Figure 2). As expected, Fc lines did not appear to affect the sprouts (Figures 2A1–2A4), and some sprouts crossed multiple lines. A similar crossing behavior could be observed for Jag1 samples (Figures 2C1–2C4), which exhibited endothelial cells on the lines, in their near vicinity, and in the space between lines. Therefore, visual assessment of the Jag1 samples did not indicate that patterning is controlled by this ligand. In contrast, in agreement with our previous findings, the sprouts in the Dll4 samples did seem to remain confined to the space between lines, consistent with negative patterning (Figures 2B1–2B4).

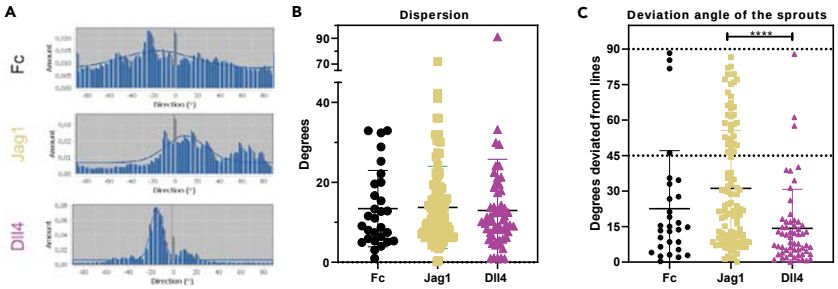

Figure 3. The effects of ligand patterns on sprout direction

Direction of sprouts analyzed with directionality plugIn (ImageJ).

(A–C) Representative histograms for sprouts on Jag1, Dll4, and Fc of selected single ROIs, normalized to the direction of the ligand lines. The dispersion of the fitted graph through the histogram for every ROI is reported in (B). The deviation angles of the sprouts with respect to the line direction, shown in (C), are significantly larger for Jag1 samples compared with Dll4 samples ($p < 0.0001$). See also Figure S1. Data represented as mean ± SD, N = 29/106/58 ROIs pooled from a total of three Fc/4 Jag1/4 Dll4 microchips, respectively, from all experimental rounds combined. ROIs with a goodness of a fit that resulted less than 0.2 were not considered.

Sprouts strongly orient parallel to Dll4, but not Jag1 lines

Regions of interest (ROIs) were identified, by visual assessment, to perform image analysis. ROIs were defined as nonoverlapping regions, adjacent to the original seeding areas of the initially confined endothelial cells, where cells (1) were alive and viable; (2) displayed a sprouting phenotype; (3) were contiguous in the seeded area, mimicking a monolayer; (4) were able to sprout from the seeded area into the ROI; and (5) were exposed to visible lines of functionalized ligand.

First, we analyzed if and how the Jag1 and Dll4 functionalized lines influence the sprout orientation. For every ROI, the average orientation of the actin cytoskeleton of the cells was obtained based on fitted graphs through a direction histogram (Figure 3A). For a better comparison across samples, the orientation angles were normalized such that the ligand functionalized lines of the corresponding sample have a 0° angle. The resulting dispersions of the fitted graphs were not significantly different across samples (Figure 3B). Similarly, when orientation angles between −90° and +90° were considered (Figure S1), no significant difference across samples was observed for the average orientation angles, with angle averages around 0° in all conditions; this is consistent with the symmetry of the system with respect to the direction of the lines. To analyze whether the ligand lines induce sprouts to follow the line direction or to deviate from it, we computed the absolute value of the orientation angles, which we refer to as "deviation angle" (Figure 3C). The deviation angles of sprouts of Jag1 samples were significantly larger than those of the Dll4 samples (Figure 3C). Taken together these results indicate that, although sprouts generally orient in the direction of the lines, the sprouts of Jag1 samples are not hindered to sprout further on reaching Jag1 lines nor are dictated to follow the direction of the lines, in contrast to sprouts on Dll4-patterns.

In contrast to Dll4, Jag1 lines cannot influence the sprout location

To further characterize the difference between Jag1 and Dll4 lines, the efficiency of controlled sprouting (Ef_{cs}) was calculated (Tiemeijer et al., 2018) (Figure 4). Ef_{cs} represents the control of the functionalized lines over the spatial location of the endothelial sprouts. In particular, different sprouting patterns (Figure 1E) correspond to different Ef_{cs} values: $Ef_{cs} \approx 50\%$ for random patterning; $Ef_{cs} \lesssim 50\%$ for positive patterning; and $Ef_{cs} \gtrsim 50\%$ for negative patterning. Moreover, Ef_{cs} values closer to extreme percentages (0 and 100%) correspond to higher spatial control. To calculate the Ef_{cs}, the ROIs were divided into two subregions with identical surface areas adjacent to each other. The subregions were located on the lines or in between the lines (On and Off). The number of cells in those areas were counted and used in the formula depicted in Figure 4A. Here, Ef_{cs} is the percentage of the number of cells that stay in between the lines (C_{off}) calculated from the total number of cells in that ROI. C_{on} is the number of cells that are on the ligand-functionalized lines. The Ef_{cs} of the Jag1 samples was found to be around 50% and was not significantly different from the Ef_{cs} of the control. The Ef_{cs} of the Dll4 samples (Ef_{cs} = 70.17 ± 28.59, mean ± SD) was significantly

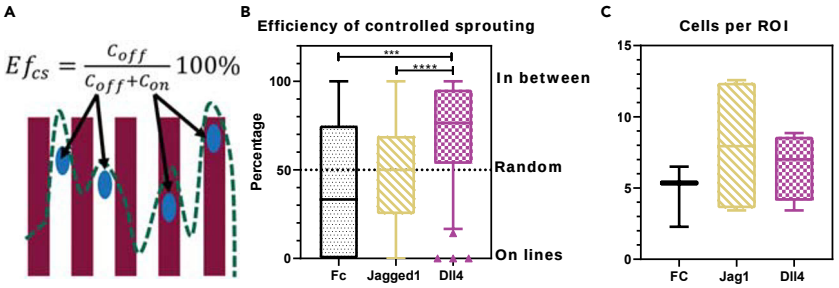

Figure 4. The efficiency of controlled sprouting (Ef_{cs}) induced by ligand patterns

(A and B) Ef_{cs} is defined by the formula in (A) and quantifies the level and type of control of the functionalized lines over the spatial location of the endothelial sprouts. Below the formula, a schematic is presented of the patterned lines (red lines), the cell nuclei (blue ellipses), and the corresponding outline of the sprouting front (discontinuous green line). The formula of Ef_{cs} then accounts for the amount of cells in the subregion of the ROI in between the ligand lines (C_{off}, white area) as a percentage of the total amount of cells (C_{off} + C_{on}) in that ROI. In the definition, C_{on} represents the number of cells in the subregion of the ROI on top of the ligand lines (red area). This definition of Ef_{cs} enables the identification of different sprouting patterns and control: $Ef_{cs} \approx 50\%$ for random patterning and no control; $Ef_{cs} \approx 0\%$ for high control toward positive patterning; and $Ef_{cs} \approx 100\%$ for high control toward negative patterning. Comparison of the Ef_{cs} between Fc, Jag1, and Dll4 line samples is shown in (B), where boxplots represent N = 31/112/58 ROIs pooled from a total of three Fc/four Jag1/4 Dll4 microchips, respectively. There is a significant difference between the Ef_{cs} of Jag1 and Dll4 samples ($p < 0.0001$) and between the Fc and Dll4 ($p = 0.0004$).

(C) No significant difference in the number of cells per ROI. In (B) and (C), data are represented as boxplots, where the boxes span from the 25th until the 75th percentile, the whiskers extend down to the 10th percentile and up to the 90th percentile, and the horizontal lines represent the median values.

increased compared with both control and Jag1 samples (Fc: $Ef_{cs} = 42 \pm 38.57$ and Jag1: $Ef_{cs} = 47.77 \pm 30.69$, mean $\pm$ SD) (Figure 4B). The Ef_{cs} was computed based on multiple nuclei per ROI. To ensure that the difference in Ef_{cs} did not result from a difference in cell number per ROI per sample group, the number of cells per ROI in the samples was analyzed; no significant difference was observed (Figure 4C). Overall, these data show that Dll4 lines are more potent than Jag1 lines in dictating the sprout location.

Simulations qualitatively mimic cell fate differences on different lines

To investigate the underlying mechanisms determining the differential behavior of endothelial cells exposed to Dll4 and Jag1 lines, we simulated our experiments by adapting a previous mathematical model of Notch cross-talking with VEGF that considers Dll4- and Jag1-mediated signaling (Boareto et al., 2015a). Briefly, the model simulates signaling among neighboring cells by assuming that both Dll4 and Jag1 lead to Notch activation, with faster Dll4-Notch1 binding rate and activation compared with Jag1-Notch1. This assumption is motivated by the higher affinity of Dll4 to Notch1, which leads to a higher probability of Dll4-mediated Notch1 activation, compared with Jag1-mediated activation, in a shorter time (Luca et al., 2017). The model also assumes that Notch activation downregulates VEGFR. This signaling crosstalk leads to three possible phenotypes based on the level of VEGFR activity: migratory tip cells with very high activity; proliferative stalk cells with very low activity; and slowly migrating tip/stalk hybrid cells, with moderate activity. To simulate our experiments, taking advantage of the spatial periodicity of the system, we considered cell signaling among cells on a limited area of the substrate, corresponding to cells located in between (half of) two patterned lines (Figure 5A). The Notch receptors of the cells on top of the lines were assumed to bind and be activated by the Notch ligands on the patterns in the same way as Notch ligands of neighboring cells. A more detailed model and parameter description can be found in the supplemental information.

Cell-cell signaling was simulated among 12 adjacent endothelial cells for 12 h, in accordance and within the time frame of the experiments. Representative images of the computational results (Figure 5B) show that most cells had a hybrid tip/stalk phenotype when not presented to Notch functionalized ligands, corresponding to randomly distributed (slowly) migrating cells (Figure 5B, bottom row). With increasing Notch ligand concentrations, Dll4 patterns increasingly forced the cells on top of the lines to obtain a stalk phenotype (Figure 5B right), in agreement with experiments where the tip cells were observed only in between the

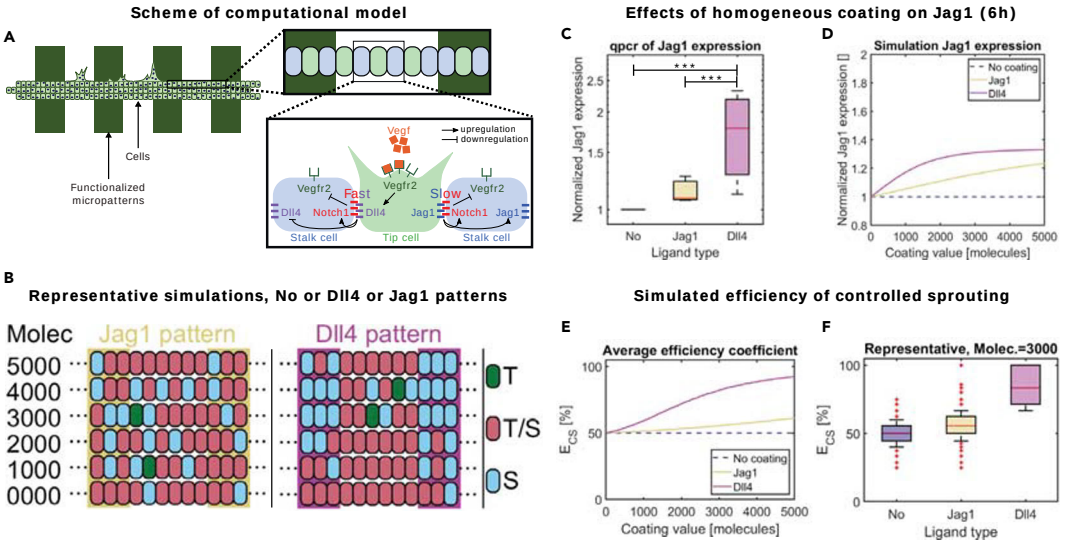

Figure 5. The computational model quantitatively replicates the experiments

(A) Due to periodicity, cell-cell signaling was modeled only for a small portion of the cells on the patterned substrate. The first enlargement shows the cells that were analyzed in the simulations. The second enlargement shows the main features of the simulated signaling network.

(B) Representative computational results, with each row corresponding to one simulation, with different ligand concentrations on the micropatterns (decreasing from top to bottom). Without ligands on the patterns (bottom row) most cells have a tip/stalk (T/S) hybrid phenotype (red). With increasing concentration, Dll4 induces the stalk (S, blue) phenotype for cells on top of the lines, whereas Jag1 does not have evident effects. Only few tip (T, green) cells were observed.

(C and D) The effects of homogeneous coating of Fc, Jag1, or Dll4 on the gene expression of Jag1 were compared between experimental (C) and computational (D) data for the time period of 6 h. qPCR revealed a significant difference of Jag1 expression for Dll4 versus Fc samples ($p < 0.0001$) and for Dll4 versus Jag1 samples ($p < 0.001$). For the computational data, averages over 10,000 simulations for each concentration are reported.

(E) The efficiency of controlled sprouting was computed for simulations of cells on patterned lines with varying ligand densities. The graph reports the averages of the computed values over 10,000 simulations.

(F) Boxplots obtained for the simulations with $D_{line} = J_{line} = 3000$ molecules. The simulations captured the higher spatial control of Dll4 lines, compared with Jag1 lines, on the location of the sprouts (E and F). In (C) and (F), data are represented as boxplots, where the boxes span from the 25th until the 75th percentile, the whiskers extend down to the 10th percentile and up to the 90th percentile, and the horizontal lines represent the median values.

lines (Figure 4B). Jag1, on the other hand, did not have any evident effect on the phenotypes (Figure 5B left), also corresponding to the experimental results (Figure 4B).

Simulations quantitatively mimic the experiments in terms of tip cell distribution

To better compare the experiments and simulations, we calibrated the model parameters D_{line} and J_{line}, corresponding to the Notch ligand content coated on top of the lines. For calibration, via qPCR, we obtained the Jag1 expression of HUVECs exposed to homogeneously coated ligands for 6 h (Figure 5C), and we simulated these experiments by considering different ligand densities (Figure 5D). The computational results mimicked the higher Jag1 expression response elicited by Dll4 coating, compared with Jag1 coating (Figures 5C and 5D). As a result of this comparison, we chose $D_{line} = J_{line} = 3000$ molecules as a representative ligand content for the simulations, considering this as a parameter value leading to a very high Dll4 response balanced by relatively low Jag1 effects.

After calibration, a quantitative comparison between sprouting experiments and simulations was obtained by plotting the boxplots of Ef_{cs} values resulting from 10,000 simulations, performed with the identified representative ligand concentration. The model could quantitatively mimic the experiments (Figure 5F): Dll4 ligands induced Ef_{cs} values around the value 100%, corresponding to sprouts only in between the lines; Jag1 elicited a random sprout distribution, very similar to the Fc control, corresponding to Ef_{cs} values around the value 50%. Further simulations (Figure 5E) indicated that increasing the Dll4 concentration on the patterns causes an increasing distribution of tip cells in between the lines, and stalk cells on top

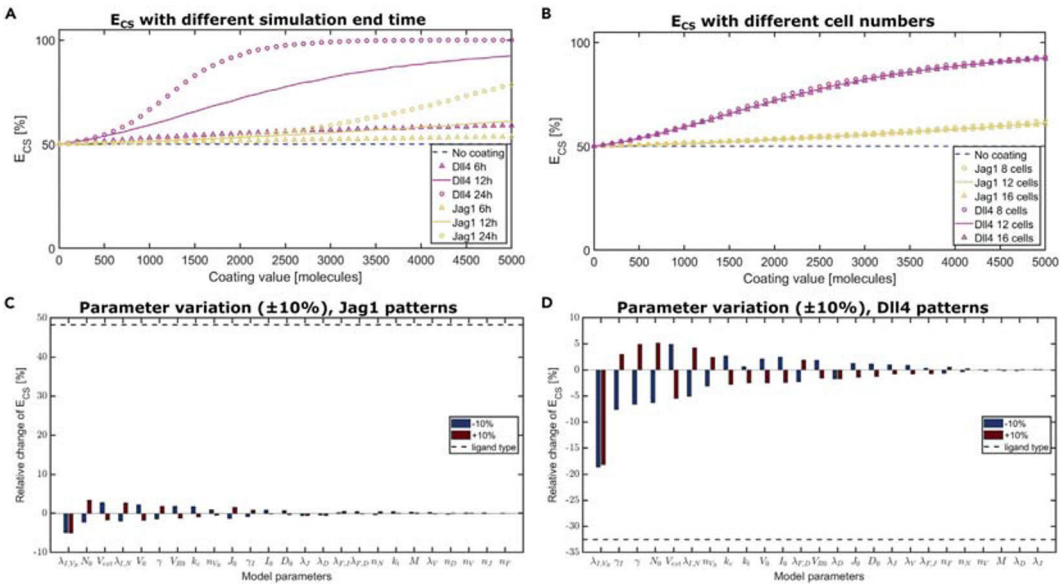

Figure 6. Parameter exploration identifies duration of ligand induction as a major determinant of efficiency of control

(A and B) Efficiency of controlled sprouting computed for simulations with varying ligand content on the patterns, for different end time of the simulations (A), and different number of cells on the patterns (B).

(C and D) Sensitivity of the efficiency of controlled spatial sprouting computed for Jag1 patterns (C) and Dll4 patterns (D) to 10% variations of the parameters describing the signaling dynamics, compared with switching the ligand type (dashed lines). In all cases, the values reported are averages over 10,000 simulations obtained by varying the initial protein content in each cell.

of the lines, whereas Jag1 has a much lower effect even at very high concentrations. Overall, these simulations indicate that the experimentally observed response of cells to the lines can be replicated with a computational model assuming that Dll4-Notch1 activation occurs at a higher rate than the Jag1-Notch1 counterpart, highlighting a possible role of the signaling temporal dynamics.

Parameter exploration confirms that Notch signaling temporal dynamics is a key factor

After verifying that the model can replicate the experiments, we performed additional simulations to confirm the importance of the signaling temporal dynamics compared with other parameters. To this aim, we performed a parameter exploration by varying the final time of the simulations between 6 and 24 h (Figure 6A), the number of cells on the lines (Figure 6B) and the other model parameters describing the cell signaling dynamics (Figures 6C and 6D). Interestingly, Figure 6A shows that the timing of cell migration away from the original configuration is a major determinant of the effects of Dll4 and Jag1. Generally, the effect of the ligand functionalized lines positively correlates with the time necessary for cells to leave the patterned lines; a longer time spent on the patterns gives a stronger effect. The simulations suggest that Jag1 might have a higher effect if the cells stay on top of the patterns for a longer period, so as to allow a longer time for Jag1 to activate Notch1. Overall, variations of the other model parameters (Figures 6B–6D) did not cause large variations of the results, especially compared with the variations caused by switching the ligand type (Dll4 to Jag1 and vice-versa, Figures 6C and 6D). In conclusion, the simulations indicate that the choice of ligand and the temporal dynamics are major determinants of the endothelial sprouting response of cells to the functionalized lines.

DISCUSSION

A spatially organized vasculature is important for tissue functionality, and spatially controlling angiogenesis is fundamental for regenerative medicine and TE applications (Jain et al., 2005; Rouwkema and Khademhosseini, 2016; Kant and Coulombe, 2018). Current approaches do not enable optimal control over

the location and direction of dynamic sprouts. We believe that spatially controlling the initiation of endothelial sprouting is key for applying further control over angiogenesis in an engineered vasculature context. Notch signaling is a key regulator of sprouting angiogenesis (Holderfield and Hughes, 2008; Phng and Gerhardt, 2009). Engineering micropatterns of Notch ligands might thus enable spatial control of sprouts. Here, by combining *in vitro* and *in silico* models, we investigated the potential and underlying mechanisms of Jag1 and Dll4 lines controlling the location and direction of endothelial sprouts. In agreement with our previous findings (Tiemeijer et al., 2018), we confirmed the potency of Dll4 lines for negative patterning of endothelial sprouting (Figure 1E). Our results indicate that spatially controlled external patterns of Dll4 can overrule the native Dll4-mediated tip-stalk cell selection and dictate the location of stalk cells. Despite the opposite role of Jag1 in native angiogenesis (Benedito et al., 2009; Marchetto et al., 2020), Jag1 lines did not elicit positive patterning but rather random patterning (Figure 1E). Specifically, Jag1 lines had a very low efficiency to control the sprout location (Figure 4) and a higher deviation angle between the lines and the sprout orientation (Figure 3). Dll4 is therefore much more potent than Jag1 in spatially controlling sprouting. Our simulations indicate that this difference arises from the distinct affinity of the ligands to Notch1 (Luca et al., 2017).

The lower affinity of Jag1 to Notch1, compared with Dll4, causes a slower rate of Jag1-mediated Notch1 activation (Kakuda and Haltiwanger, 2017); this is a key assumption of the computational model and enabled the simulations to capture the experimental results (Figure 5). In the simulations, the μCP Dll4 rapidly activates the Notch1 receptor of cells on Dll4 lines, thereby forcing them to the stalk cell phenotype and allowing sprout formation only in between the patterns. In contrast, Jag1 requires a longer time to activate Notch1 because of its lower affinity (Luca et al., 2017). Cells can therefore sprout on Jag1 lines before being forced to a stalk phenotype. Previous studies have highlighted the temporal dynamics of Notch as a key factor for native angiogenesis (Bentley and Chakravartula, 2017). Our findings provide a different angle, emphasizing the importance of the receptor-ligand binding and activation rate for the spatial control of angiogenesis with Notch micropatterns. In particular, our results suggest that a higher spatial control of endothelial sprouts could be achieved by controlling the time of ligand exposure (Figure 6A) or by engineering ligands with higher affinity to Notch1.

To model signaling among cells, the original assumptions of the model of Boareto et al. (2015b) were adopted, including the assumption that Dll4 and Jag1 have different affinity to Notch1 because of Fringe activity. Fringes are enzymes that glycosylate the Notch extracellular domain (Brückner et al., 2000); as a result of their activity, Dll4- and Jag1-mediated activation of Notch1 increases or decreases, respectively (Benedito et al., 2009). Recent studies indicate that Dll4 and Jag1 have different affinity irrespective of Fringe (Luca et al., 2017). The computational model could be modified to account for this, but our conclusions would not change: Jag1 patterns would require more time to activate Notch1 compared with Dll4. This time difference arises from affinity and probability. As reported by Luca et al. (Luca et al., 2017), "the probability that a Notch1 receptor is engaged with a ligand during the period of cellular tension application to the receptor is higher if the affinity is higher." In other words, higher affinity translates into a higher probability of Notch1 activation and, thus, a larger Notch1 activation in a limited amount of time; this can be rephrased by saying that having a higher affinity among ligands and receptors is equivalent to having a higher rate of Notch1 activation as mediated by such ligand-receptor interaction. In principle, at least in the computational model, the lower rate of Jag1-mediated Notch1 activation might be compensated by a higher concentration of Jag1 on the patterns: this would increase the probability of successful binding and Notch1 activation in a fixed time and therefore increase the activation rate. However, it is unclear whether this high concentration of Jag1 could lead to physiological sprouting, due to the dose-dependent effect of this ligand in the context of angiogenesis. In fact, as indicated by a recent study (Kang et al., 2019) combining a 3D *in vitro* model of angiogenesis and an extension of the model adapted in the present study (Boareto et al., 2015b), excessive concentrations of Jag1 can result in antiangiogenic responses (Kang et al., 2019). Therefore, future applications should still focus on Dll4 patterns rather than Jag1 patterns.

Our findings can be translated toward controlling angiogenesis for TE and regenerative medicine. Spatially controlling the initiation of endothelial sprouting can be a central step toward providing a controlled functional vasculature. Here, Dll4 ligands were clearly more potent than Jag1 in dictating the location of endothelial sprouts. Therefore, future studies in this context should choose Dll4 rather than Jag1, although the use of Dll4 might present challenges in 3D. In 2D, we were able to confine the sprouts in between two Dll4

lines because of the inhibitory effect of this ligand. However, cells have increased freedom in 3D, which makes their confinement and guidance more challenging. Dll4 functionalized materials might nevertheless be used in 3D to avoid cells from sprouting through specific homogeneously functionalized surfaces, to avoid sprouting toward some areas.

In conclusion, by combining *in vitro* and *in silico* models, we demonstrated that engineering patterns of Jag1 have a lower potential to control the location and direction of endothelial sprouts than Dll4 patterns. The simulations indicate that this difference arises from the lower affinity of Jag1 to Notch1 compared with Dll4, which results in a slower Jag1-mediated activation of Notch1. To achieve a higher spatial control of endothelial sprouting, future studies could aim at engineering Notch ligands with higher affinity to Notch1.

Limitations of the study

The present study presents some limitations, which were minimized to enhance the accuracy of the data interpretation. The experimental method involves manual steps that could result in small sample imperfections. To drastically limit their possible influence on the data analysis, the criteria for the ROI selection were set very strictly. In addition, in contrast to native angiogenesis, our *in vitro* and *in silico* models do not expose cells to VEGF gradients; their inclusion would tremendously increase the complexity of the *in vitro* system design and validation. In particular, it would require a more controlled addition of VEGF within microchips, similar to Zheng et al. (Zheng et al., 2017); however, combining these devices with the micropatterning of Notch ligands would be extremely challenging. Computationally, the effects of VEGF gradients could be investigated by extending the computational model with filopodia formation (Venkatraman et al., 2016), cell shape changes, and movement (Vega et al., 2020). These mechanisms, affected by VEGF gradients (Gerhardt et al., 2003), were not considered here because we focused on the initial response of cells leaving the original seeding area. The absence of these factors may explain why the computational model did not predict alternating tip-stalk phenotypes for cells on control substrates (Figure 5B), in contrast to previous predictions for native angiogenesis (Boareto et al., 2015b). In absence of VEGF gradients, filopodia formation, and of cell shape changes, several feedback loops in the VEGF-Notch crosstalk are necessary to establish the tip-stalk pattern at the gene level (Bentley and Chakravartula, 2017). Each loop has a period of around 4 to 6 h (Ubezio et al., 2016). Therefore, in agreement with experiments, our simulation end time of 12 h is too short for cells to establish the characteristic tip-stalk pattern. Choosing 12 h is here justified by the short time necessary for cells to leave the initial seeding position in our devices, much shorter than both 24 h (our experiment end time) and the asymptotic conditions simulated for native angiogenesis (Boareto et al., 2015b).

STAR★METHODS

Detailed methods are provided in the online version of this paper and include the following:

- KEY RESOURCES TABLE
- RESOURCE AVAILABILITY
  - Lead contact
  - Materials availability
  - Data and code availability
- EXPERIMENTAL MODEL AND SUBJECT DETAILS
  - Primary cells source
- METHOD DETAILS
  - Experimental design (objectives and design of study)
  - Fabrication of the soft lithography masters
  - Fabrication of μCP stamps and cell seeding channels
  - Cell culture
  - μCP of ligand functionalized lines
  - Confined cell seeding and sprouting assay
  - Fluorescent microscopy and image analysis
  - qPCR
  - Computational model
- QUANTIFICATION AND STATISTICAL ANALYSIS
  - Experimental results

SUPPLEMENTAL INFORMATION

Supplemental information can be found online at https://doi.org/10.1016/j.isci.2022.104306.

ACKNOWLEDGMENTS

Funding: this study was supported by the Academy of Finland, grant numbers 307133, 316882, and 330411 (LAT, OMJAS, CMS); the Marie Sklodowska-Curie Global Fellowship, grant number 846617 (to TR); ERC ForceMorph, grant number 771168 (OMJAS, CMS). LAT was supported by the Turku Doctoral Network in Molecular Biosciences at Åbo Akademi University. CSC was supported by NIH (EB00262 and HL147585). KB was supported by the Francis Crick Institute, which receives its core funding from Cancer Research UK (FC001751), the UK Medical Research Council (FC001751), and the Wellcome Trust (FC001751). We gratefully acknowledge the Gravitation Program "Materials Driven Regeneration", funded by the Netherlands Organisation for Scientific Research (024.003.013) (CVB), the InFLAMES Flagship Program of the Academy of Finland (337531) (LAT, CMS), and the Åbo Akademi University Foundation's Center of Excellence in Cellular Mechanostasis (CellMech) (CMS).

AUTHOR CONTRIBUTIONS

Conceptualization: LAT, TR, CMS. Formal Analyses: LAT, TR, OMJAS. Funding Acquisition: TR, KB, CS, CVCB, CMS. Investigation: LAT, TR, JJJB, JJA, OMJAS. Methodology: LAT, TR, CMS. Project Administration: LAT, TR, CMS. Resources: CSC, CVCB, CMS. Software: TR, JJJB. Supervision: CSC, KB, CVCB, CMS. Validation: LAT, TR, CMS. Visualization: LAT, TR. Writing—Original Draft: LAT, TR. Writing—Review and Editing: LAT, TR, OMJAS, CSC, KB, CVCB, CMS.

DECLARATION OF INTERESTS

Authors declare that they have no competing interests.

Received: October 7, 2021
Revised: February 25, 2022
Accepted: April 22, 2022
Published: May 20, 2022

REFERENCES

Antfolk, D., Sjoqvist, M., Cheng, F., Isoniemi, K., Duran, C.L., Rivero-Muller, A., Antila, C., Niemi, R., Landor, S., Bouten, C.V.C., et al. (2017). Selective regulation of Notch ligands during angiogenesis is mediated by vimentin. Proc. Natl. Acad. Sci. U S A *114*, E4574–E4581. https://doi.org/10.1073/pnas.1703057114.

Benedito, R., Roca, C., Sorensen, I., Adams, S., Gossler, A., Fruttiger, M., and Adams, R.H. (2009). The notch ligands Dll4 and Jagged1 have opposing effects on angiogenesis. Cell *137*, 1124–1135. https://doi.org/10.1016/j.cell.2009.03.025.

Bentley, K., Mariggi, G., Gerhardt, H., and Bates, P.A. (2009). Tipping the balance: robustness of tip cell selection, migration and fusion in angiogenesis. PLoS Comput. Biol. *5*, e1000549. https://doi.org/10.1371/journal.pcbi.1000549.

Bentley, K., Franco, C.A., Philippides, A., Blanco, R., Dierkes, M., Gebala, V., Stanchi, F., Jones, M., Aspalter, I.M., Cagna, G., et al. (2014). The role of differential VE-cadherin dynamics in cell rearrangement during angiogenesis. Nat. Cell Biol. *16*, 309–321. https://doi.org/10.1038/ncb2926.

Bentley, K., and Chakravartula, S. (2017). The temporal basis of angiogenesis. Phil. Trans. R. Soc. B Biol. Sci. *372*, 20150522. https://doi.org/10.1098/rstb.2015.0522.

Bentley, K., Gerhardt, H., and Bates, P.A. (2008). Agent-based simulation of notch-mediated tip cell selection in angiogenic sprout initialisation. J. Theor. Biol. *250*, 25–36. https://doi.org/10.1016/j.jtbi.2007.09.015.

Blanco, R., and Gerhardt, H. (2013). VEGF and Notch in tip and stalk cell selection. Cold Spring Harbor Perspect. Med. *3*. a006569–19. https://doi.org/10.1101/cshperspect.a006569.

Boareto, M., Jolly, M.K., Lu, M., Onuchic, J.N., Clementi, C., and Ben-Jacob, E. (2015a). Jagged–Delta asymmetry in Notch signaling can give rise to a Sender/Receiver hybrid phenotype. Proc. Natl. Acad. Sci. U S A *112*, E402–E409. https://doi.org/10.1073/pnas.1416287112.

Boareto, M., Jolly, M.K., Ben-Jacob, E., and Onuchic, J.N. (2015b). Jagged mediates differences in normal and tumor angiogenesis by affecting tip-stalk fate decision. Proc. Natl. Acad. Sci. U S A *112*, E3836–E3844. https://doi.org/10.1073/pnas.1511814112.

Brückner, K., Perez, L., Clausen, H., and Cohen, S. (2000). Glycosyltransferase activity of fringe modulates notch–delta interactions. Nature *406*, 411–415. https://doi.org/10.1038/35019075.

Cao, L., Arany, P.R., Kim, J., Rivera-Feliciano, J., Wang, Y.S., He, Z., Rask-Madsen, C., King, G.L., and Mooney, D.J. (2010). Modulating Notch signaling to enhance neovascularization and reperfusion in diabetic mice. Biomaterials *31*, 9048–9056. https://doi.org/10.1016/j.biomaterials.2010.08.002.

Carmeliet, P. (2005). Angiogenesis in life, disease and medicine. Nature *438*, 932–936. https://doi.org/10.1038/nature04478.

van Engeland, N.C.A., Suarez Rodriguez, F., Rivero-Muller, A., Ristori, T., Duran, C.L., Stassen, O.M.J.A., Antfolk, D., Driessen, R.C.H., Ruohonen, S., Ruohonen, S.T., et al. (2019). Vimentin regulates Notch signaling strength and arterial remodeling in response to hemodynamic stress. Scientific Rep. *9*, 12415. https://doi.org/10.1038/s41598-019-48218-w.

Frimat, J.P., Menne, H., Michels, A., Kittel, S., Kettler, R., Borgmann, S., Franzke, J., and West, J. (2009). Plasma stencilling methods for cell patterning. Anal. Bioanal. Chem. *395*, 601–609. https://doi.org/10.1007/s00216-009-2824-7.

Gale, N.W., Dominguez, M.G., Noguera, I., Pan, L., Hughes, V., Valenzuela, D.M., Murphy, A.J., Adams, N.C., Lin, H.C., Holash, J., et al. (2004). Haploinsufficiency of delta-like 4 ligand results in embryonic lethality due to major defects in arterial and vascular development. Proc. Natl. Acad. Sci. U S A

101, 15949–15954. https://doi.org/10.1073/pnas.0407290101.

Gerhardt, H., Golding, M., Fruttiger, M., Ruhrberg, C., Lundkvist, A., Abramsson, A., Jeltsch, M., Mitchell, C., Alitalo, K., Shima, D., and Betsholtz, C. (2003). VEGF guides angiogenic sprouting utilizing endothelial tip cell filopodia. J. Cell Biol. *161*, 1163–1177. https://doi.org/10.1083/jcb.200302047.

Hellström, M., Phng, L.K., Hofmann, J.J., Wallgard, E., Coultas, L., Lindblom, P., Alva, J., Nilsson, A.K., Karlsson, L., Gaiano, N., et al. (2007). Dll4 signalling through Notch1 regulates formation of tip cells during angiogenesis. Nature *445*, 776–780. https://doi.org/10.1038/nature05571.

Holderfield, M.T., and Hughes, C.C.W. (2008). Crosstalk between vascular endothelial growth factor, notch, and transforming growth factor-β in vascular morphogenesis. Circ. Res. *102*, 637–652. https://doi.org/10.1161/CIRCRESAHA.107.167171.

Jain, R.K., Au, P., Tam, J., Duda, D.G., and Fukumura, D. (2005). Engineering vascularized tissue. Nat. Biotechnol. *23*, 821–823. https://doi.org/10.1038/nbt0705-821.

Jakobsson, L., Franco, C.A., Bentley, K., Collins, R.T., Ponsioen, B., Aspalter, I.M., Rosewell, I., Busse, M., Thurston, G., Medvinsky, A., et al. (2010). Endothelial cells dynamically compete for the tip cell position during angiogenic sprouting. Nat. Cell Biol. *12*, 943–953. https://doi.org/10.1038/ncb2103.

Kakuda, S., and Haltiwanger, R.S. (2017). Deciphering the fringe-mediated notch code: identification of activating and inhibiting sites allowing discrimination between ligands. Dev. Cell *40*, 193–201. https://doi.org/10.1016/j.devcel.2016.12.013.

Kang, T.Y., Bocci, F., Jolly, M.K., Levine, H., Onuchic, J.N., and Levchenko, A. (2019). Pericytes enable effective angiogenesis in the presence of proinflammatory signals. Proc. Natl. Acad. Sci. U S A *116*, 23551–23561. https://doi.org/10.1073/pnas.1913373116.

Kangsamaksin, T., Murtomaki, A., Kofler, N.M., Cuervo, H., Chaudhri, R.A., Tattersall, I.W., Rosenstiel, P.E., Shawber, C.J., and Kitajewski, J. (2015). NOTCH decoys that selectively block DLL/NOTCH or JAG/NOTCH disrupt angiogenesis by unique mechanisms to inhibit tumor growth. Cancer Discov. *5*, 182–197. https://doi.org/10.1158/2159-8290.CD-14-0650.

Kant, R.J., and Coulombe, K.L.K. (2018). Integrated approaches to spatiotemporally directing angiogenesis in host and engineered tissues. Acta Biomater. *69*, 42–62. https://doi.org/10.1016/j.actbio.2018.01.017.

Kim, S., Lee, H., Chung, M., and Jeon, N.L. (2013). Engineering of functional, perfusable 3D microvascular networks on a chip. Lab Chip *13*, 1489. https://doi.org/10.1039/c3lc41320a.

Kofler, N.M., Shawber, C.J., Kangsamaksin, T., Reed, H.O., Galatioto, J., and Kitajewski, J. (2011). Notch signaling in developmental and tumor angiogenesis. Genes and Cancer *2*, 1106–1116. https://doi.org/10.1177/1947601911423030.

Kopan, R., and Ilagan, M.X.G. (2009). The canonical notch signaling pathway: unfolding the activation mechanism. Cell *137*, 216–233. https://doi.org/10.1016/j.cell.2009.03.045.

Krebs, L.T., Xue, Y., Norton, C.R., Shutter, J.R., Maguire, M., Sundberg, J.P., Gallahan, D., Closson, V., Kitajewski, J., Callahan, R., et al. (2000). Notch signaling is essential for vascular morphogenesis in mice. Genes Dev. *14*, 1343–1352. https://doi.org/10.1101/gad.14.11.1343.

Limbourg, F.P., Takeshita, K., Radtke, F., Bronson, R.T., Chin, M.T., and Liao, J.K. (2005). Essential role of endothelial Notch1 in angiogenesis. Circulation *111*, 1826–1832. https://doi.org/10.1161/01.CIR.0000160870.93058.DD.

Lobov, I.B., Renard, R.A., Papadopoulos, N., Gale, N.W., Thurston, G., Yancopoulos, G.D., and Wiegand, S.J. (2007). Delta-like ligand 4 (Dll4) is induced by VEGF as a negative regulator of angiogenic sprouting. Proc. Natl. Acad. Sci. U S A *104*, 3219–3224. https://doi.org/10.1073/pnas.0611206104.

Lobov, I., and Mikhailova, N. (2018). The role of dll4/notch signaling in normal and pathological ocular angiogenesis: dll4 controls blood vessel sprouting and vessel remodeling in normal and pathological conditions. J. Ophthalmol. *2018*, 3565292. https://doi.org/10.1155/2018/3565292.

Loerakker, S., Stassen, O.M.J.A., ter Huurne, F.M., Boareto, M., Bouten, C.V.C., and Sahlgren, C.M. (2018). Mechanosensitivity of Jagged-Notch signaling can induce a switch-type behavior in vascular homeostasis. Proc. Natl. Acad. Sci. U S A *115*, E3682–E3691. https://doi.org/10.1073/pnas.1715277115.

Luca, V.C., Kim, B.C., Ge, C., Kakuda, S., Wu, D., Roein-Peikar, M., Haltiwanger, R.S., Zhu, C., Ha, T., and Garcia, K.C. (2017). Notch-Jagged complex structure implicates a catch bond in tuning ligand sensitivity. Science *355*, 1320–1324. https://doi.org/10.1126/science.aaf9739.

Malheiro, A., Wieringa, P., Mota, C., Baker, M., and Moroni, L. (2016). Patterning vasculature: the role of biofabrication to achieve an integrated multicellular ecosystem. ACS Biomater. Sci. Eng. *2*, 1694–1709. https://doi.org/10.1021/acsbiomaterials.6b00269.

Manderfield, L.J., High, F.A., Engleka, K.A., Liu, F., Li, L., Rentschler, S., and Epstein, J.A. (2012). Notch activation of Jagged1 contributes to the assembly of the arterial wall. Circulation *125*, 314–323. https://doi.org/10.1161/CIRCULATIONAHA.111.047159.

Marchetto, N.M., Begum, S., Wu, T., O'Besso, V., Yarborough, C.C., Valero-Pacheco, N., Beaulieu, A.M., Kitajewski, J.K., Shawber, C.J., and Douglas, N.C. (2020). Endothelial jagged1 antagonizes dll4/notch signaling in decidual angiogenesis during early mouse pregnancy. Int. J. Mol. Sci. *21*, 6477. https://doi.org/10.3390/ijms21186477.

Morales, A.V., Yasuda, Y., and Ish-Horowicz, D. (2002). Periodic Lunatic fringe expression is controlled during segmentation by a cyclic transcriptional enhancer responsive to Notch signaling. Dev. Cell *3*, 63–74. https://doi.org/10.1016/S1534-5807(02)00211-3.

Moya, M.L., Hsu, Y.H., Lee, A.P., Hughes, C.C., and George, S.C. (2013). In vitro perfused human capillary networks. Tissue Eng. Part C Methods *19* (9), 730–737. https://doi.org/10.1089/ten.tec.2012.0430.

Phng, L.K., and Gerhardt, H. (2009). Angiogenesis: a team effort coordinated by notch. Dev. Cell *16*, 196–208. https://doi.org/10.1016/j.devcel.2009.01.015.

Potente, M., and Carmeliet, P. (2017). The link between angiogenesis and endothelial metabolism. Annu. Rev. Physiol. *79*, 43–66. https://doi.org/10.1146/annurev-physiol-021115-105134.

Potente, M., Gerhardt, H., and Carmeliet, P. (2011). Basic and therapeutic aspects of angiogenesis. Cell *146*, 873–887. https://doi.org/10.1016/j.cell.2011.08.039.

Raghavan, S., Nelson, C.M., Baranski, J.D., Lim, E., and Chen, C.S. (2010). Geometrically controlled endothelial tubulogenesis in micropatterned gels. Tissue Eng. Part A *16* (7), 2255–2263. https://doi.org/10.1089/ten.tea.2009.0584.

Ristori, T., Stassen, O.M.J.A., Sahlgren, C.M., and Loerakker, S. (2020). Lateral induction limits the impact of cell connectivity on Notch signaling in arterial walls. Int. J. Numer. Methods Biomed. Eng. *36*, e3323. https://doi.org/10.1002/cnm.3323.

Rouwkema, J., and Khademhosseini, A. (2016). Vascularization and angiogenesis in tissue engineering: beyond creating static networks. Trends Biotechnol. *34*, 733–745. https://doi.org/10.1016/j.tibtech.2016.03.002.

Sainson, R.C.A., and Harris, A.L. (2008). Regulation of angiogenesis by homotypic and heterotypic notch signalling in endothelial cells and pericytes: from basic research to potential therapies. Angiogenesis *11*, 41–51. https://doi.org/10.1007/s10456-008-9098-0.

Schindelin, J., Arganda-Carreras, I., Frise, E., Kaynig, V., Longair, M., Pietzsch, T., Preibisch, S., Rueden, C., Saalfeld, S., Schmid, B., et al. (2012). Fiji: an open-source platform for biological-image analysis. Nat. Methods *9*, 676–682. https://doi.org/10.1038/nmeth.2019.

Shimojo, H., Ohtsuka, T., and Kageyama, R. (2011). Dynamic expression of notch signaling genes in neural stem/progenitor cells. Front. Neurosci. *5*, 1–7. https://doi.org/10.3389/fnins.2011.00078.

Sprinzak, D., Lakhanpal, A., Lebon, L., Santat, L.A., Fontes, M.E., Anderson, G.A., Garcia-Ojalvo, J., and Elowitz, M.B. (2010). Cis-interactions between Notch and Delta generate mutually exclusive signalling states. Nature *465*, 86–90. https://doi.org/10.1038/nature08959.

Tiemeijer, L.A., Frimat, J.P., Stassen, O.M.J.A., Bouten, C.V.C., and Sahlgren, C.M. (2018). Spatial patterning of the Notch ligand Dll4 controls endothelial sprouting in vitro. Sci. Rep. *8*, 6392. https://doi.org/10.1038/s41598-018-24646-y.

Ubezio, B., Blanco, R.A., Geudens, I., Stanchi, F., Mathivet, T., Jones, M.L., Ragab, A., Bentley, K., and Gerhardt, H. (2016). Synchronization of endothelial Dll4-Notch dynamics switch blood vessels from branching to expansion. eLife *5*, e12167. https://doi.org/10.7554/eLife.12167.

Vega, R., Carretero, M., Travasso, R.D.M., and Bonilla, L.L. (2020). Notch signaling and taxis mechanisms regulate early stage angiogenesis: a mathematical and computational model. PLoS Comput. Biol. *16*, e1006919. https://doi.org/10.1371/journal.pcbi.1006919.

Venkatraman, L., Regan, E.R., and Bentley, K. (2016). Time to decide? Dynamical analysis predicts partial tip/stalk patterning states arise during angiogenesis. PLoS One *11*. e0166489–23. https://doi.org/10.1371/journal.pone.0166489.

Xue, Y., Gao, X., Lindsell, C.E., Norton, C.R., Chang, B., Hicks, C., Gendron-Maguire, M., Rand, E.B., Weinmaster, G., and Gridley, T. (1999). Embryonic lethality and vascular defects in mice lacking the Notch ligand Jagged1. Hum. Mol. Genet. *8*, 723–730. https://doi.org/10.1093/hmg/8.5.723.

Zakirov, B., Charalambous, G., Thuret, R., Aspalter, I.M., Van-Vuuren, K., Mead, T., Harrington, K., Regan, E.R., Herbert, S.P., and Bentley, K. (2021). Active perception during angiogenesis: filopodia speed up Notch selection of tip cells in silico and in vivo. Phil. Trans. R. Soc. B Biol. Sci. *376*, 20190753. https://doi.org/10.1098/rstb.2019.0753.

Zheng, Y., Wang, S., Xue, X., Xu, A., Liao, W., Deng, A., Dai, G., Liu, A.P., and Fu, J. (2017). Notch signaling in regulating angiogenesis in a 3D biomimetic environment. Lab Chip *17*, 1948–1959. https://doi.org/10.1039/C7LC00186J.

STAR★METHODS

KEY RESOURCES TABLE

REAGENT or RESOURCE	SOURCE	IDENTIFIER
Chemicals, peptides, and recombinant proteins		
active human Dll4 protein fragment	Abcam, HEK293 cells	ab108557; lot#:GR3172950-14
recombinant human Jagged1/fc chimera	R&D systems	Cat#1277-JG; Lot#RZL2219031
ChromePure human IgG Fc fragment	Jackson Immuno Research	Code: 0009-000-008; Lot#135334
protein G fluorescent particles	Spherotech	Cat#PGFP-0562-5
SYLGARD™ 184 Silicone Elastomer Kit (PDMS)	DOW	GMID: 01672921; CAS: 100-41-4
Matrigel membrane basis growth factor reduced	Corning	Cat#354230; Lot#8190005
Gelatin	Sigma, porcine	CAS: 900708,
Endothelial cell base media 2 and supplement pack endothelial cell GM2	Promocell	Cat#C-39211; Lot#454M232
Su-8 Masters, made with Su-8 2000 photoresist, Su-8-2050 and Su-8 Developer	Tiemeijer et al. 2018 master and design, MicroChem (chemicals)	www.microchem.com
Phalloidin Atto-488 Bioreagent	Merck Life Science NV	N/A
DAPI	Merck Life Science NV	CAS: 28718-90-3
HOT FIREPol® EvaGreen® qPCR Mix Plus (ROX)	Solis Biodyne	08-24-00008
Revertaid Reverse Transcriptase	Thermo fisher	EP0441
Protein G	Pierce	77675
Recombinant dll4-fc	R&D Systems	10185-D4
Recombinant jag1-fc	R&D Systems	1277-JG
Recombinant human IgG1-Fc	R&D Systems	110-HG-100
Critical commercial assays		
Nucleospin Kit	Marcherey-Nagel	740955.5
Deposited data		
Fluorescence microscopy, image analysis, quantitative PCR data, computational data	This paper	https://doi.org/10.4121/19235784
Experimental models: Cell lines		
Human: Human Umbilical Vein Endothelial Cells	Lonza	Cat#C2519A; Lot#0000704189
Oligonucleotides		
Jag1 Primer: Forward: AATGGCTACCGGTGTGTCTG; Reverse: CCCATGGTGATGCAAGGTCT	Sigma-Aldrich	N/A
Software and algorithms		
Fiji (Image J)	Schindelin et al. (Schindelin et al., 2012)	https://imagej.net/software/fiji/
GraphPad Prism 8.0.2	GraphPad	https://www.graphpad.com/scientific-software/prism/
LAS X small 3.4.2	Leica microsystems	https://www.leica-microsystems.com/products/microscope-software/p/leica-las-x-ls/
Original code	This paper	https://doi.org/10.4121/19235793
Other		
Corona Discharge Generator	Tantec HF	N/A

RESOURCE AVAILABILITY

Lead contact

Further information and requests for resources and reagents should be directed to and will be fulfilled by the lead contact, Cecilia Sahlgren (cecilia.sahlgren@abo.fi).

Materials availability

This study did not generate new unique reagents.

Data and code availability

Section 1 Data

Fluorescence microscopy, image analysis and quantitative PCR data have been deposited at 4TU.ResearchData and are publicly available as of the date of publication. DOIs are listed in the key resources table.

Section 2 Code

All original code has been deposited at 4TU.ResearchData and is publicly available as of the date of publication. DOIs are listed in the key resources table.

Section 3

Any additional information required to reanalyze the data reported in this paper is available form the lead contact upon request.

EXPERIMENTAL MODEL AND SUBJECT DETAILS

Primary cells source

HUVECs were purchased from Lonza. Product code: C2519A, Lot number: 0000704189. Tissue Acquisition number: P826. Pooled Donors. Sex: MALE/FEMALE MIXED. Race: B,B,A,C,C,C.

METHOD DETAILS

Experimental design (objectives and design of study)

In this study, the effects of Jag1 and Dll4 micropatterned lines on endothelial sprouting were compared. Fc fragments were used a control. We looked at the effects on sprout location and direction with fluorescent microscopy. Briefly, 6 different experimental rounds were performed; each round on a different day. Per round, approximately 20 million Human Umbilical Vein Endothelial Cells (HUVECs) from one passage number (P3, P4, or P6) were distributed among 8 microchips, corresponding to 2 Fc, 4 Jag1, and 2 Dll4 chips/samples per round. Thus, the experiment was performed for a total of 48 chips (12 Fc, 24 Jag1, 12 Dll4). 22 chips that showed signs of channel leakage, failed μCP or cell death during or at the end of the experimental period (24h) were omitted from further analysis. *In silico* modeling was adopted to investigate if the experiments could be explained by the effects of the Notch ligand patterns on the dynamics of cell signaling.

Fabrication of the soft lithography masters

As described in our previous study (Tiemeijer et al., 2018), standard soft lithography was used to create SU-8 masters for both μCP stamps and cell seeding channels. The same SU-8 masters were used in this study. Briefly, Su-8 2050 was spun at 500 rpm for 10 s, followed by 30 s at 2000 rpm, prebaked 5 min at 65°C and 15 min at 95°C. UV exposure was performed with a mask containing the desired features for 35 s at 13mNcm−2. Post baking 5 min at 65°C and 8 min at 95°C and finally developed for an hour with SU-8 developer.

Fabrication of μCP stamps and cell seeding channels

PDMS consisting of 10:1 w/v base to curing agent (Sylgard 184) was mixed, degassed by centrifuging and poured over the corresponding master before final removal of air bubbles in vacuum. After curing at 65°C overnight, the PDMS was taken of the masters and cut into stamps with dimensions of 100 μm lines spaced 100 μm and channels with dimensions of 150 μm and 300 μm wide, spaced by 300 or 500 μm, with 1.5 mm inlets and outlets (Figures 1A and 1C2).

Cell culture

HUVECs (Lonza, pooled, Cat#: C2519A Lot#: 0000704189) were cultured in Endothelial Cell Base Media 2 (Promocell) with addition of the supplement pack endothelial cell GM2 (Promocell) with final concentrations of 0.02 ml/ml Fetal Calf Serum (FCS), 5 ng/ml human recombinant Epidermal Growth Factor (hEGF), 10 ng/ml human recombinant basic Fibroblast Growth Factor (hbFGF), 20 ng/ml human recombinant Insulin-like Growth Factor (R3-IGF-1), 0.5 ng/ml human recombinant Vascular Endothelial Growth Factor 165 (VEGF), 1 μg/ml ascorbic acid, 22.5 μg/ml heparin, and 0.2 μg/ml hydrocortisone and was supplemented with additional 1% penicillin/streptomycin. Cell culture flasks were coated with 0.1% gelatin (Porcine, Sigma) before culture in 37°C, 5% CO_2. Cells with passage numbers of 3-6 were used for the experiments.

μCP of ligand functionalized lines

Similar to our previous study (Tiemeijer et al., 2018), 50 μl (10 μg/ml) of active human Dll4 protein fragment (Abcam) or 4.3 μl (200 μg/ml) of recombinant human Jagged1/fc chimera (R&D systems) or 0.2 μl (2.2 mg/ml) ChromePure human IgG Fc fragment (Jackson Immuno Research) was incubated with 100 μl (0.1% w/v) protein G fluorescent particles (Spherotech, purple, 0.4–0.6 μm) overnight at 5°C, resulting in μCP ink with a maximum of 0.5 μg of Dll4 ligand immobilized to the beads per sample or molar% equivalents of Jag1 and Fc fragments. Before inking of the μCP stamps with ligand-bead mixture, the stamps were made hydrophilic by treatment with atmospheric plasma for 9 s (Corona Discharge Generator, Tantec HF). μCP stamps and ink were incubated for 30 min at RT and dried using N_2 gas prior to printing on glass slides, which were sterilized with 70% ethanol and additional UV light treatment (5 min). The μCP stamps were left to adhere to the glass for 30 min at RT before removal.

Confined cell seeding and sprouting assay

Microfluidic channels were placed on the printed glass slides orientated perpendicular to the ligand functionalized lines and gently pressed to contact the substrate and seal the microchannels. P200 pipette tips (without filter) were placed in the inlets of the channels as fluidic reservoirs that allowed feeding of the system by gravity (Figure 1C). The channels were coated with 1% gelatin in PBS, pipetted in one of the tips, for 5 min at 37°C, 5% CO2, followed by careful flushing out of the gelatin solution with pre-warmed media (18 h at 37°C, 5% CO_2). HUVECs in pre-warmed media ($5*10^6$ cells/ml) were seeded directly via the pipette tips and were left to adhere for approx. 2.5 h at 37°C, 5% CO_2 monitoring against cell aggregates and ensuring sufficient flow through the channels. After cell adherence the channels were cautiously taken off the glass slides, and Matrigel®matrix (15% in total amount of media, growth factor reduced, Corning; lotnr. 00034014) was placed on top of the HUVECs, after setting shortly followed by remaining media. The HUVECs were left to sprout unconfined for 24 h in 37°C, 5% CO_2.

Fluorescent microscopy and image analysis

The cell samples were fixated for 30 min at RT with 3.7% formaldehyde in PBS. The fixed samples were permeabilized with 0.5% triton X-100 in PBS for 15 min. PBS was used as washing buffer during staining with the markers Phalloidin (Atto488) for the actin cytoskeleton and DAPI for the nuclei respectively. Tile scan acquisition was done using a Leica DMi8 TIRF microscope. Regions of interest (ROIs) were defined as mentioned in the results and identified by visual assessment. Direction analysis for every ROI was performed with the Fourier components method of the Directionality plugin in Fiji (Image J). ROIs with a "goodness of a fit" value lower than 0.2 were excluded from subsequent analysis, as the fitting graph was judged inaccurate for those cases. The average orientation and the dispersion were extracted from the graphs fitted on the histograms. The average direction was normalized to the direction of ligand functionalized lines. Sprouts that deviate to the left from the line direction would correspond to a positive direction and sprouts that deviate to the right would correspond to a negative direction. The efficiency of patterning was quantified similar to our previous study (Tiemeijer et al., 2018), by using an equation adjusted from Frimat et al. (Frimat et al., 2009):

$$Ef_{cs} = \frac{C_{off}}{C_{off} + C_{on}} 100\% \quad \text{(Equation 1)}$$

where Ef_{cs} is the efficiency of controlled sprouting of the endothelial cells in between the lines in percentage, C_{off} the number of cells in the region A of the ROI (in between the lines) and Con the number of cells in the region B of the ROI (on top of the lines), where A and B have equal dimensions and surface,

and together are one ROI. The cells were counted using the Cell Counter plugin in Fiji (Image J). Statistical analysis was done using non-parametric ANOVA (Kruskal-Wallis) with Dunn's multiple comparisons test.

qPCR

Notch response after 6-h ligand induction was tested on HUVECs cultured in wells coated with protein-G and either 25 nM recombinant Fc-Dll4, 25 nM recombinant Fc-Jag1 or 25 nM Fc. RNA was isolated using a Nucleospin kit (Macherey-Nagel) and 100–150 ng RNA was converted to cDNA by Revertaid Reverse Transcriptase (Thermo Fischer). qPCR was run on a QuantStudio3 qPCR machine (Applied Biosystems), with as mastermix Hot FirePol EvaGreen plus ROX (Solis Biodyne). Primer of Jag1 consisted of; Forward: AATGGCTACCGGTGTGTCTG, Reverse: CCCATGGTGATGCAAGGTCT.

Computational model

A previous computational model (Boareto et al., 2015b) was adopted to simulate cell-cell signaling occurring among the cells in our experiments. The model was adapted to simulate a row of endothelial cells with periodic boundary conditions (with the first cell connected to the last cell in the row), with boundaries corresponding to half of two consecutive lines patterned with ligands (Figure 5A). Half of the cells were considered in contact with functionalized ligands on the substrate. The model relies on a system of ordinary differential equations describing the time variation of the Notch and VEGF signaling proteins within each cell. Briefly, external VEGF is assumed to bind and activate VEGFR, which leads to Dll4 upregulation (Blanco and Gerhardt, 2013). Dll4 can then bind to Notch1 in both the same cell, leading to cis-inhibition (Sprinzak et al., 2010), or neighboring cells, causing transactivation. Notch cis-inhibition and transactivation can also be mediated by the other Notch ligand, Jag1. Notch activation leads to an increase in Notch intracellular domain, which in turn causes downregulation of Dll4 (Shimojo et al., 2011) and VEGFR (Blanco and Gerhardt, 2013), and upregulation of Jag1 and Notch1, in the receiving cell (Manderfield et al., 2012). Finally, the Notch intracellular domain is assumed to activate Fringe (Morales et al., 2002), which in turn influences the (cis- and trans-) binding rate of Notch1 with its ligands. This increases the Dll4-Notch1 binding rate and decreases the Jag1-Notch1 binding rate (Kopan and Ilagan, 2009).

The modelling assumptions translate into a system of ordinary differential equations describing the dynamics of VEGF and Notch signaling in each cell. In particular, the equations focus on the time variations of free Notch (N_i), Dll4 (D_i), Jag1 (J_i), Notch intracellular domain (I_i), VEGFR ($V_{R,i}$), and activated VEGFR (V_i), for each cell with index $i \in N$. The variation over time of these proteins is described by the following system of ordinary differential equations:

$$\frac{dN_i}{dt} = N_0 H^S(I_i,\ \lambda_{I,N}, n_N) - N_i\left[(k_C D_i + k_T D_{i,\text{ext}})H^S(I_i,\ \lambda_{F,D}, n_F) + (k_C J_i + k_T J_{i,\text{ext}})H^S(I_i,\ \lambda_{F,J}, n_F)\right] - \gamma N_i \quad \text{(Equation 2)}$$

$$\frac{dD_i}{dt} = D_0 H^S(I_i,\ \lambda_{I,D}, n_D)H^S(V_i,\ \lambda_{V,D}, n_D) - D_i\left[k_C H^S(I_i,\ \lambda_{F,D}, n_F)N_i + k_T N_{i,\text{ext}}\right] - \gamma D_i \quad \text{(Equation 3)}$$

$$\frac{dJ_i}{dt} = J_0 H^S(I_i,\ \lambda_{I,J}, n_J) - J_i\left[k_C H^S(I_i,\ \lambda_{F,J}, n_F)N_i + k_T N_{i,\text{ext}}\right] - \gamma J_i \quad \text{(Equation 4)}$$

$$\frac{dI_i}{dt} = k_T N_i\left[D_{i,\text{ext}} H^S(I_i,\ \lambda_{F,D}, n_F) + J_{i,\text{ext}} H^S(I_i,\ \lambda_{F,J}, n_F)\right] - \gamma_S I_i \quad \text{(Equation 5)}$$

$$\frac{dV_{R,i}}{dt} = V_{R0} H^S\left(I_i,\ \lambda_{I,V_R}, n_{V_R}\right) - k_T V_{R,i} V_{\text{ext}} - \gamma V_{R,i} \quad \text{(Equation 6)}$$

$$\frac{dV_i}{dt} = k_T V_{R,i} V_{\text{ext}} - \gamma_S V_i \quad \text{(Equation 7)}$$

Here, N_0, D_0, J_0, V_{R0} represent the production rate of Notch1, Dll4, Jag1, and VEGFR, respectively. γ is the degradation rate of Notch ligands, VEGF ligands, and inactive receptors; γ_S indicates the degradation rate of activated Notch and VEGFR. k_C and k_T label the rate of cis-inhibition and transactivation of Notch receptors by Notch ligands when no Fringe is expressed. k_T also represents the rate of activation of VEGFR by external VEGF (indicated with the model parameter V_{ext}). The rate of protein production, cis-inhibition, and transactivation varies over time as influenced by Notch and VEGFR activation, as captured by the shifted Hill function $H^S(X,\ \lambda_{X,Y}, n) = \lambda_{X,Y} + (1 - \lambda_{X,Y})/(1 + (X/X_0)^n)$. X and Y are here auxiliary labels to indicate that H^S describes the variation in production of Y due to variations in the activation of X with respect to a reference value X_0. n represents the sensitivity of the production rate to these variations.

Finally, $\lambda_{X,Y}$ describes the effect of these variations on Y: $\lambda_{X,Y} = 1$ has no effects; $\lambda_{X,Y}<1$ corresponds to downregulation; and $\lambda_{X,Y}>1$ corresponds to upregulation. Similarly, $H^S(I, \lambda_{F,D}, n_F)$ and $H^S(I, \lambda_{F,J}, n_F)$ represent the production rate of the enzyme Fringe and, indirectly, the influence of Fringe on the binding and activation rate of Notch1 to Dll4 (with $\lambda_{F,D}$) and Jag1 (with $\lambda_{F,J}$), respectively. Finally, in the present study we define $N_{i,ext}$, $D_{i,ext}$, and $J_{i,ext}$ as the summation of Notch1, Dll4, and Jag1 content on the patterned lines and on neighboring cells, such that:

$$N_{i,ext} = (N_{i-1} + N_{i+1})/2 \quad \text{(Equation 8)}$$

$$D_{i,ext} = \begin{cases} (D_{i-1} + D_{i+1})/2 + D_{line} & \textit{cell } i \textit{ is on a Dll4 line} \\ (D_{i-1} + D_{i+1})/2 & \textit{otherwise} \end{cases} \quad \text{(Equation 9)}$$

$$J_{i,ext} = \begin{cases} (J_{i-1} + J_{i+1})/2 + J_{line} & \textit{cell } i \textit{ is on a Jag1 line} \\ (J_{i-1} + J_{i+1})/2 & \textit{otherwise} \end{cases} \quad \text{(Equation 10)}$$

The indices $i-1$ and $i+1$ correspond to the direct neighbors of the cells. As in Boareto et al. (2015a, 2015b), we therefore assumed that the rate of Notch transactivation is proportional to the average content of Notch proteins in their neighbors. In the present study, we added the parameters D_{line} and J_{line} to consider the Dll4 and Jag1 concentrations coated on the ligand-functionalized lines, thereby assuming that the Notch ligands printed on the patterns bind and activate the Notch receptors present in the cells on top of the patterned lines. The parameters D_{line} and J_{line} were calibrated via a comparison between simulations and experiments of cells on homogeneous coatings (see Figures 5C and 5D). The remaining parameter values were chosen in agreement with Boareto et al. (2015a, 2015b) and they are reported in Table S1.

Due to the periodicity of the system, only cells within a limited portion of the substrate were simulated, corresponding to the cells in between the middle portion of two adjacent patterned lines (Figure 5A). Periodic boundary conditions were assigned to cells at the edges of this area, such that the first cell was considered in contact and signaling with the last cell. Practically, if we are simulating $M \in N$ cells, in Equations 8, 9, and 10 the value of the function mod M applied to $i-1$ and $i+1$ is taken for the cells with indices 1 and M, respectively. This is performed to ensure that cell 1 is a neighbor of the cells with indices 2 and M, while cell M is a neighbor of the cells with indices 1 and $M-1$. The system of equations was solved with an explicit scheme, with a time-step $dt = 0.01$ h. The simulations were run with a limited end time t_{fin} equal to 12 h, unless stated otherwise. Finally, a phenotype was assigned to each endothelial cell according to the final VEGFR activation, represented by the value $V_i(t_{fin})$: if $0 < V_i(t_{fin}) < 100$, a stalk (S) cell phenotype was assigned; $100 \leq V_i(t_{fin}) \leq 300$ corresponded to a hybrid tip/stalk (T/S) phenotype; and cells with $V_i(t_{fin}) > 300$ corresponded to tip cells (T). For the calculation of Ef_{cs}, we considered that: cells predicted as tip cells and tip/stalk cells correspond to sprouting migrating cells; cells predicted as stalk cells correspond to non-sprouting cells. Ef_{cs} was computed via Equation 1, by counting the tip and tip/stalk hybrid cells that were localized on top (C_{on}) or off (C_{off}) the patterns.

The solutions at the limited time point of 12 h depend on the initial conditions. To account for that, all simulations were repeated 10000 times, with random initial conditions chosen such that $0 < N_i(0)$, $D_i(0)$, $J_i(0)$, $V_{R,i}(0)<6000$ molecules, and $0 < I_i(0)$, $V_i(0)<600$ molecules for all indices i. Averages and boxplots of the simulated Jag1 expression and Ef_{cs} were computed over the 10000 simulation runs. Random initial conditions are justified because, in the *in vitro* experiments, HUVECs were exposed to VEGF already during the initial cell culture step, before the microchip seeding. As a result of VEGF exposure, cell-cell signaling, and random cell movement, we can assume that cells in the culture flasks exhibit a random mix of tip, stalk, and hybrid phenotypes. This supports our choice of random phenotypes and protein contents as initial conditions for the microchip simulations, similar to studies with analogous models (Boareto et al., 2015a, 2015b; Loerakker et al., 2018; Ristori et al., 2020). Even changing this assumption by choosing specific ratios of phenotypes as initial conditions would not significantly change the computational results. Irrespective of the initial conditions, when strong effects from the patterns are absent, cells obtain an approximately homogeneous hybrid phenotype (Figure 5B). This general tendency towards a homogeneous hybrid phenotype would therefore cancel out any chosen distribution of cell phenotypes as initial condition and only strong and relatively fast effects from the patterns would force cells into the stalk phenotype (as in Figure 5B).

QUANTIFICATION AND STATISTICAL ANALYSIS

Experimental results

After fluorescent imaging, multiple ROIs per chip could be potentially identified. Due to the stringent criteria for ROI selection, successful ROI identification was limited to a total of 3 Fc, 4 Jag1, 4 Dll4 chips

from 4 experimental rounds. For statistical analysis, data from the selected ROIs were pooled per experimental condition from the different experimental rounds. Per experimental condition, the data were represented by at least 3 chips, each containing at least 7 ROIs. The data in the results and figure legends are reported as mean $\pm$ SD, N corresponds to the number of ROIs. In the directionality analysis, ROIs with a fit of the graph less than 0.2 were dismissed resulting in 29 Fc, 106 Jag1 and 58 Dll4 ROIs analyzed. Both the Efficiency of controlled sprouting and the Directionality results were analyzed with a Kruskal-Wallis test and a Dunn's multiple comparisons test as normal distributions were not assumed.

qPCR was performed was performed in 3 separate replications, with 3 or 4 wells per condition (Fc, Jag1, Dll4), per replication (averaged for statistical analysis). These results were analyzed by repeated measures ANOVA (to take into account different baseline between separate replications), and by Tukey's post hoc test.

iScience, Volume *25*

Supplemental information

Engineered patterns of Notch ligands Jag1 and Dll4 elicit differential spatial control of endothelial sprouting

Laura A. Tiemeijer, Tommaso Ristori, Oscar M.J. A. Stassen, Jaakko J. Ahlberg, Jonne J.J. de Bijl, Christopher S. Chen, Katie Bentley, Carlijn V.C. Bouten, and Cecilia M. Sahlgren

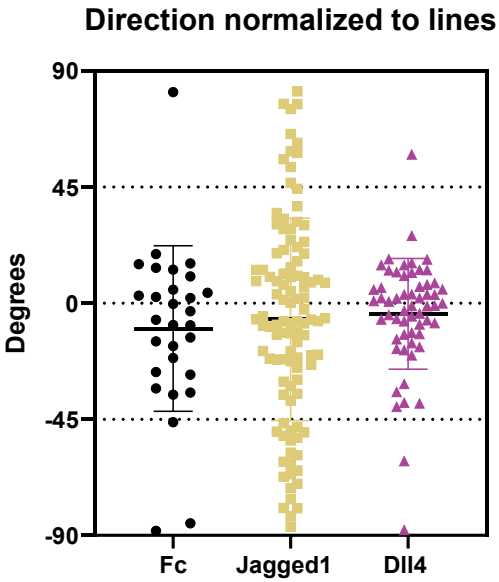

Figure S1. Directions of normalized lines, related to Figure 3
The average direction for every ROI, normalized to the direction of the lines (0 degrees). There is no significant difference between the mean direction between the sample groups. Data represented as Mean ± SD, N=29/106/58 ROI for Fc/Jag1/Dll4 respectively. Data points that represented ROIs with a "goodness of a fit" value lower than 0.2 were excluded.

Table S1. Parameter values, related to STAR Methods.

Parameter	Value	Description
N_0	$1200\ molec\ \cdot h^{-1}$	Notch1 baseline production
D_0, V_{R0}	$1000\ molec\ \cdot h^{-1}$	Dll4 and VEGFR baseline production
J_0	$800\ molec\ \cdot h^{-1}$	Jag1 baseline production
I_0, V_0	$200\ molec$	reference value of Notch and VEGFR activation
V_{ext}	$1000\ molec$	external VEGF present in the cell environment
γ	$0.1\ h^{-1}$	Notch protein degradation rate
γ_S	$0.5\ h^{-1}$	activated Notch and VEGFR degradation rate
k_T	$2.5 \cdot 10^{-5}\ h^{-1}$	transactivation rate
k_C	$5 \cdot 10^{-4}\ h^{-1}$	cis-inhibition rate
n_N, n_D, n_V, n_{V_R}	2.0	sensitivity of protein production to signaling activation
n_J	5.0	sensitivity of Jag1 production to Notch1 activation
n_F	1.0	sensitivity of Fringe production to Notch1 activation
$\lambda_{I,N}, \lambda_{I,J}, \lambda_{V,D}$	2.0	effect of signaling activation on protein production
$\lambda_{I,D}, \lambda_{I,V_R}$	0.0	effect of signaling activation on protein production
$\lambda_{F,D}$	3.0	effect of Notch1 activation on Dll4-Notch1 binding as mediated by Fringe
$\lambda_{F,J}$	0.3	effect of Notch1 activation on Jag1-Notch1 binding as mediated by Fringe
D_{line}, J_{line}	$0 - 5000\ molec$	Dll4 and Jag1 proteins on the printed micropatterns

Laura Tiemeijer

Spatial Control of Angiogenesis by Engineered Patterns of Notch Ligands

In tissue engineering, vascularization of engineered tissues is imperative for constructs larger than a few cells thick. Common approaches for the engineering of vasculature rely on a preset structural support for the cells which limits integration into engineered and native tissues. Self-assembly of vascular constructs are promising but lack the ability to dictate structure and organization of the vasculatures. Therefore, spatial control over vascularization is required for tissue engineered constructs to remain alive and functioning. During angiogenesis, the native growth of existing vasculature, migrating tip cells emerge from the vascular endothelium and sprout towards the oxygen gradient, closely followed by proliferating stalk cells forming a vascular tube. The selection of tip and stalk cell phenotypes is partly regulated via the Notch signaling pathway, a highly conserved cell-cell signaling pathway involved in numerous cell fate decisions and the patterning of tissues. Here, Dll4/Notch1 signaling is responsible for tip and stalk cell selection while Jag1/Notch1 signaling modulates this signaling. The role of Jag1 in this selection needs to be further elucidated. Local activation of Notch signaling, especially to target angiogenesis has not yet been widely addressed.

This thesis describes an in vitro method to use spatial patterns of parallel lines of Notch signaling ligands to locally modulate endothelial tip/stalk cell selection and thereby gain spatial control over endothelial sprouting. We showed that line patterns of Dll4 induced controlled unidirectional and restricted sprouting on the lines, resulting in localization of endothelial sprouts between the lines (negative patterning). In contrast to Dll4, Jag1 patterns did not exert control over endothelial sprouting location and direction. The difference in control between stimulation with Dll4 and Jag1 could not be explained by the corresponding gene expression profiles. Computational modeling, revealed that underlying differences in signaling dynamics are likely the cause for the lack of control over endothelial sprouting exerted by Jag1. Finally, alternative techniques for complex patterning of ligands were considered and investigated, but require further optimization. In summary, we have shown the potential of engineered patterns of ligands to control endothelial sprouting during angiogenesis, which is valuable for the design of biomaterials, engineering of organized vasculature and regenerative medicine. Additionally, the method developed in this thesis allows for the screening of the functionality of engineered (mutated) ligands and consequent revealing disease phenotypes.

ISBN 978-952-12-4219-9